CO_2 Fixation into Cyclic Carbonates Catalyzed by Single-Site Aprotic Organocatalysts

Ala'a F. Eftaiha*[a] Abdussalam K. Qaroush,*[b] Areej K. Hasan,[b] Wissam Helal,[b] and Feda'a M. Al-Qaisi[a]

[a] Department of Chemistry, Faculty of Science, The Hashemite University, P.O. Box 330127, Zarqa 13133, Jordan. E-mail: alaa.eftaiha@hu.edu.jo

[b] Department of Chemistry, Faculty of Science, The University of Jordan, Amman 11942, Jordan. E-mail: a.qaroush@ju.edu.jo

Table of contents

Figure SE 2. The DFT-optimized molecular geometries of the species present in the reaction profile of ECH and CO_2 to form CC catalyzed by (**5'**, **6'**, and **7'**). The reported bond lengths are in angstrom (Å)..62

Table S1. Different benchmark studies reported organocatalysts for CO_2 cycloaddition

	Paul J. Dyson[1]	Werner and Ludwig[2]	W. Wu[3]	This work
The reported families	Aprotic Imidazolium and ammonium salts	Aprotic Ammonium and phosphonium salts	Protic ionic liquids: imidazolium, ammonium, pyridinium	Aprotic Imidazolium, ammonium, phosphonium, and pyridinium salts
Atmospheric Conditions	Yes	High (10 bar)	High (15 bar)	Yes
Experimental Conditions	ECH, catalyst (5 mol%), 50 °C, 3 h	1,2-epoxybutane, catalyst (2 mol%), 90 °C, 6 h.	PO, catalyst (1 mol%), 120 °C, 2 h.	ECH, catalyst (5 mol%), 90 °C, 6 h
Further studies	DFT	DFT and Kinetics	-	DFT
Catalysts Physical status	Homogeneous	Homogeneous	Homogeneous	Homogeneous vs. Heterogeneous
Product Analysis	NMR conversion	n.a.	Isolated yields and selectivity (GC)	NMR conversions and Isolated yields
Derivatives	Mono-functionalized	Mono-functionalized	Mono-functionalized	Mono-, bi-functionalized and polymeric material

n.a.: not available.

1. Synthesis and characterization of the organocatalysts (1-8)

1.1. Synthesis of 3-(3-(1,3-dioxoisoindolin-2-yl)propyl)-1-methyl-1*H*-imidazole-3-ium bromide (1)

In a 250 ml round-bottom flask equipped with a stirring bar, 8.00 g of N-(3-Bromopropyl) phthalimide (0.0298 mol) dissolved in 25 ml ethyl acetate (EtOAc), after the solution became clear, 2.4 ml of 1-methylimidazole (0.0301 mol) was added. The solution was refluxed in an oil bath at 80 °C for 4 h, EtOAc was removed by rotary evaporation, and a white precipitate was obtained, washed with copious amounts of diethyl ether (Et_2O), 7.46 g was obtained (71.5 % yield). Melting point (not corrected): 209.6 °C.

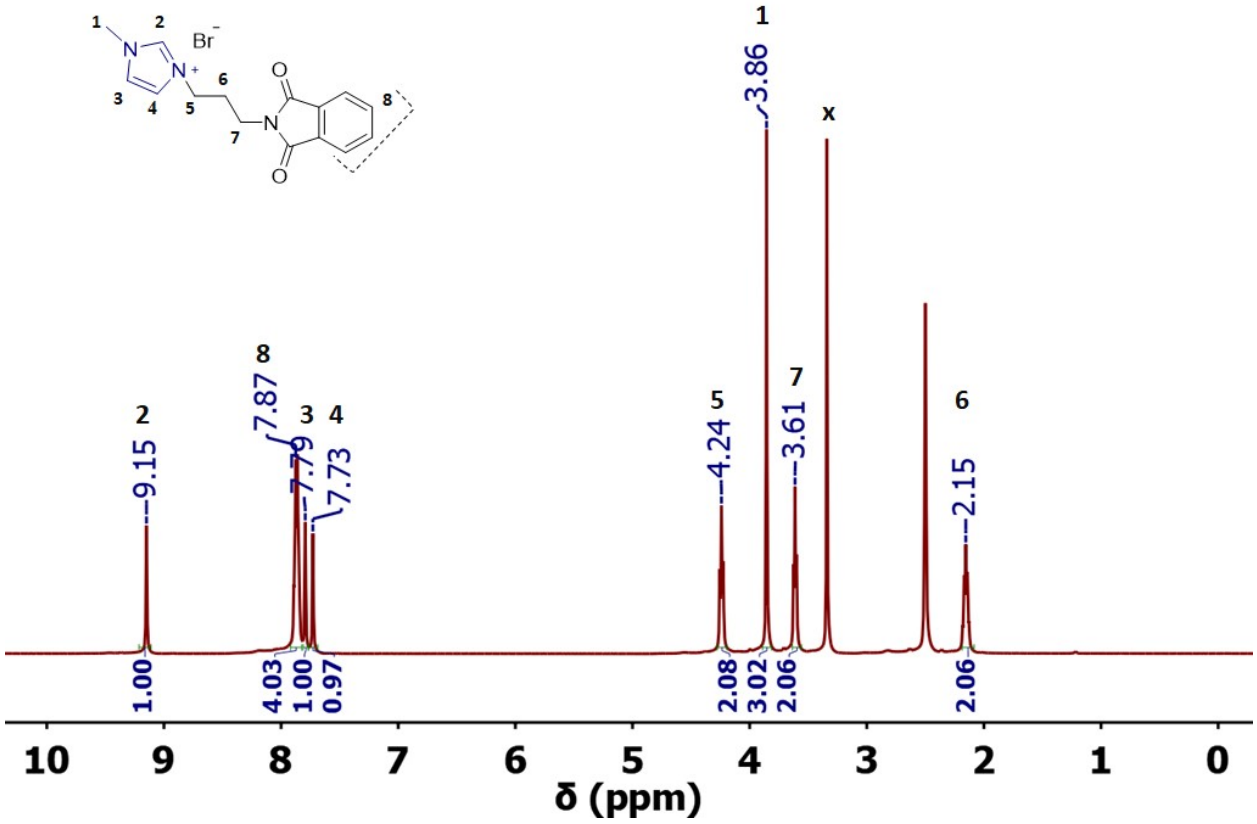

Figure SA 1. ^{1}H NMR spectra of **1** in DMSO-d_6, **S**: Solvent, **x**: H_2O.

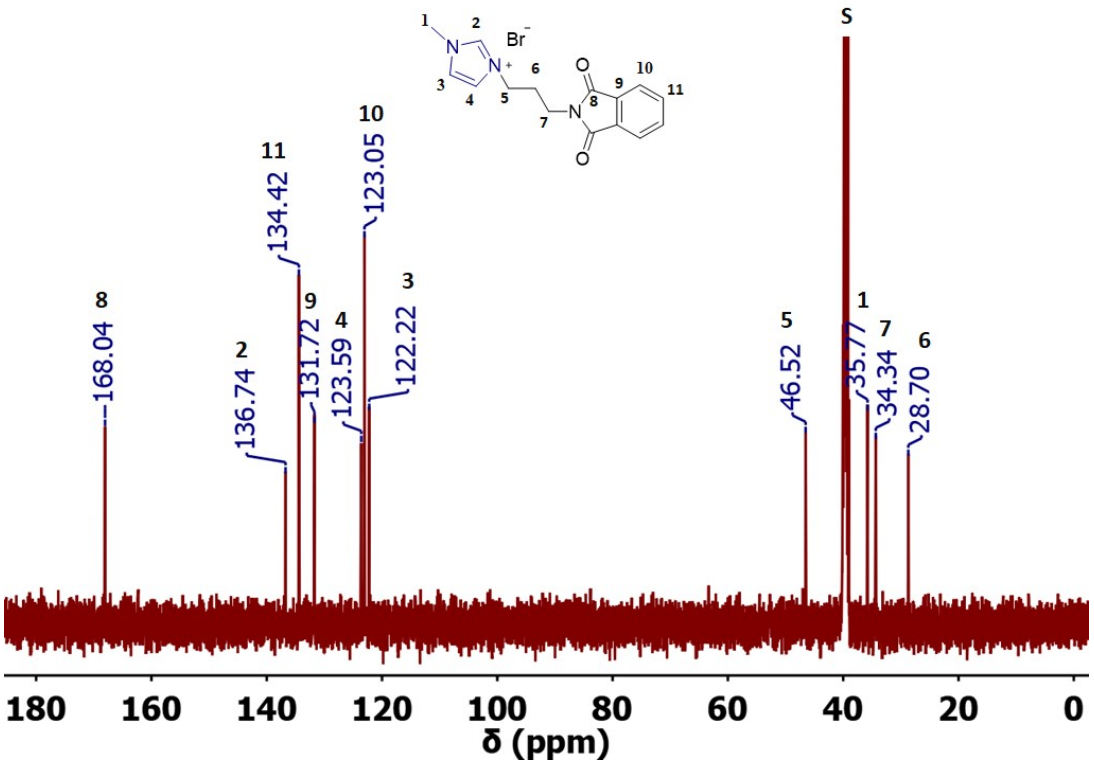

Figure SA 2. [13] C NMR spectrum NMR of **1** in DMSO-d_6, **S**: Solvent.

The ATR-FTIR was also used to investigate the synthesis of **1**, the presence of the imidazolium unit was verified by the four characteristic ring stretching bands (**3**, **Figure SA 3**) at 3094 (C-H), 1629 ($C=N^+$), 1573 (C=C), and 1166 (C-N) cm^{-1}.[4] The phthalimide ring bands were observed at 1609 cm^{-1} ($C=C_{aromatic}$), the bands at 1768 and 1629 were assigned for the symmetrical and asymmetrical stretching of (N-C=O) bond, respectively.[5] Herein, the disappearance of the (C-Br) stretching band in **3** at 532 cm^{-1} was a clear proof of the quaternization process,[6] due to the nucleophilic substitution of 1-methylimdazole with the phthalimide alkyl halide which resulted in the release the bromide anion as a leaving group.

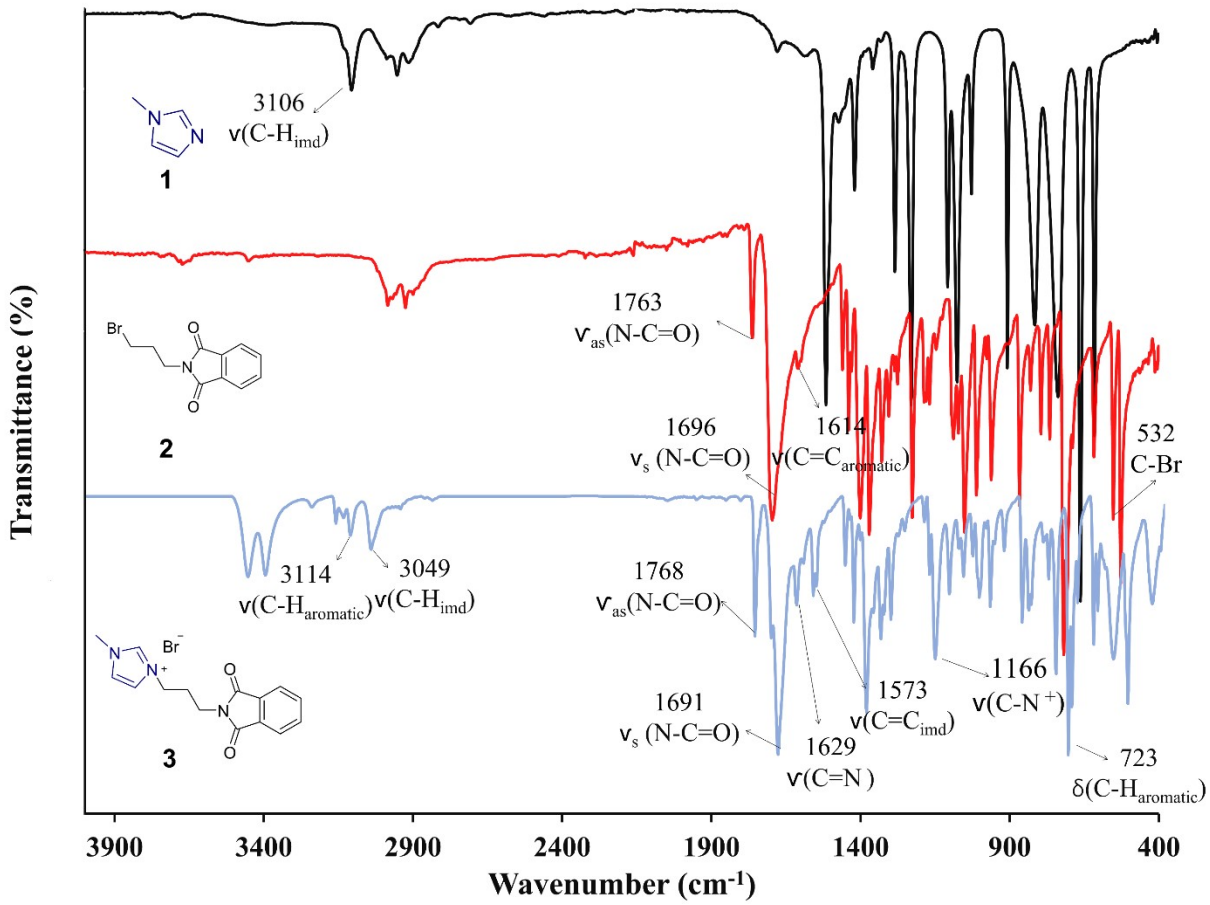

Figure SA 3. ATR-FTIR spectra of **1.** 1-methylimidazole (black traces), **2.** N-(3-Bromopropyl)phthalimide (red traces), and **3.** 1-methylimidazolium-based catalyst (**1**, blue traces).

1.2. Synthesis of 3-(3-(1,3-dioxoisoindolin-2-yl)propyl) -1,2-dimethyl-1H-imidazole-3-ium bromide (2)

In a 250 ml round-bottom flask equipped with a stirring bar, 3.01 g of N-(3-Bromopropyl) phthalimide (0.0112 mol) dissolved in 20 ml of ACN with 1.07 g of 1,2-dimethylimidazole (0.0112 mol), the reaction mixture refluxed in an oil bath at 80 °C for 4 h, a white solid was precipitated, washed with ACN to get rid of any starting materials, and then with Et_2O to obtain 3.69 g, yield: 90.5%. Melting point (not corrected): 250.4 °C.

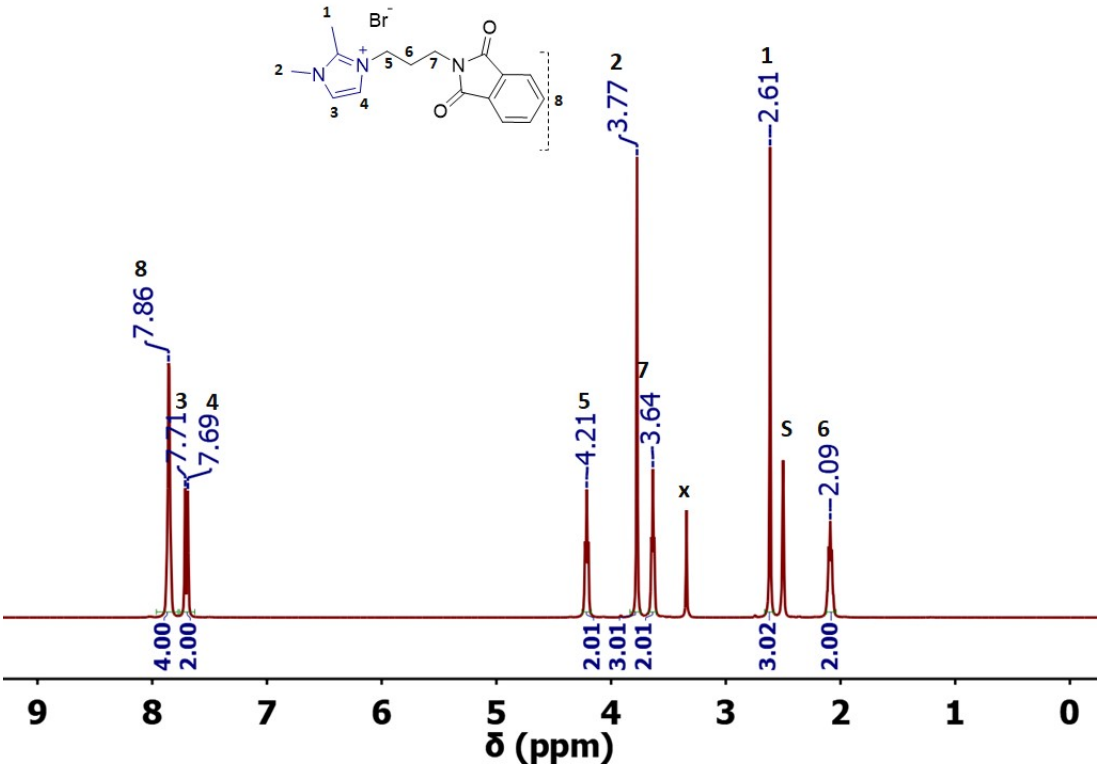

Figure SA 4. [1]H NMR spectrum of **2** in DMSO-d_6, **S**: solvent, **x**: H_2O.

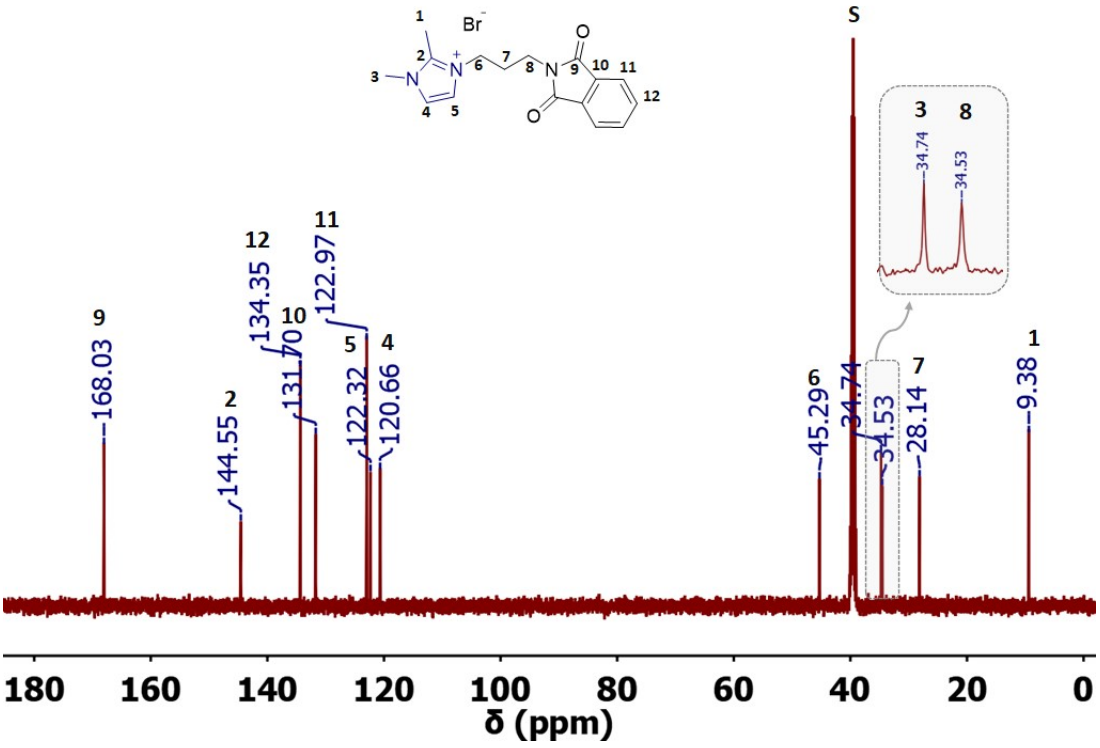

Figure SA 5. [13] C NMR spectrum of **2** in DMSO-d_6, **S**: solvent.

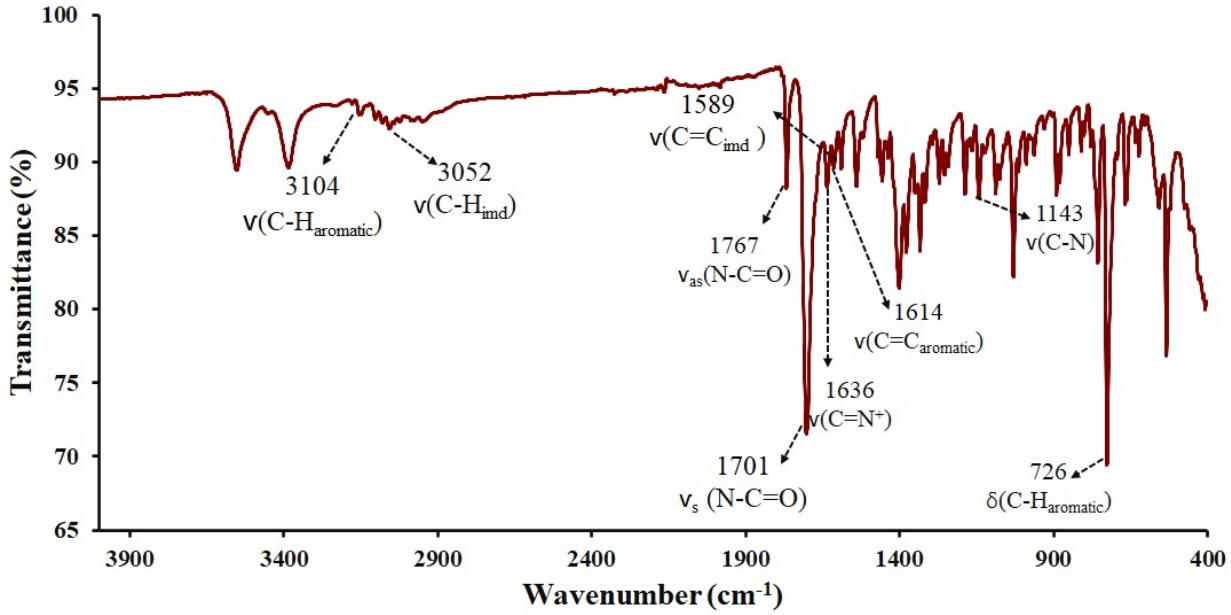

Figure SA 6. ATR-FTIR spectrum of **2**.

1.3. Synthesis of 3,3'-(1,4-phenylenebis(methylene))bis(1-methyl-1H-imidazole-3-ium) bromide (3)

In a 250 ml round-bottom flask equipped with a stirring bar, 0.500 g of 1,4-bis (bromomethyl)benzene (0.00189 mol) dissolved in 25 ml of ACN, after the mixture became clear, 0.30 ml of 1-methylimidazole (0.00378 mol) was added drop wisely to the reaction mixture, then refluxed in an oil bath at 82 °C for 6 h, a white precipitate was formed, washed ACN, 0.361 g was obtained (yield: 45%). Melting point (not corrected): 255.9 °C.

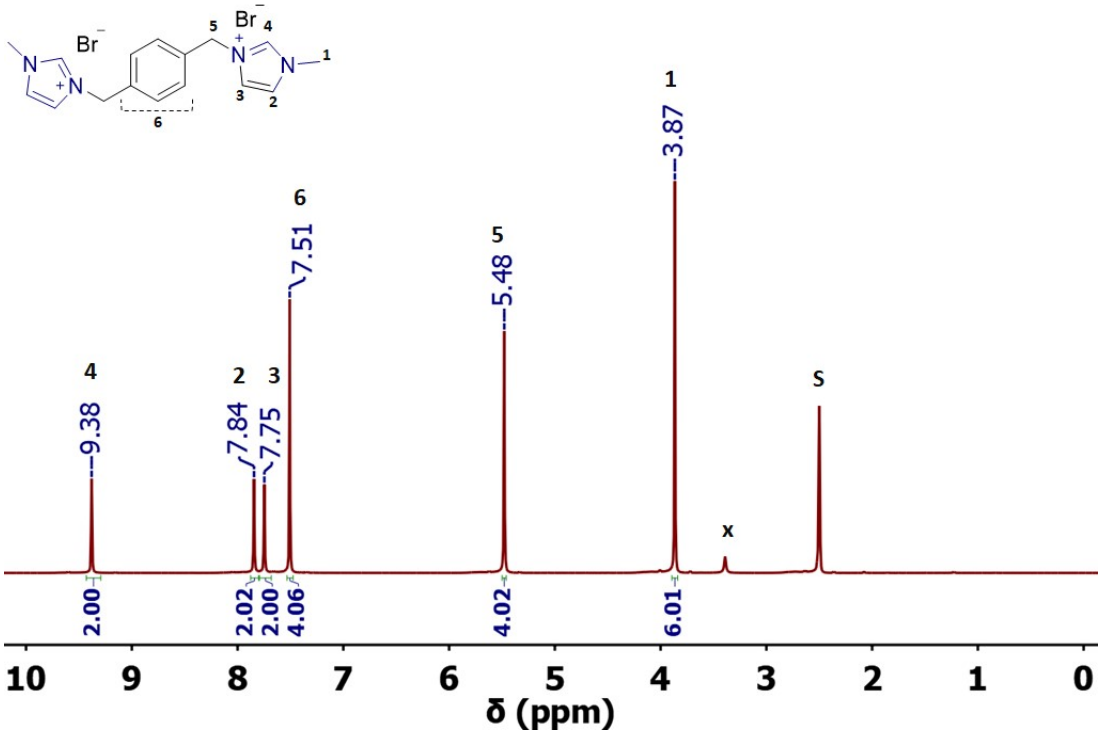

Figure SA 7. [1]H NMR spectra of **3** in DMSO-d_6, **S**: Solvent, **x**: H_2O.

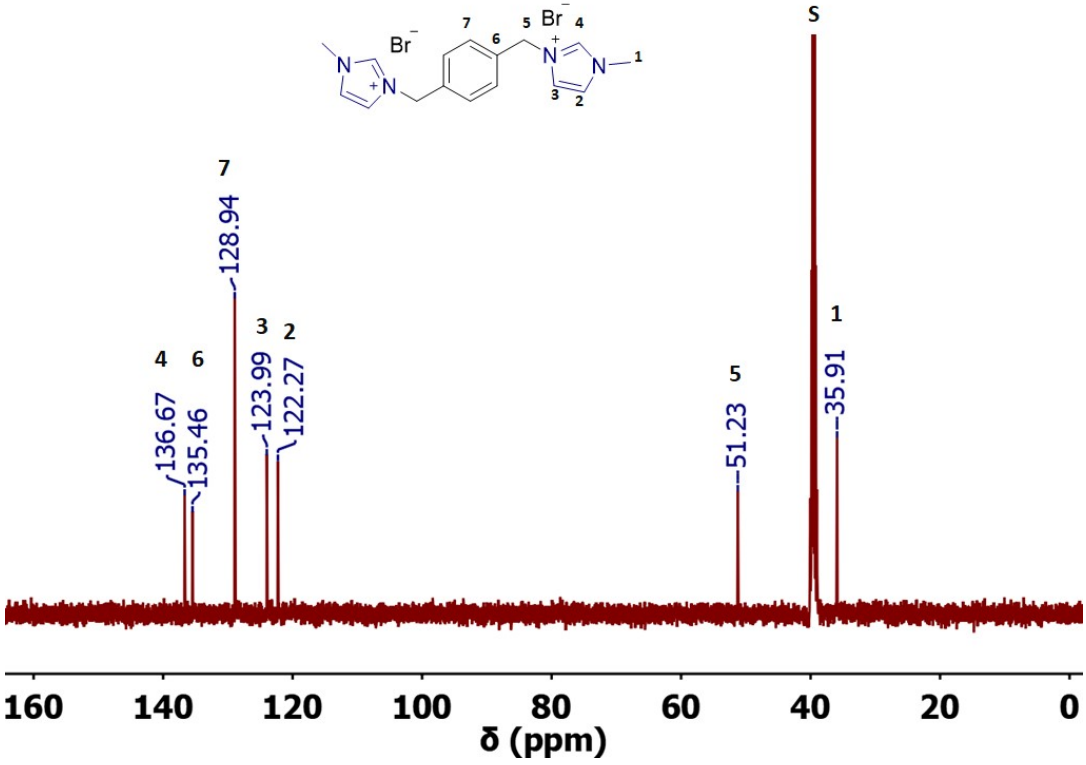

Figure SA 8. [13]C NMR spectrum of **3** in DMSO-d_6, **S**: Solvent.

The ATR-FTIR of (**3**) in comparison with 1-methyl imidazole and 1,4-bis(bromomethyl) benzene are shown in **Figure SA 9**, the imidazolium ring stretching bands appeared at 3049 (C-H), 1640 (C=N$^+$), 1560(C=C) and 1162 (C-N) cm^{-1}.[4] The disappearance of the (C-Br) stretching band in 1,4-bis(bromomethyl) benzene at 609 cm^{-1} was clear proof of the quaternization process. The stretching and rocking band of the aromatic C-H bond was observed at 3110 and 619 cm^{-1} in addition to the C=C ring stretch at 1512, 1420, and 1419 cm^{-1}.[7]

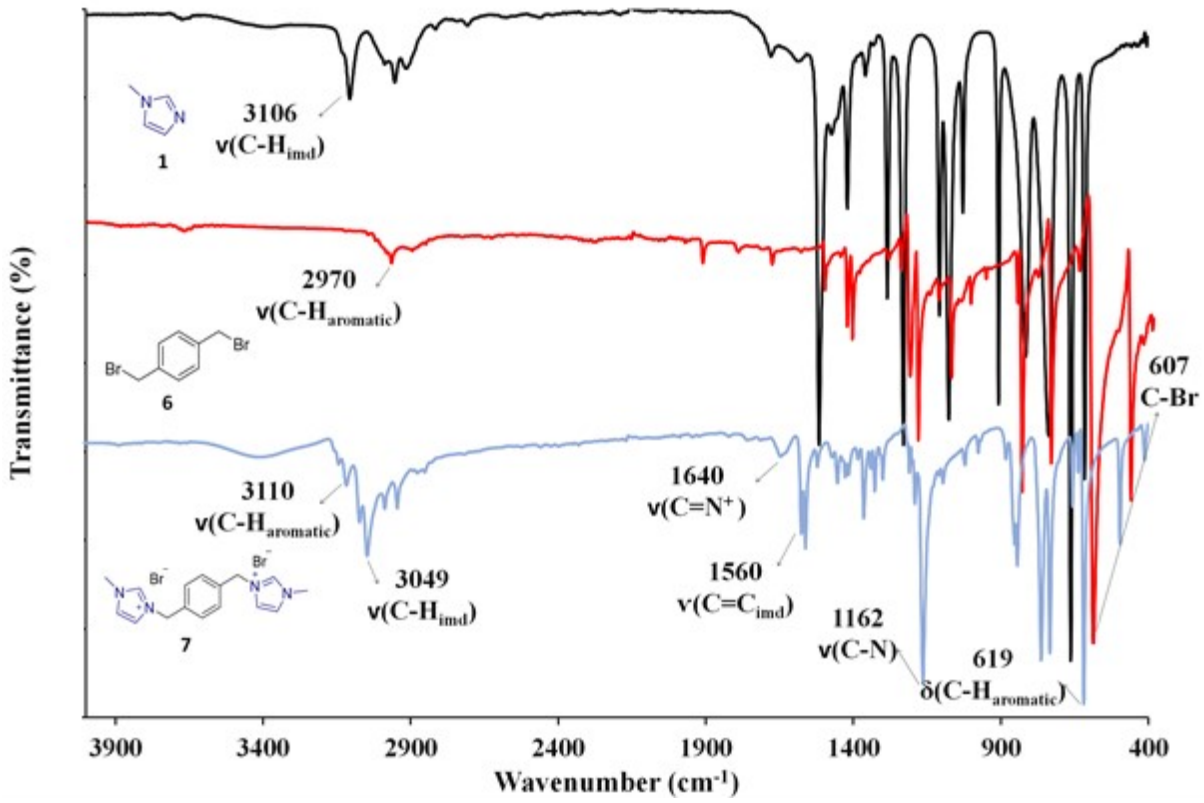

Figure SA 9. ATR-FTIR spectra of 1-methylimidazole (black traces), 1,4-bis (bromomethyl)benzene (red traces), and 1,4-diimdazolium-based catalyst (**3**, blue traces).

1.4. Synthesis of poly 3-(4-methylenbenzyl)-1H-imidazole-3-ium bromide (4)

In a 250 ml round-bottom flask equipped with a stirring bar, 2.60 g of imidazole (0.0382 mol) dissolved in 20 ml anhydrous tetrahydrofuran (THF) and added to 0.50 g of sodium hydride (NaH) formerly dissolved in THF at 30 °C to form the imidazolide species. Separately, 2.7 g of

1,4-bis (bromomethyl)benzene (0.0102 mol) was dissolved in THF and drop wisely added to the imidazolide mixture, the reaction mixture was refluxed at 70 °C for 72 h, the white precipitate was washed with 100 ml THF and stored. (3.76 g). Melting point (not corrected): 303.2.

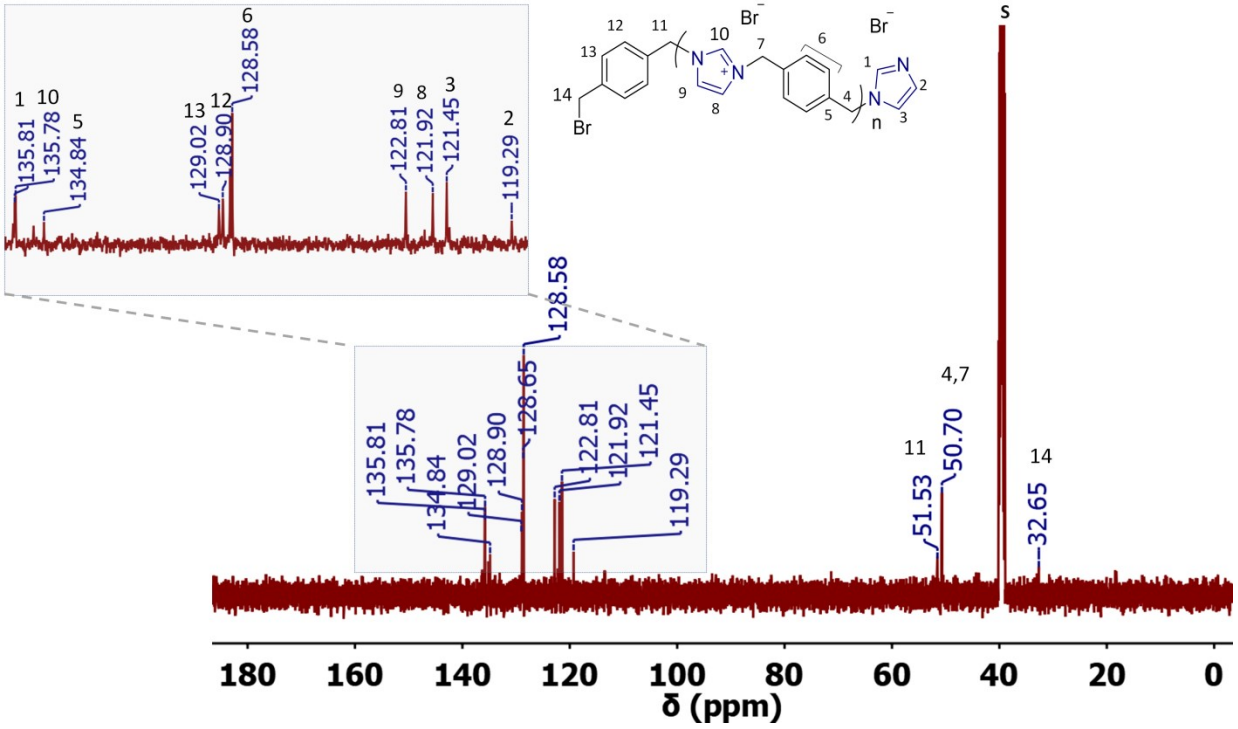

Figure SA 10. ^{13}C NMR spectrum of **4** in DMSO-d_6, **S**: Solvent.

ATR-FTIR spectra of **4** (**Figure SA 11**), shows the characteristic imidazolium ring stretching bands at 3085 ν(C-H_{imd}), 1614 ν(C=C_{imd}), 1556(C=C_{imd}), 1150 ν(C-N^+). The rocking band of the aromatic C-H bond was observed and 712 cm^{-1} as well as the C=C ring stretch at 1518, 1441, and 1403 cm^{-1}. The stretching mode of the aromatic C-H may be hidden by the broad O-H peak. ATR-FTIR revealed the polymer's susceptibility to moisture, with a broad peak at 3408 cm^{-1} ascribed to O-H stretching vibrational mode accompanied by a bending mode at 1403 cm^{-1} ascribed to the water traces in the sample. In addition, ^{1}H NMR (**Figure SA 12**) confirmed that with abroad peak at 3.57 ppm [8].

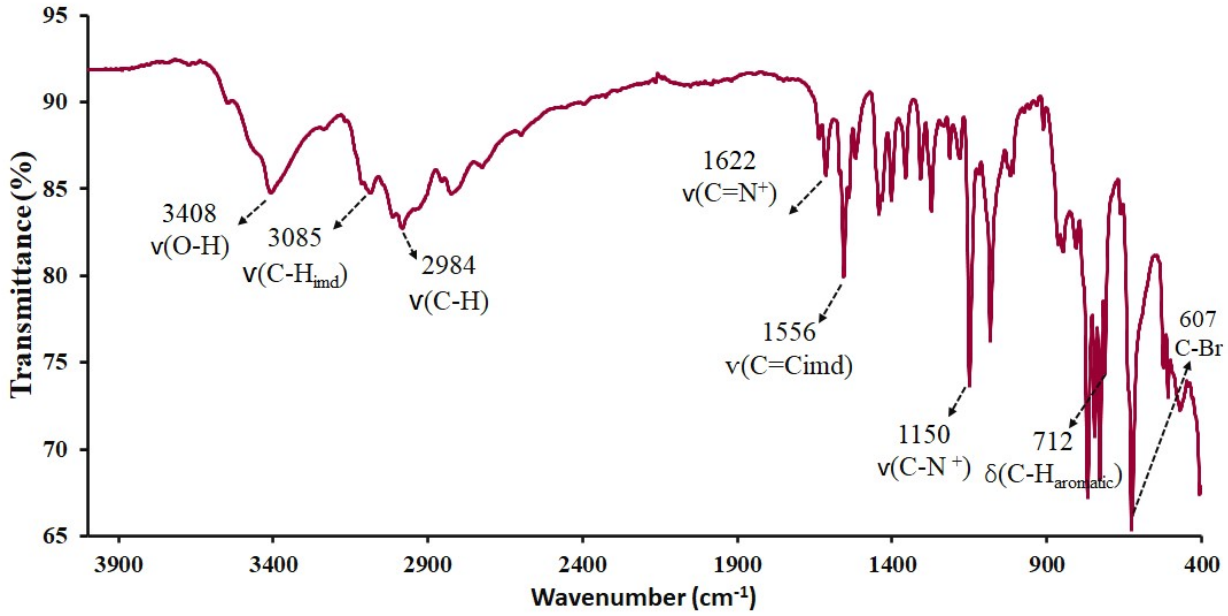

Figure SA 11. ATR-FTIR spectrum of **4**.

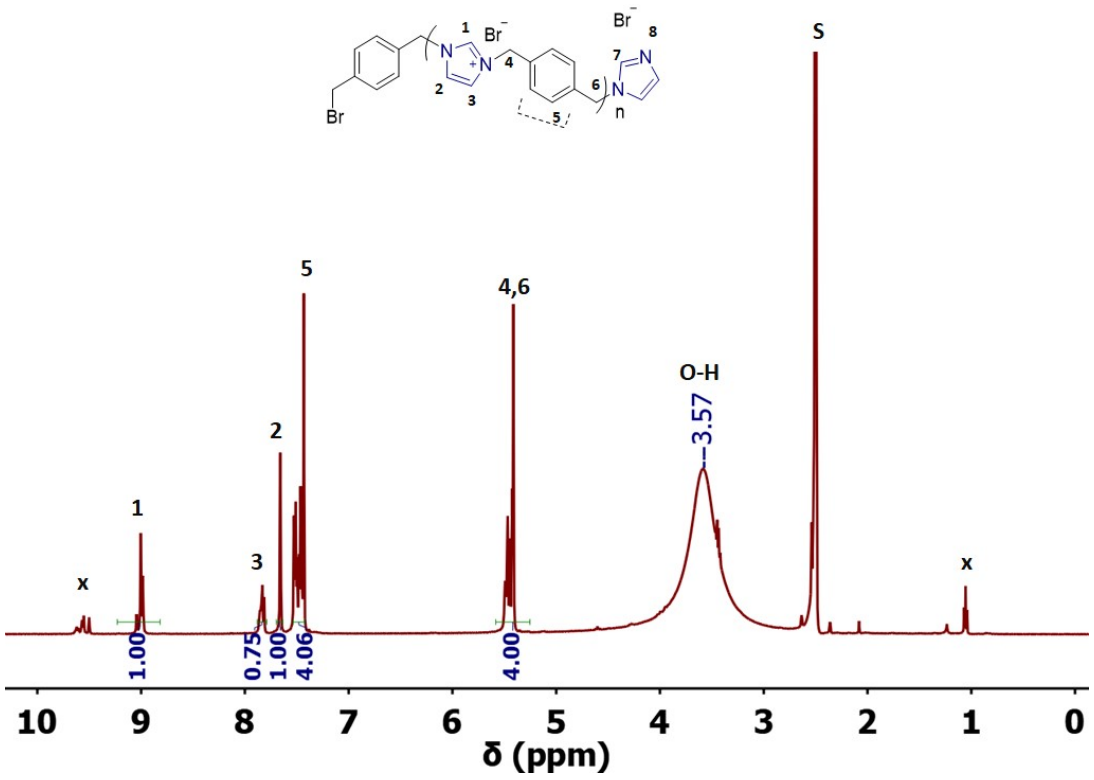

Figure SA 12. ^{1}H NMR spectrum of **4** in DMSO-d_6, **S**: Solvent, **x**: impurities.

1.5. Synthesis of N-(3-(1,3-dioxoisoindolin-2-yl)propyl)-dimethylbenzenaminium bromide (**5**)

In a 100 ml round-bottom flask equipped with a stirring bar, 6.00 g of N-(3-Bromopropyl) phthalimide (0.0224 mol) reacted with 2.8 ml of *N*, *N*-dimethyl aniline (0.0221 mol) without any solvent at 80 °C for 16 h, a yellow precipitate was formed. The reaction workup involved washing with ethyl copious amounts EtAOc to get rid of any starting material (monitored under the ultraviolet lamp) and washing with hexane to yield a white precipitated powder (6.54 g, yield: 75.8%). Melting point (not corrected): 135.1 °C.

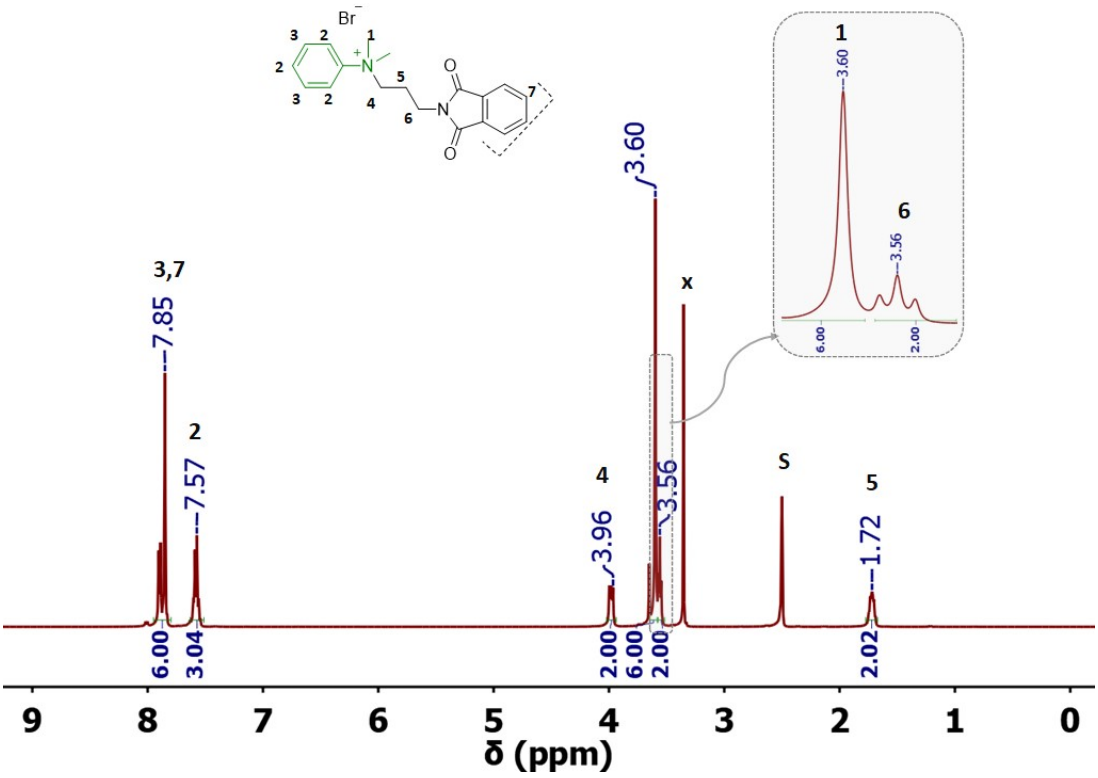

Figure SA 13. ^{1}H NMR spectrum of **5** in DMSO-d_6, **S**: solvent, **x**: H_2O.

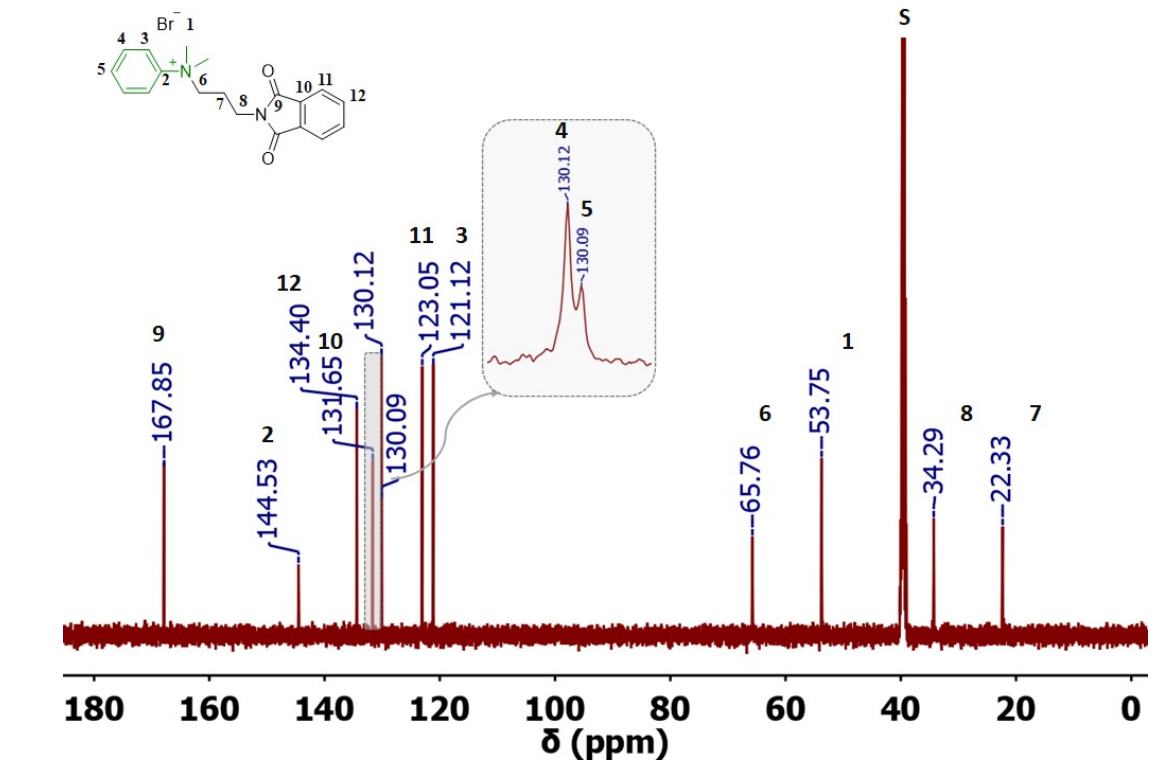

Figure SA 14. ^{13}C NMR spectrum of **5** in DMSO-d_6, **S**: solvent.

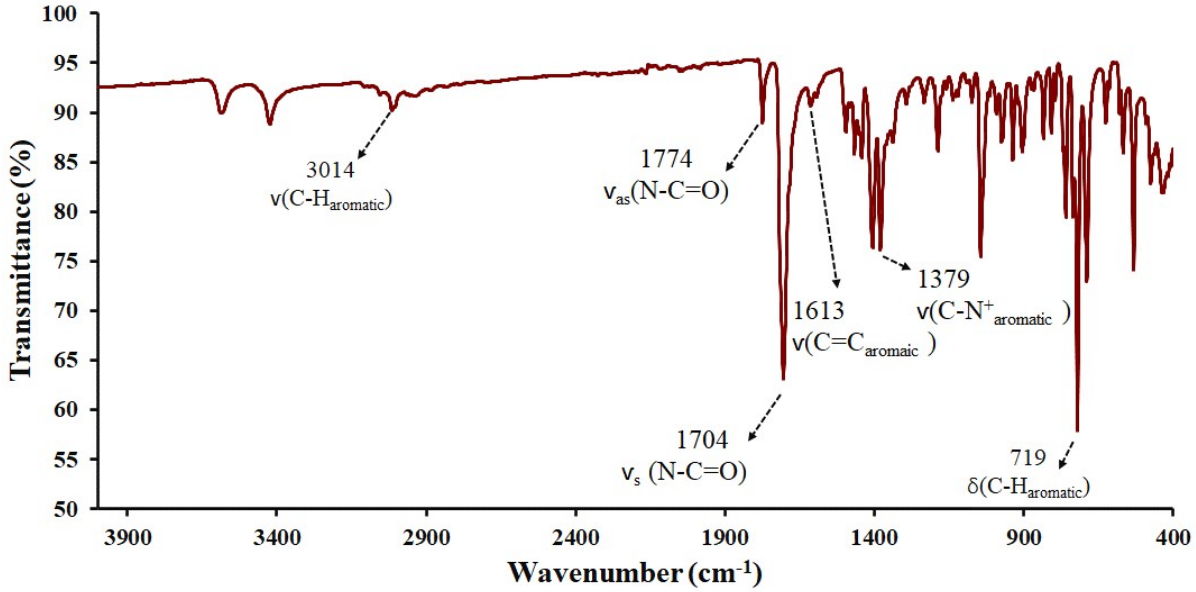

Figure SA 15. ATR-FTIR spectrum of **5**.

1.6. Synthesis of (3-(1,3-dioxoisoindolin-2-yl)propyl)triphenylphosphonium bromide (6)

In a 250 ml round-bottom flask equipped with a stirring bar, 3.13 g of N-(3-Bromopropyl) phthalimide (0.0116 mol) dissolved in 20 ml acetonitrile (ACN) with 3.00 g of triphenylphosphine (0.0114 mol), the reaction mixture refluxed at 80 °C for 5 h, the pale-yellow solution was evaporated resulting in a white precipitate, then was washed with EtAOc to get rid of the starting materials (5.71 g, yield: 94.1%). Melting point: 210 °C (Corrected: 218-221 °C).

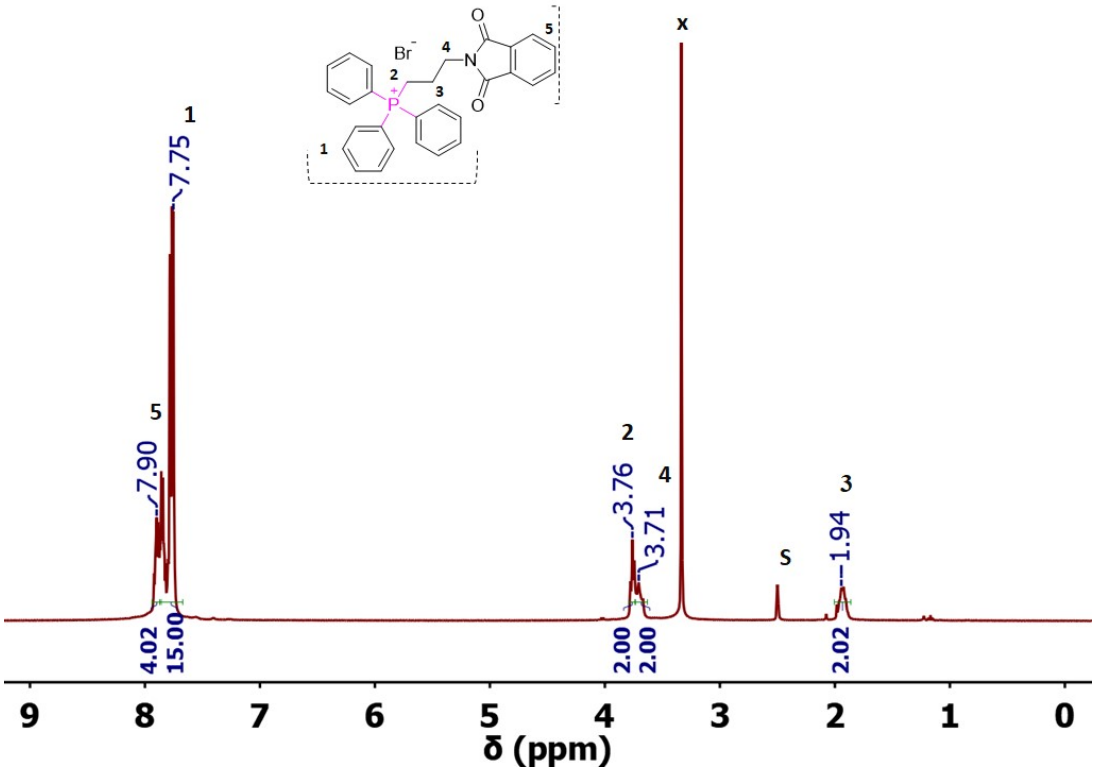

Figure SA 16. ^{1}H NMR spectrum of **6** in DMSO-d_6, **S**: solvent, **x**: H_2O.

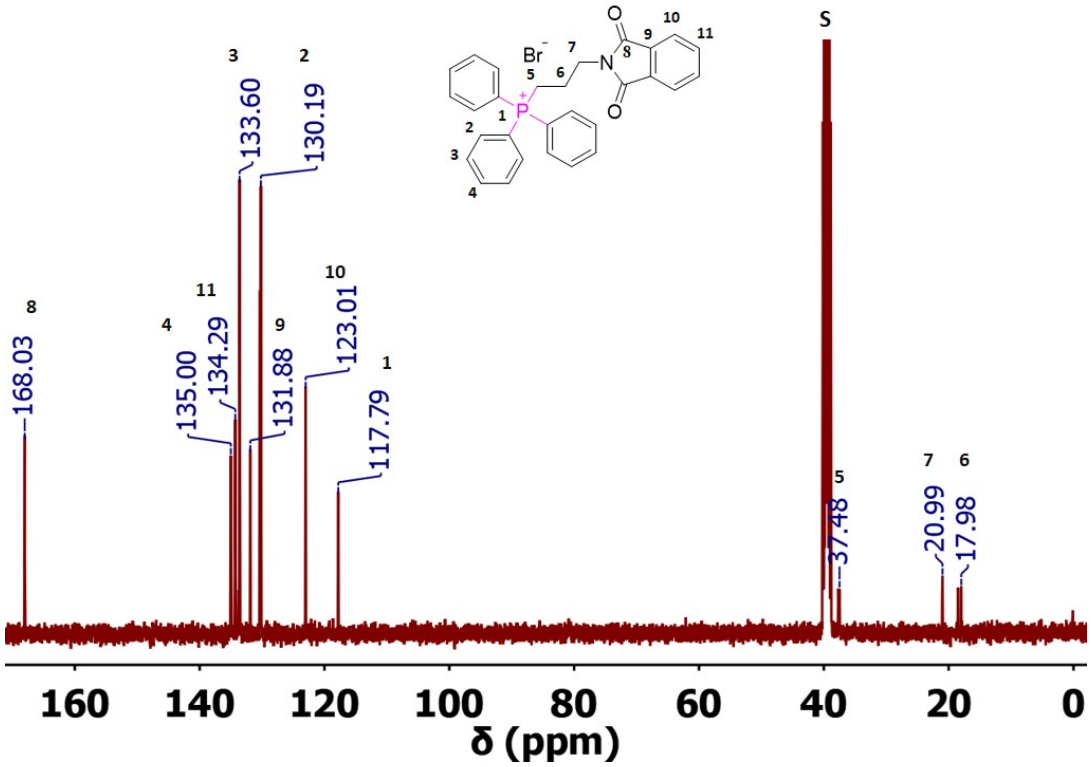

Figure SA 17. ^{13}C NMR spectrum of **6** in DMSO-d_6, **S**: solvent.

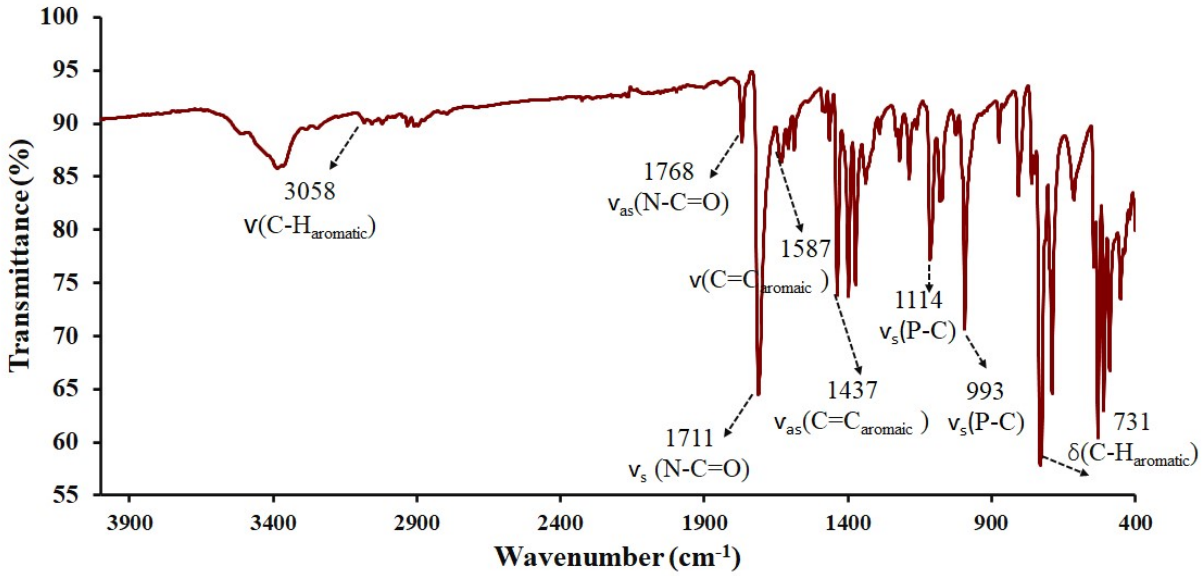

Figure SA 18. ATR-FTIR spectrum of **6**.

1.7. Synthesis of 1-(3-(1,3-dioxoisoindolin-2-yl)propyl) pyridin-1-ium bromide (7)

In a 250 ml round-bottom flask equipped with a stirring bar, 1.00 g of N-(3-Bromopropyl) phthalimide (0.0373 mol) dissolved in 15 ml ACN, after the solution became clear, 0.30 ml of pyridine (0.0372 mol) was added drop wisely to the reaction mixture, then refluxed at 82 °C for 5 h, the white solid was obtained (0.665 g, 51.6 % yield). Melting point (not corrected): 252.3 °C.

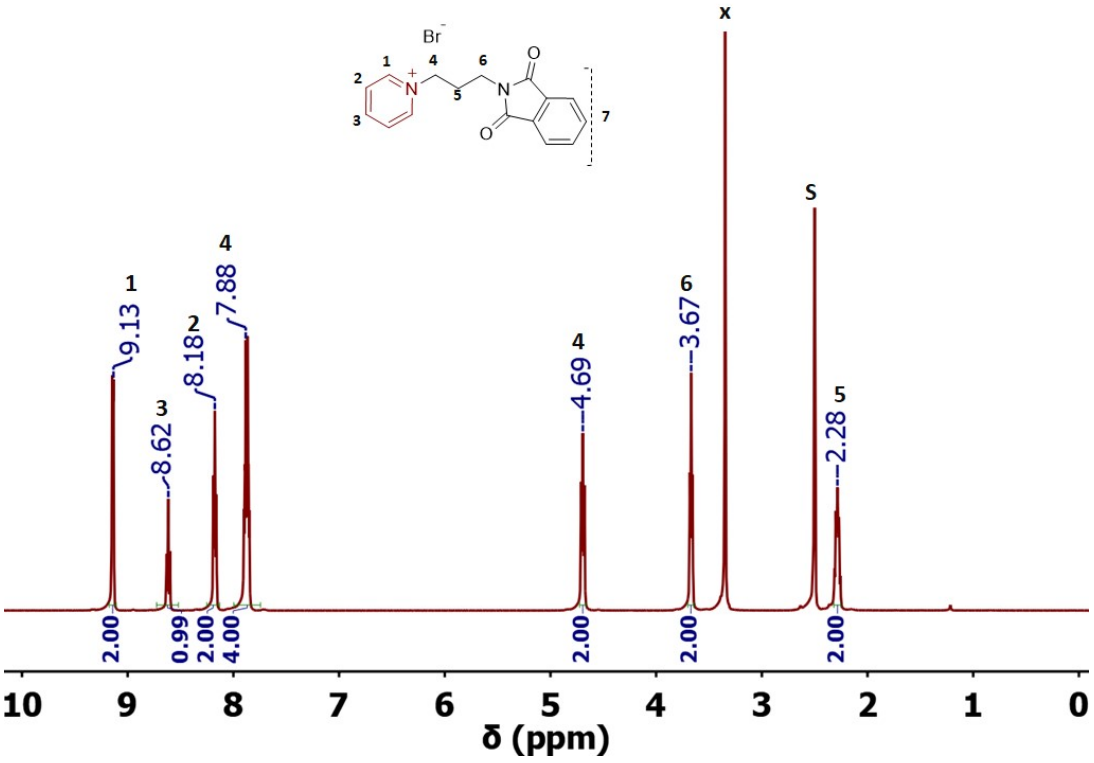

Figure SA 19. ^{1}H NMR spectrum of **7** in DMSO-d_6, **S**: solvent, **x**: H_2O.

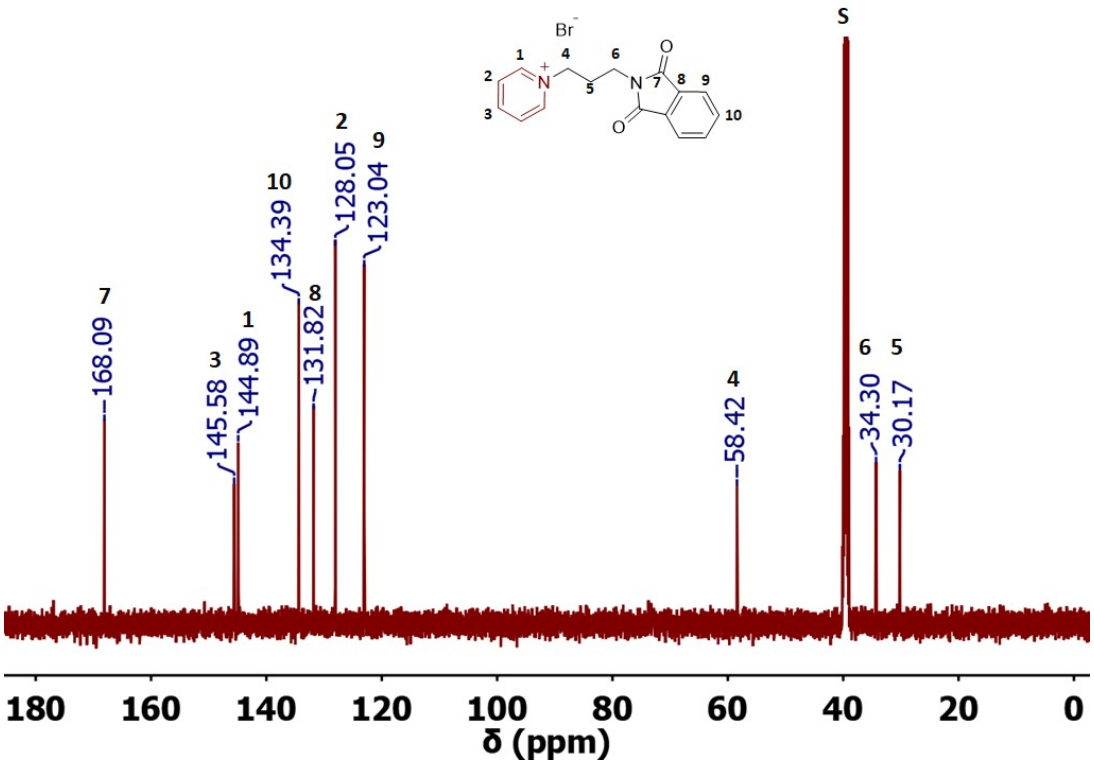

Figure SA 20. ^{13}C spectrum NMR of **7** in DMSO-d_6, **S** solvent.

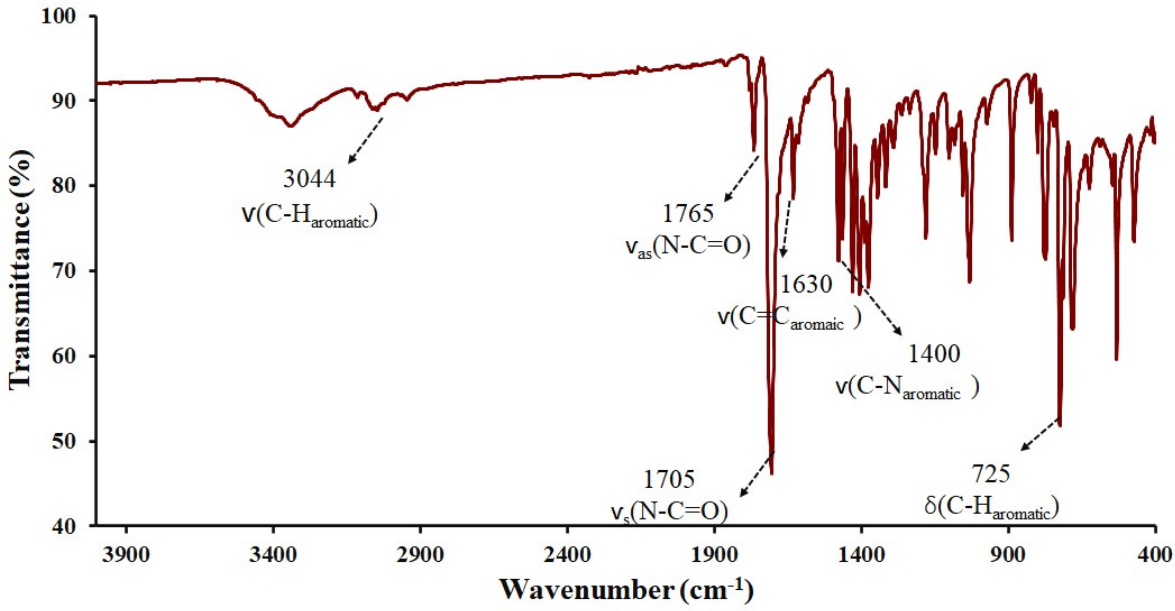

Figure SA 21. ATR-FTIR spectrum of **7**.

1.8. Synthesis of 4-(dimethylamino)-1-(3-(1,3-dioxoisoindoline-2yl)propyl) pyridine -1-ium bromide (**8**)

In a 250 ml round-bottom flask equipped with a stirring bar, 1.19 g of N-(3-Bromopropyl) phthalimide (0.0438 mol) dissolved in 20 ml of EtOAc with 0.501 g of 4-(dimethylamino) pyridine (0.0411 mol), the reaction mixture refluxed in an oil bath at 80 °C for 4 h, the white precipitate washed EtOAc to get rid of ant starting materials, then was with Et_2O (0.886 g, yield: 81%). Melting point (not corrected): 230.3 °C.

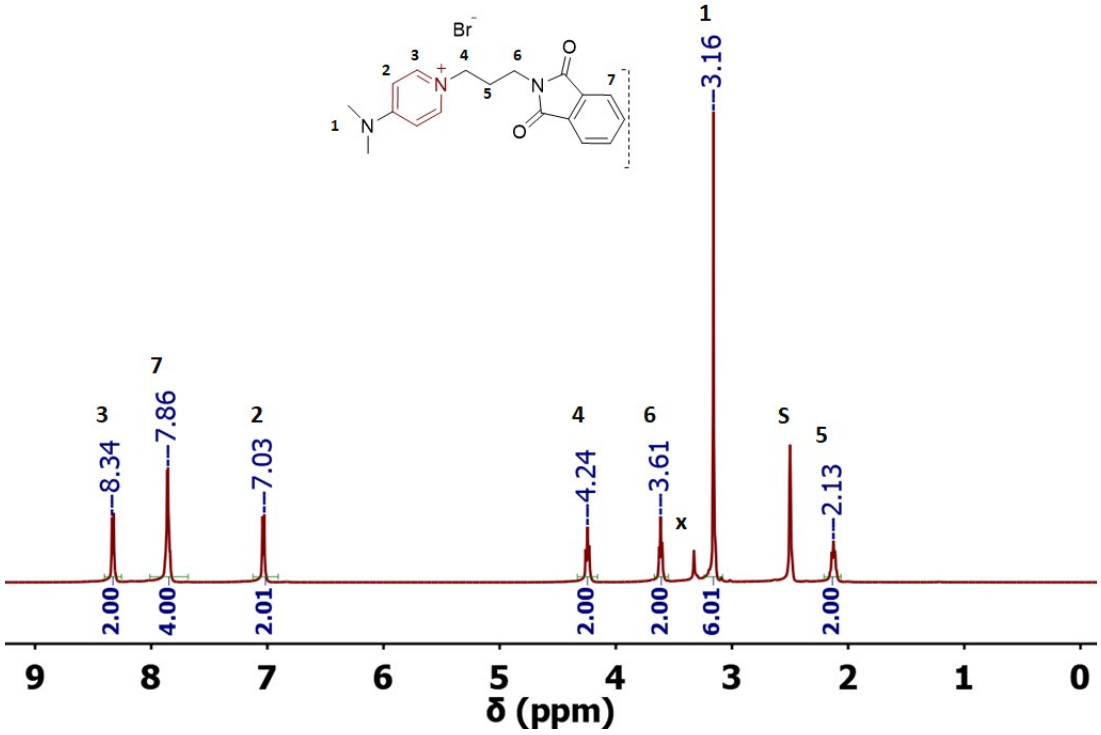

Figure SA 22. ^{1}H NMR spectrum of **8**in DMSO-d_6, **S**: solvent, **x**: H_2O.

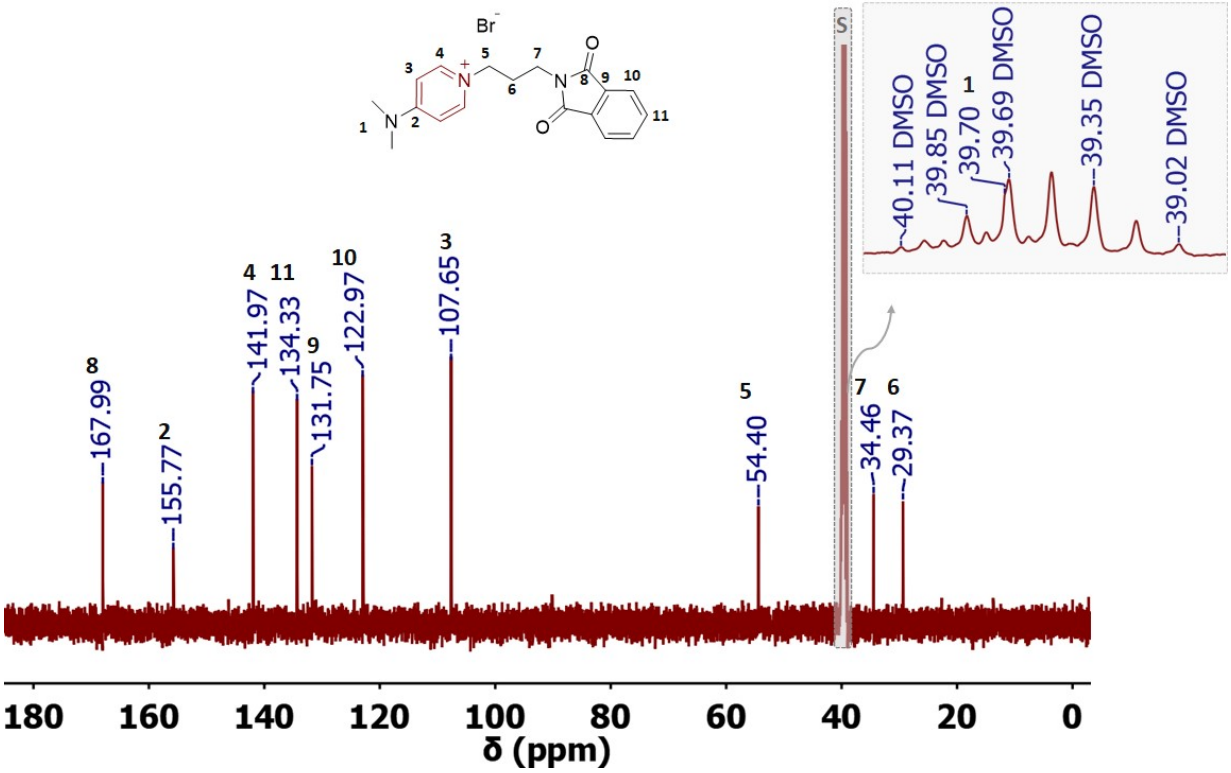

Figure SA 23. ^{13}C spectrum NMR of **8** in DMSO-d_6, **S**: solvent.

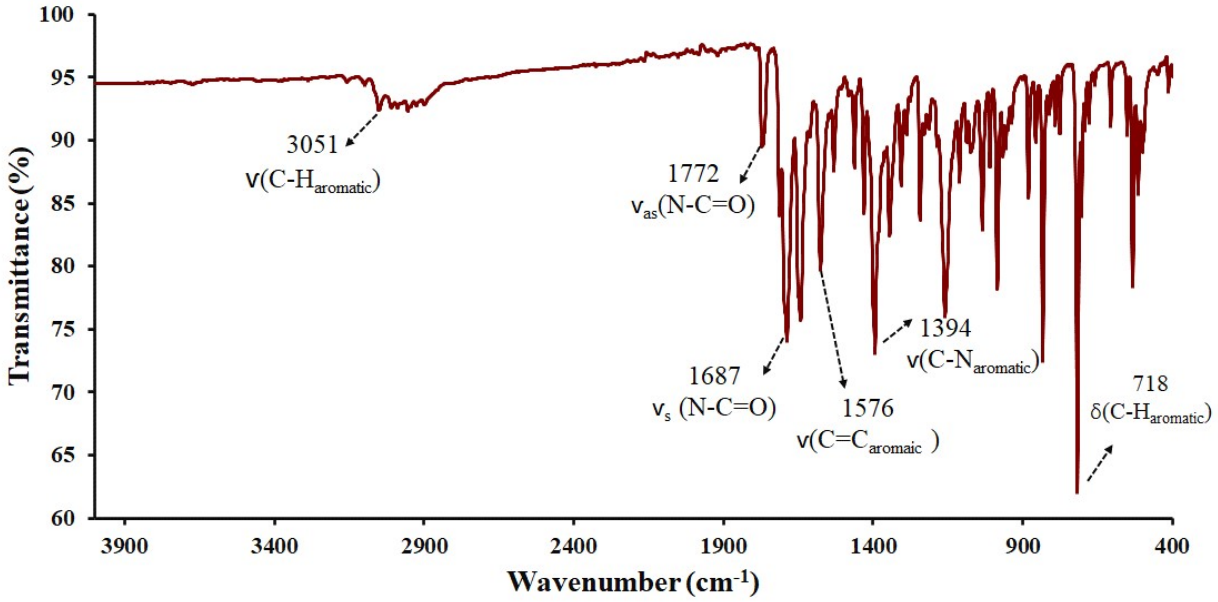

Figure SA 24. ATR-FTIR spectrum of **8**.

2. Thermal properties (TGA) traces

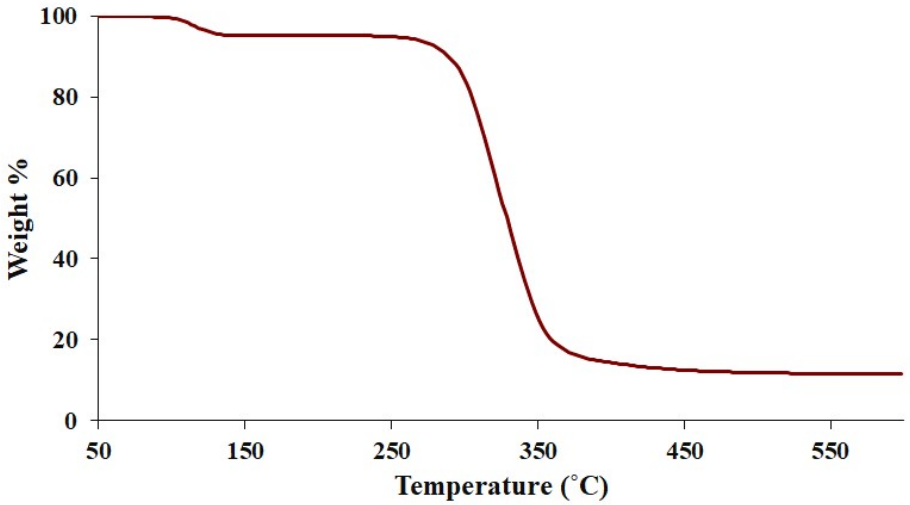

Figure SB 1. TGA traces of **1**. No weight loss up to 288 °C, the decomposition temperature at 50% weight loss ($\mathbf{T}_{d50}$) took place at 328 °C.

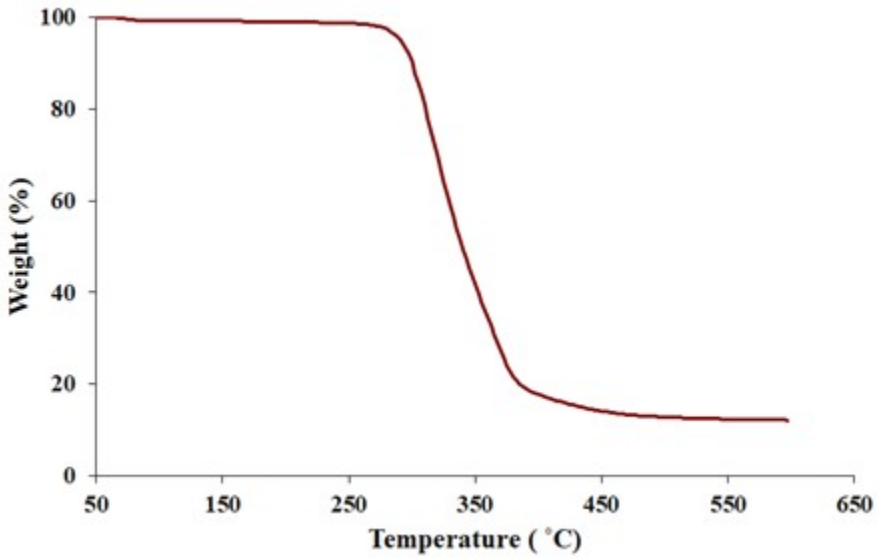

Figure SB 2. TGA traces of **2**. No weight loss up to 280 °C, the decomposition temperature at 50% weight loss ($\mathbf{T}_{d50}$) took place at 340 °C.

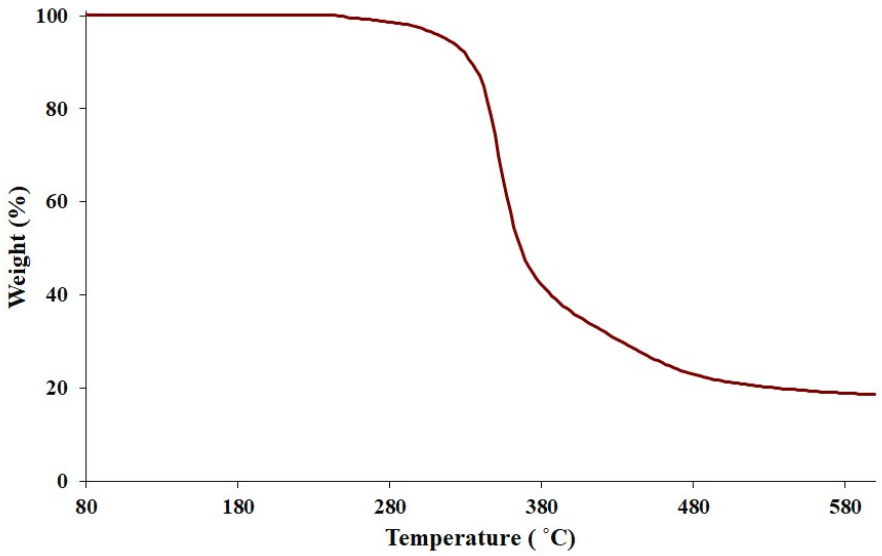

Figure SB 3. TGA traces of **3**. No weight loss up to 300 °C, the decomposition temperature at 50% weight loss ($\mathbf{T}_{d50}$) took place at 360 °C.

Figure SB 4. TGA traces of **4**. No weight loss up to 300 °C, the decomposition temperature at 50% weight loss ($\mathbf{T}_{d50}$) took place at 360 °C.

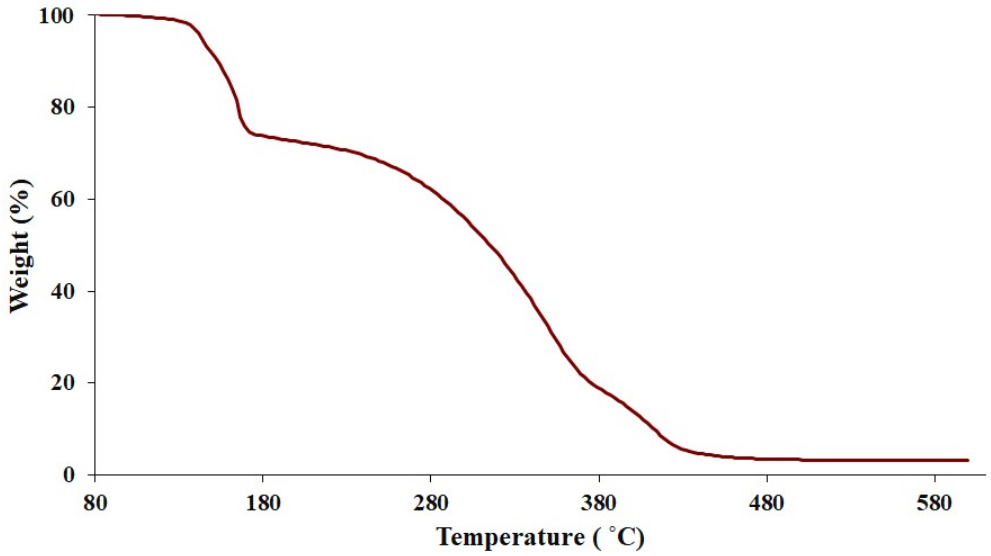

Figure SB 5. TGA traces of **5**. No weight loss up to 100 °C, the decomposition temperature at 75% weight loss took place at 170 °C. (This degradation pattern was observed for other trialkylammonium salts.[9]

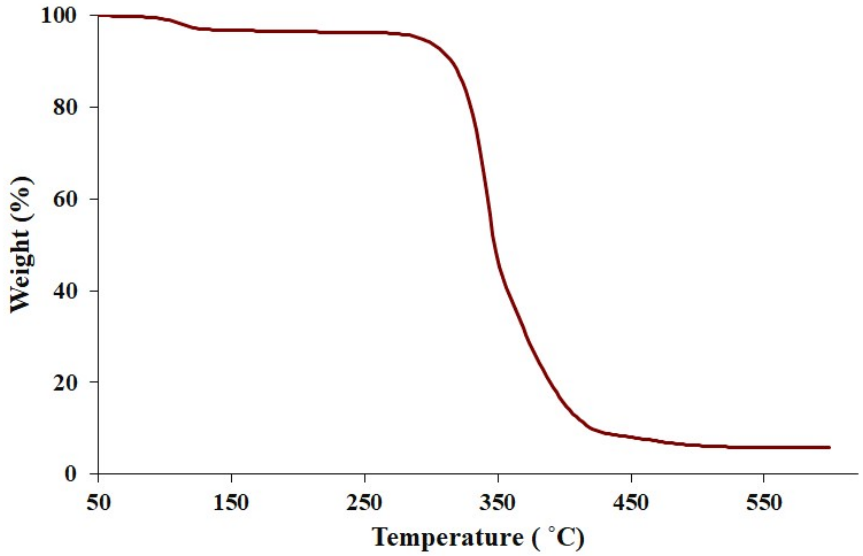

Figure SB 6. TGA traces of **6**. No weight loss up to 300 °C, the decomposition temperature at 50% weight loss (T_{d50}) took place at 345 °C.

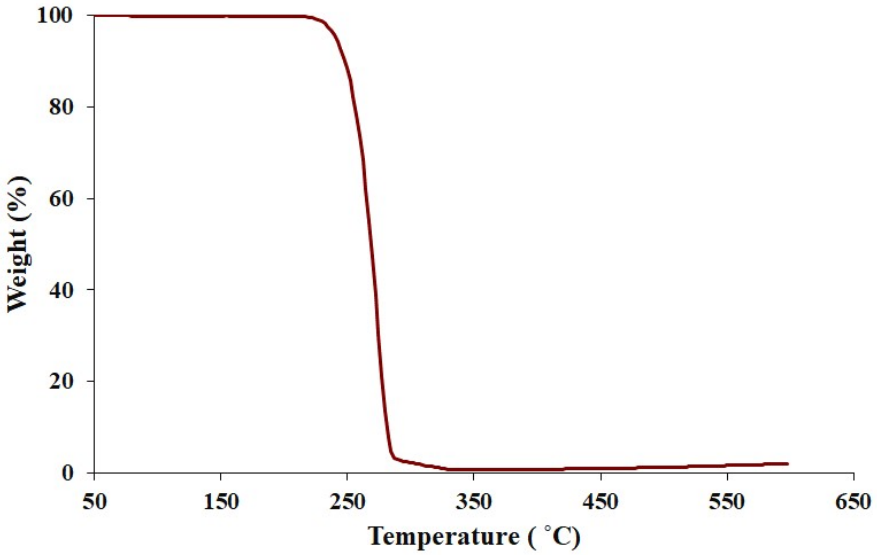

Figure SB 7. TGA traces of **7**. No weight loss up to 230 °C, the decomposition temperature at 50% weight loss ($\mathbf{T}_{d50}$) took place at 370 °C.

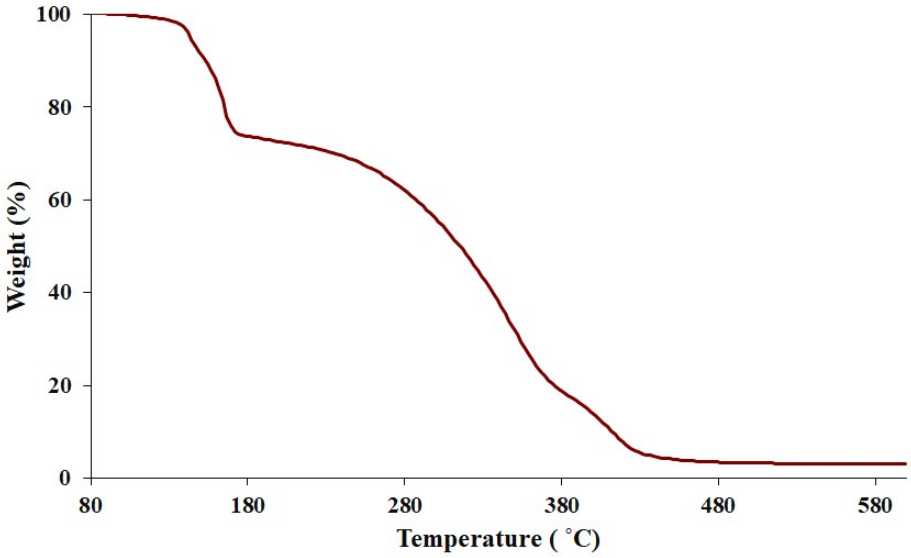

Figure SB 8. TGA trace of **8**. No weight loss up to 140 °C, the decomposition temperature at 50% weight loss ($\mathbf{T}_{d50}$) took place at 314 °C. (This degradation pattern was observed for other trialkylammonium salts. [9]

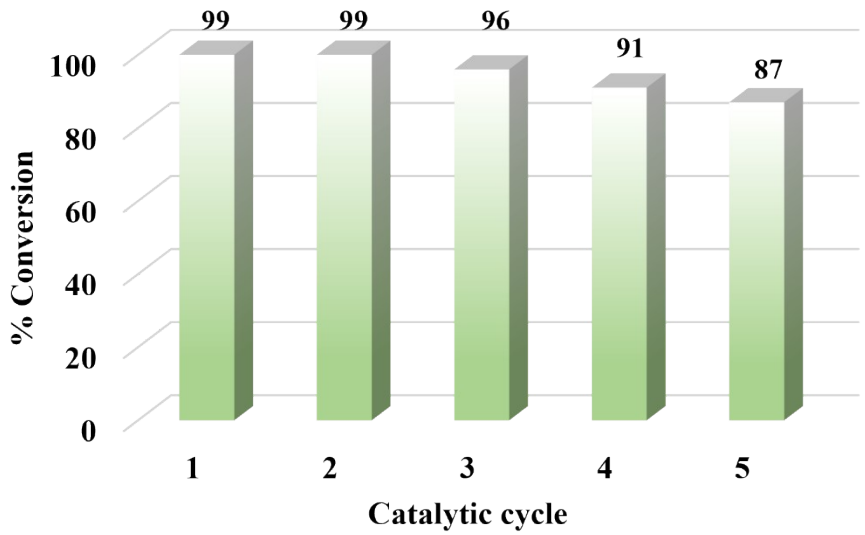

Figure SB 9. Reusability of **4** in the cycloaddition of CO_2 and ECH for five catalytic cycles. The reaction conditions: 6.38 mmol ECH, 0.20 g of **4**, 90 °C, 8 h, and 1 atm of CO_2. The Representative ^{1}H NMR spectrum for each entry is shown in the supporting information (**Figure SC 21-25**, **SI**).

3. ^{1}H NMR spectra of cycloaddition reaction

The conversion percent between the ^{1}H NMR spectra and the tables may appear to differ slightly (Approximately 2 percent). The conversion percent in the tables reflect the average of two experiments

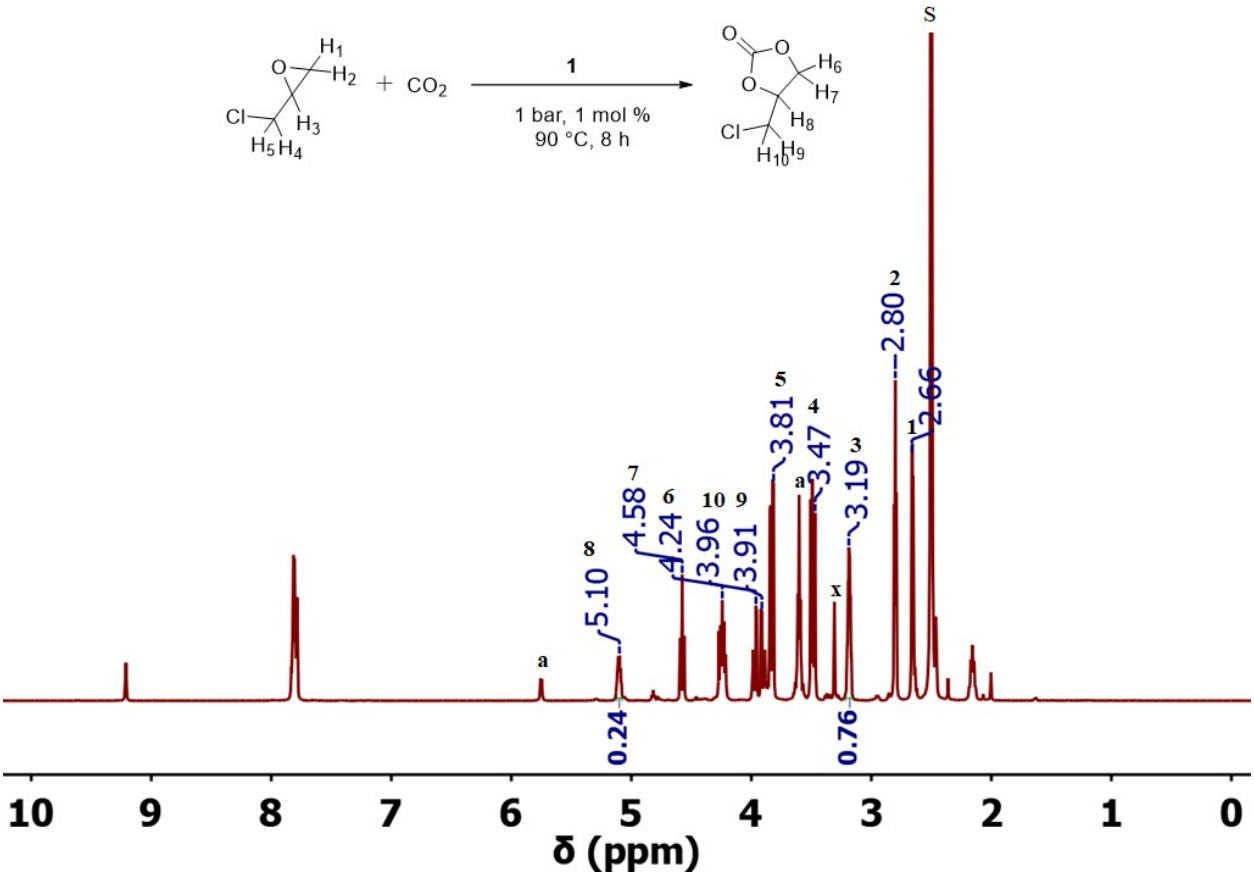

Figure SC 1. ^{1}H NMR spectrum of ECH conversion in DMSO-d_6 using 1 mol % of **1**, **S**: solvent, **x**: H_2O, **a**: 1,2-diol, peaks at 2.15, 7.65,7.73,7.80, and 9.14 ppm are corresponding to the catalyst (**Figure 2A**).

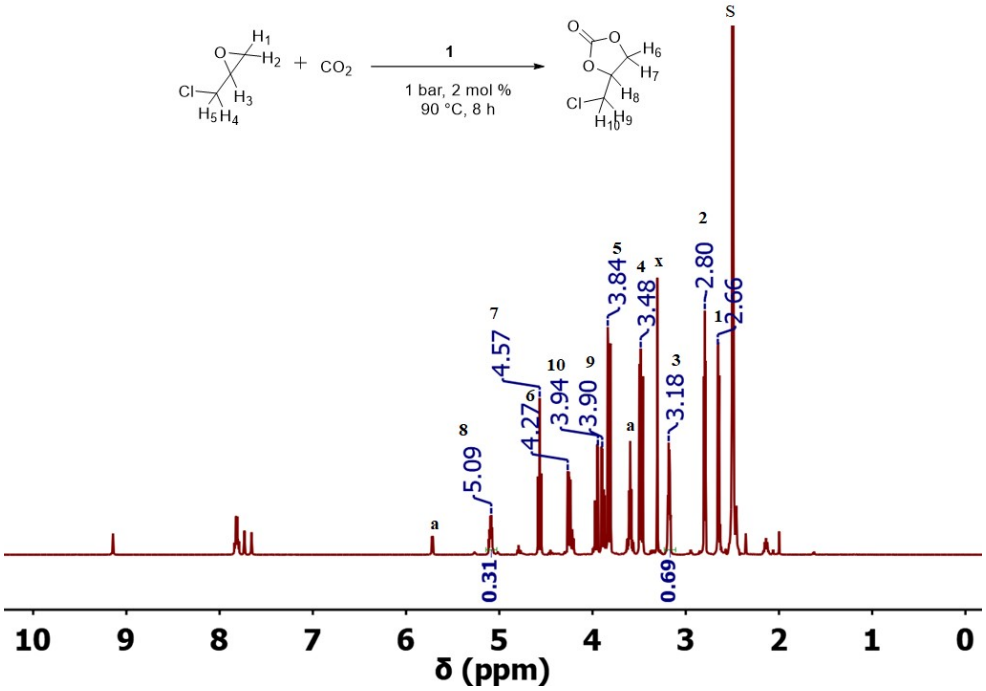

Figure SC 2. ^{1}H NMR spectrum of ECH conversion in DMSO-d_6 using 2 mol % of **1**, **S**: solvent, **x**: H_2O, **a**: 1,2-diol, peaks at 2.15, 7.65,7.73,7.80, and 9.14 ppm are corresponding to the catalyst (**Figure 2A**).

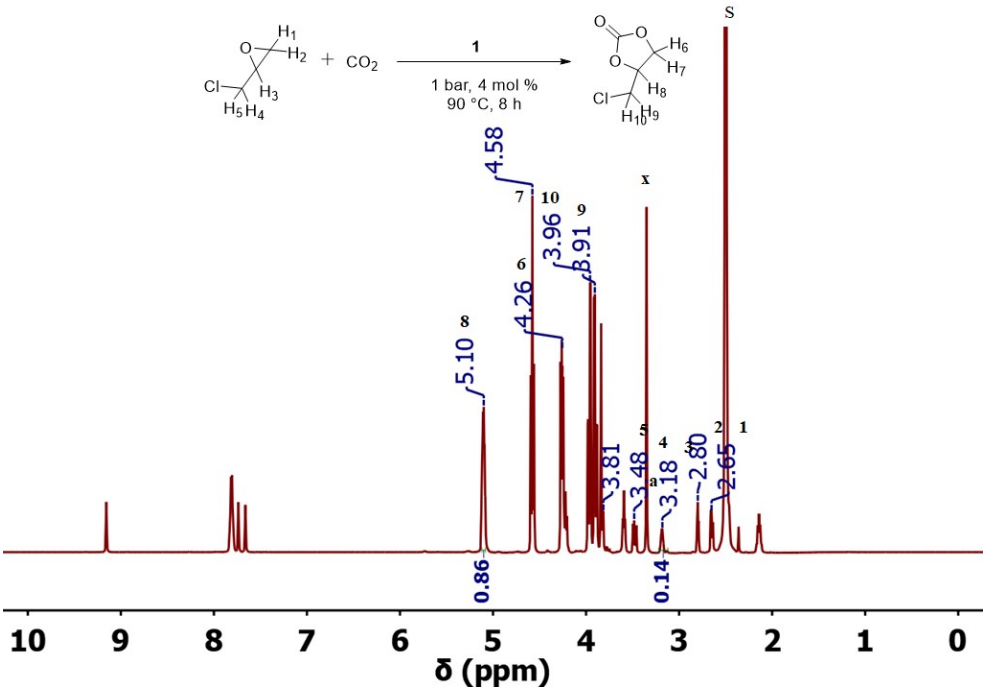

Figure SC 3. ^{1}H NMR spectrum of ECH conversion in DMSO-d_6 using 4 mol % of **1**, **S**: solvent, **x**: H_2O, **a**: 1,2-diol, peaks at 2.15, 7.65,7.73,7.80, and 9.14 ppm are corresponding to the catalyst (**Figure 2A**).

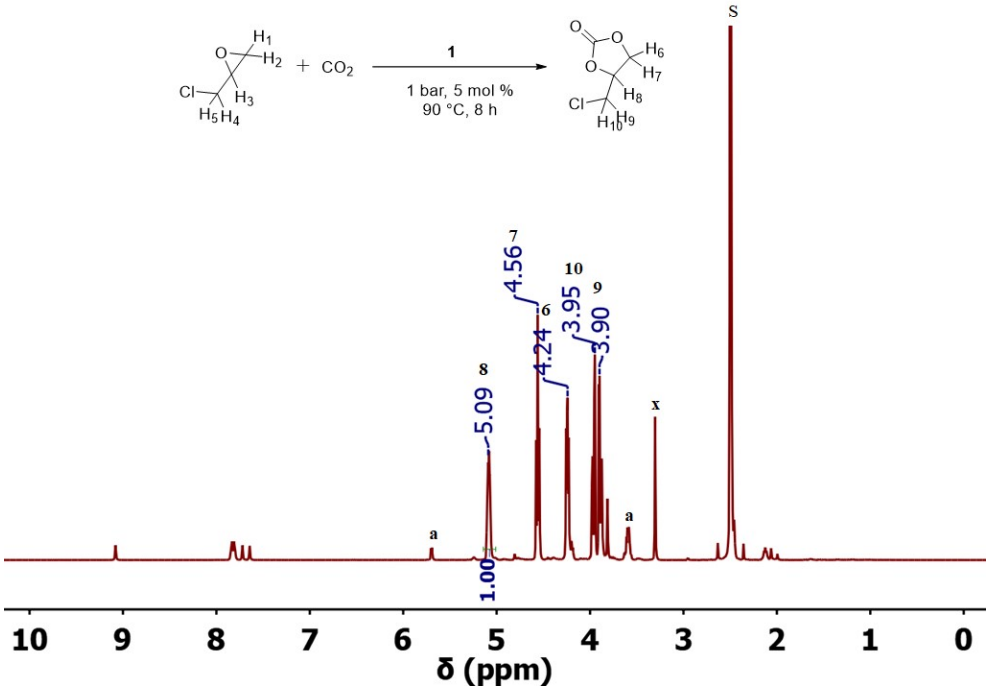

Figure SC 4. [1]H NMR spectrum of ECH conversion in DMSO-d_6 using 5 mol % of **1**, **S**: solvent, **x**: H_2O, **a**: 1,2-diol, peaks at 2.15, 7.65,7.73,7.80, and 9.14 ppm are corresponding to the catalyst (**Figure 2A**).

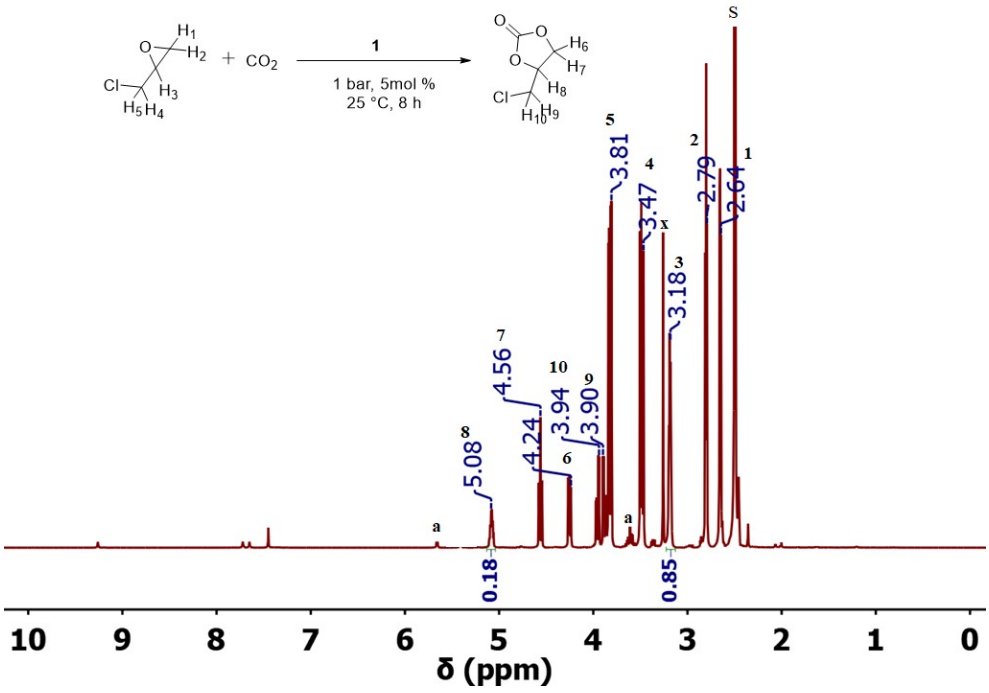

Figure SC 5. [1]H NMR spectrum of ECH conversion in DMSO-d_6 using **1** at 25 °C, **S**: solvent, **x**: H_2O, **a**: 1,2-diol, peaks at 2.15, 7.65,7.73,7.80, and 9.14 ppm are corresponding to the catalyst (**Figure 2B**).

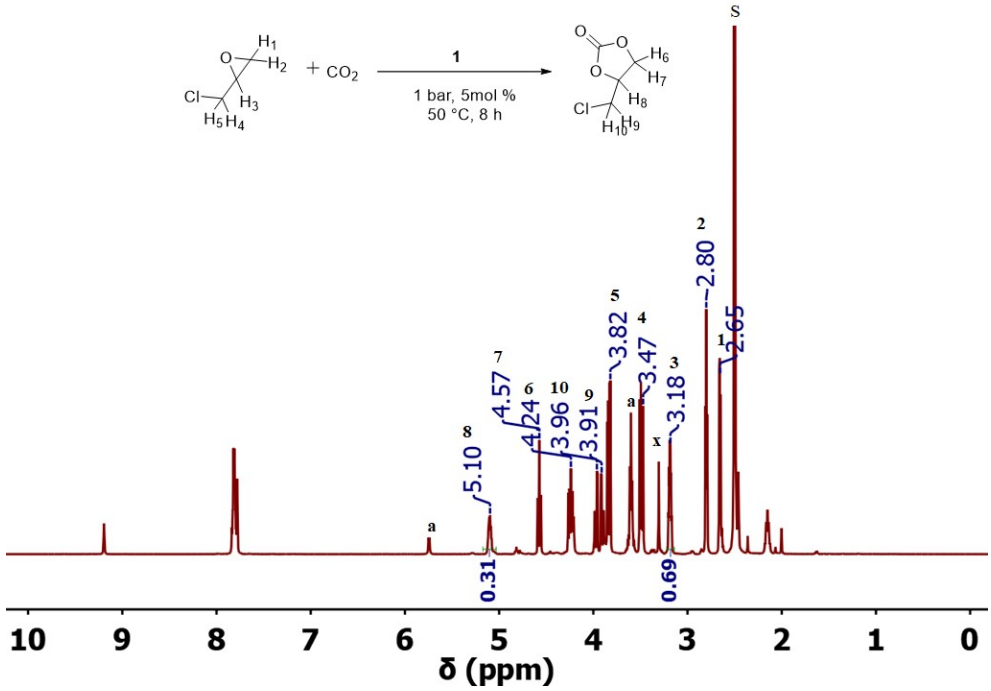

Figure SC 6. ^{1}H NMR spectrum of ECH conversion in DMSO-d_6 using **1** at 50 °C, **S**: solvent, **x**: H_2O, **a**: 1,2-diol, peaks at 2.15, 7.65,7.73,7.80, and 9.14 ppm are corresponding to the catalyst (**Figure 2B**).

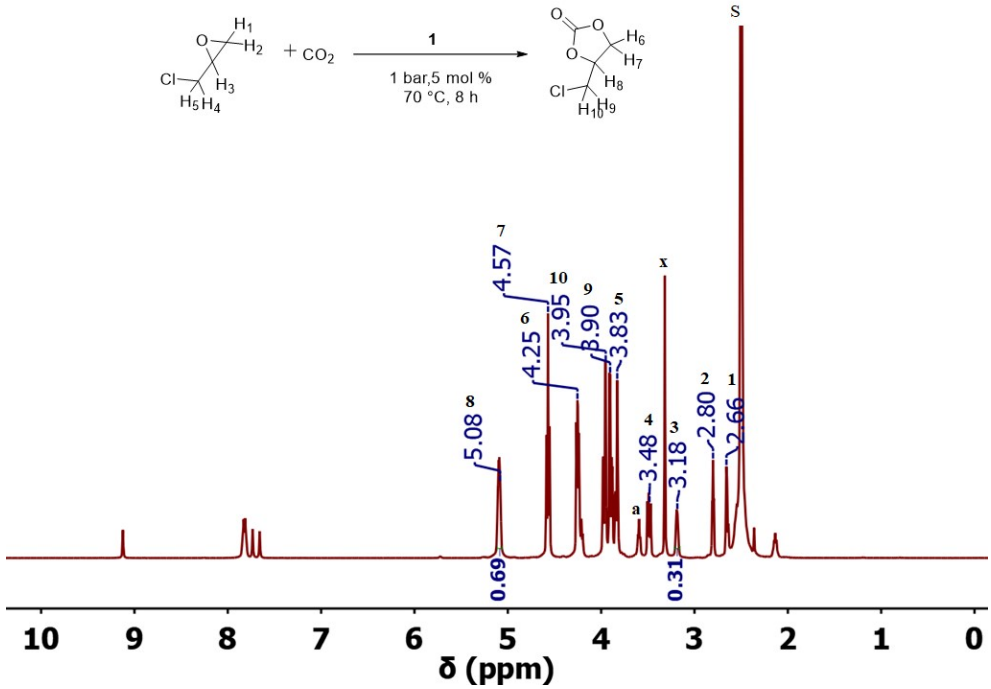

Figure SC 7. ^{1}H NMR spectrum of ECH conversion in DMSO-d_6 using **1** at 70 °C, **S**: solvent, **x**: H_2O, **a**: 1,2-diol, peaks at 2.15, 7.65,7.73,7.80, and 9.14 ppm are corresponding to the catalyst (**Figure 2B**).

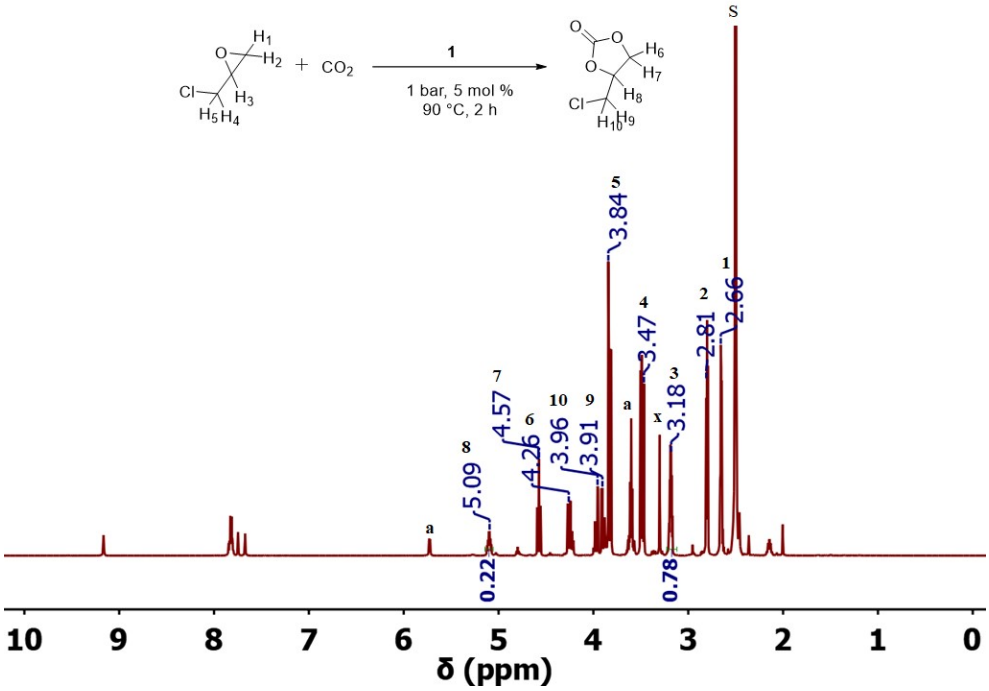

Figure SC 8. [1]H NMR spectrum of ECH conversion in DMSO-d_6 using **1** for 2 h, **S**: solvent, **x**: H_2O, **a**: 1,2-diol, peaks at 2.15, 7.65,7.73,7.80, and 9.14 ppm are corresponding to the catalyst (**Figure 2C**).

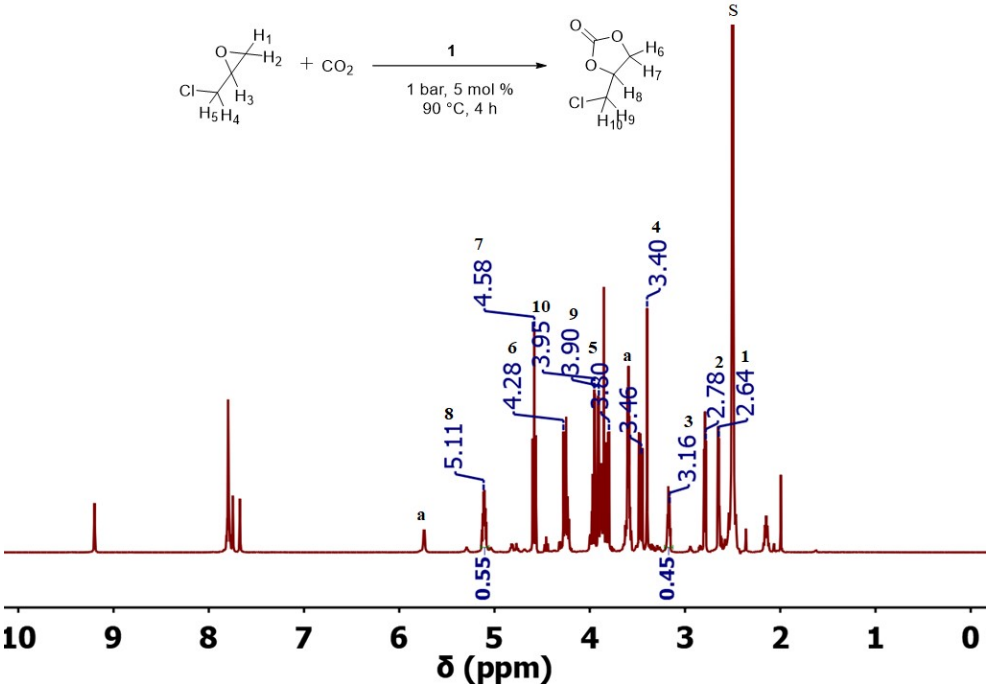

Figure SC 9. [1]H NMR spectrum of ECH conversion in DMSO-d_6 using **1** for 4 h, **S**: solvent, **x**: H_2O, **a**: 1,2-diol, peaks at 2.15, 7.65,7.73,7.80, and 9.14 ppm are corresponding to the catalyst (**Figure 2C**).

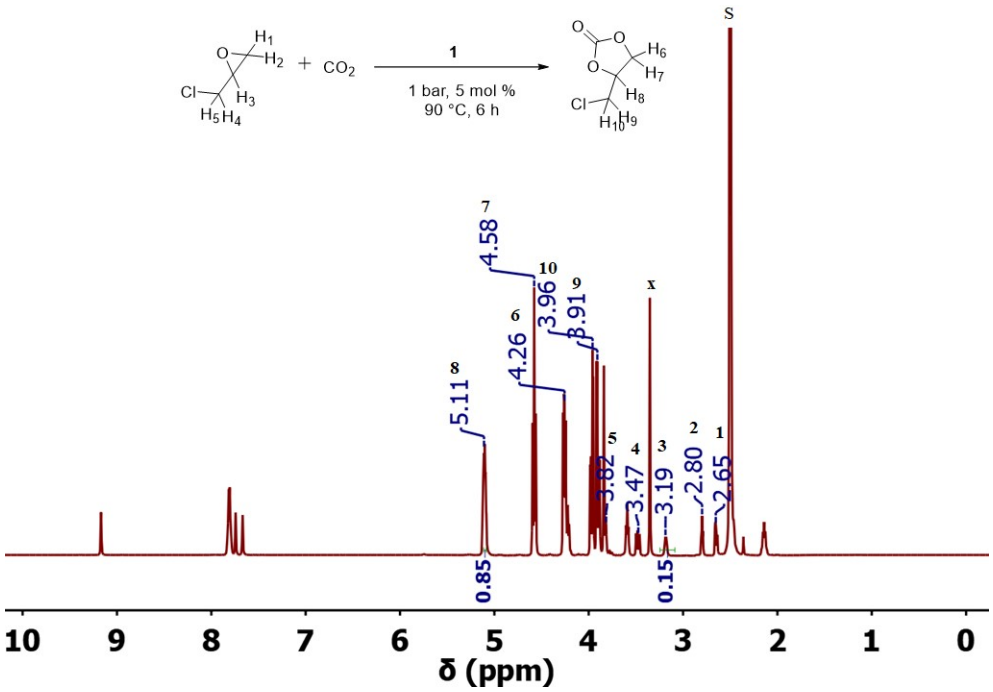

Figure SC 10. ^{1}H NMR spectrum of ECH conversion in DMSO-d_6 using **1** for 6 h, **S**: solvent, **x**: H_2O, **a**: 1,2-diol, peaks at 2.15, 7.65,7.73,7.80, and 9.14 ppm are corresponding to the catalyst (**Figure 2C**).

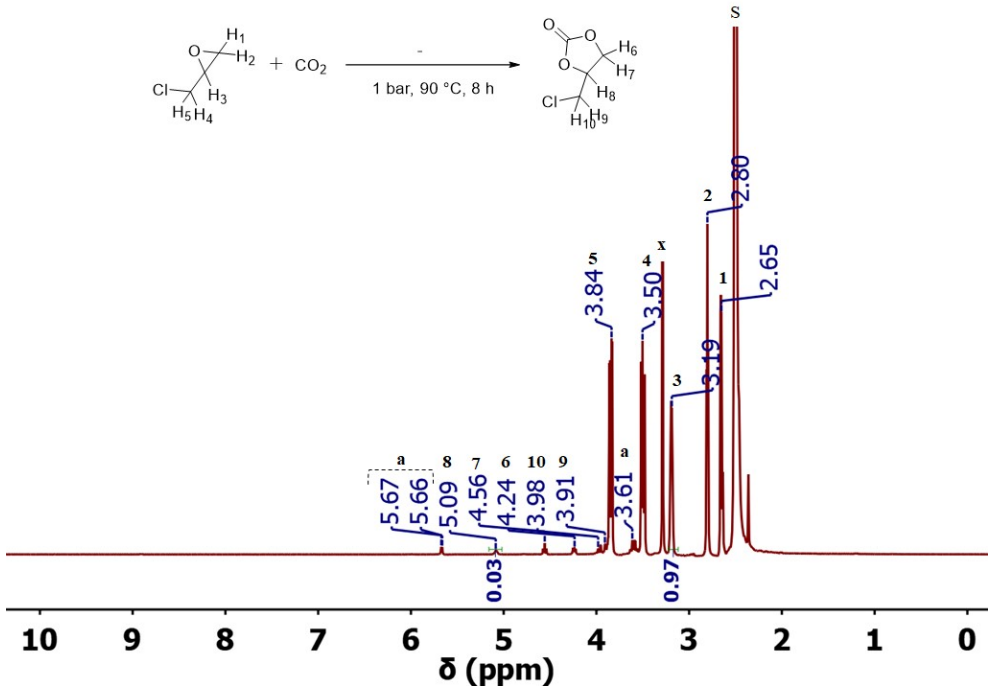

Figure SC 11. ^{1}H NMR spectrum of ECH conversion in DMSO-d_6, **S**: solvent, **x**: H_2O, **a**: 1,2-diol (**Table 1**, entry 1).

Figure SC 12. ^{1}H NMR spectrum of ECH conversion in DMSO-d_6 using **1**, **S**: solvent, **x**: H_2O, **a**: 1,2-diol, peaks at 2.15, 7.65,7.73,7.80, and 9.14 ppm are corresponding to the catalyst (**Table 1**, entry 2).

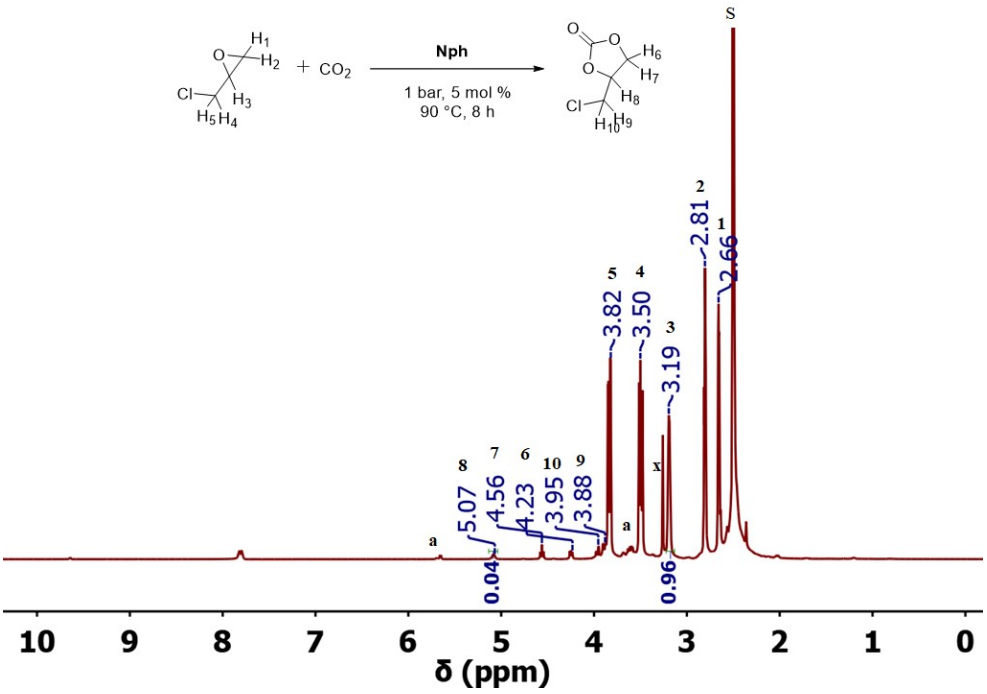

Figure SC 13. ^{1}H NMR spectrum of ECH conversion in DMSO-d_6 using **Nph**, **S**: solvent, **x**: H_2O, **a**: 1,2-diol, peaks at 7.80 ppm are corresponding to the catalyst (**Table 1**, entry 3).

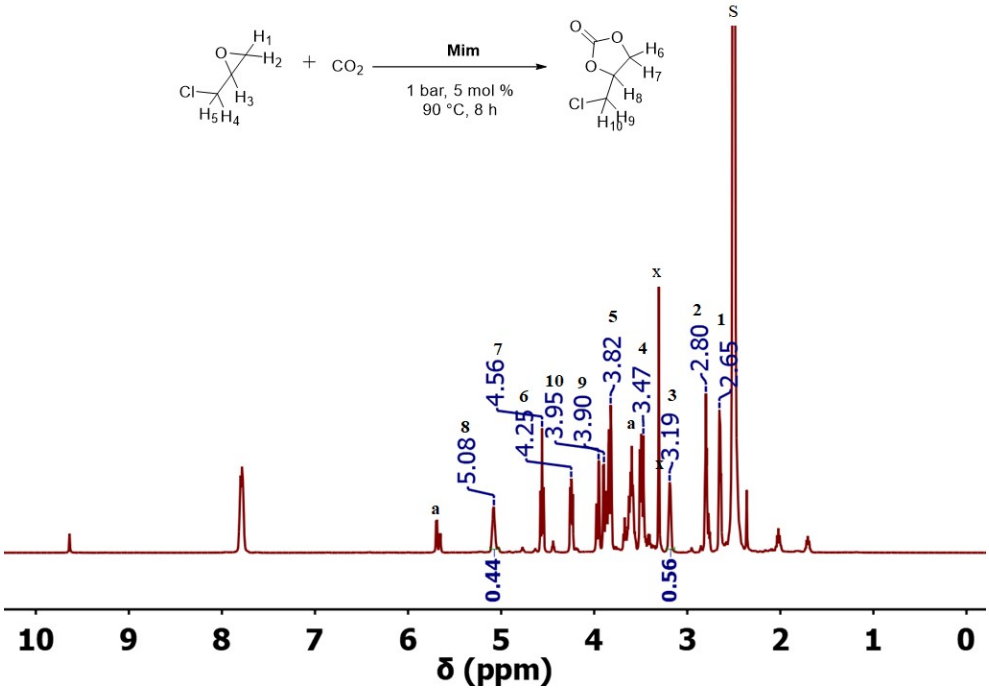

Figure SC 14. ^{1}H NMR spectrum of ECH conversion in DMSO-d_6 using **Mim**, **S**: solvent, **x**: H_2O, **a**: 1,2-diol, peaks at 2.02, 7.78, and 9.64 ppm are corresponding to the catalyst (**Table 1**, entry 4).

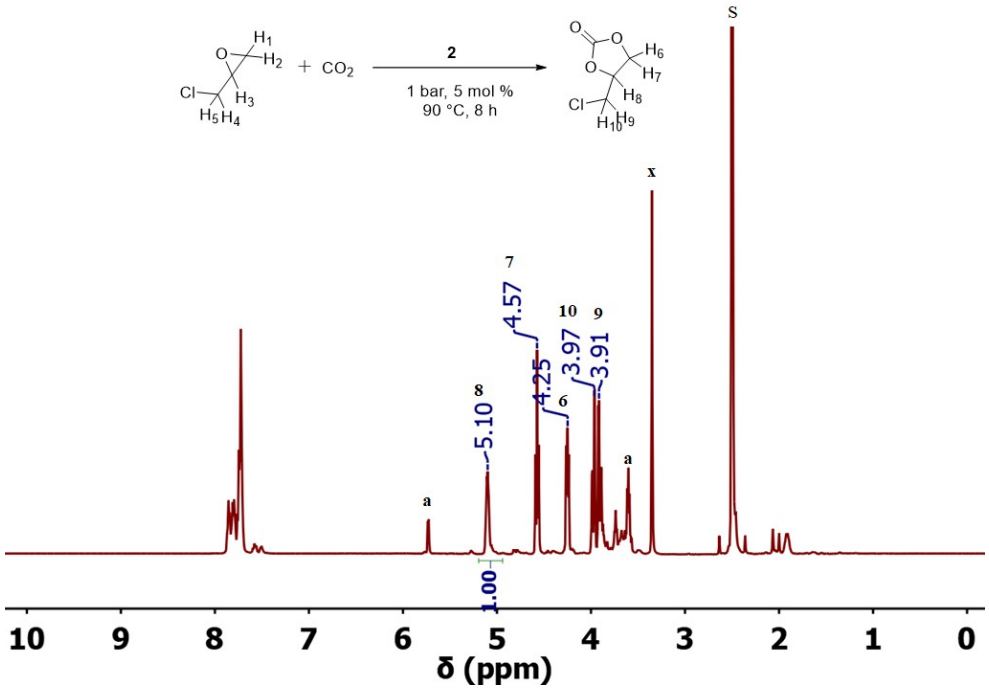

Figure SC 15. ^{1}H NMR spectrum of ECH conversion in DMSO-d_6 using **2**, **S**: solvent, **x**: H_2O, **a**: 1,2-diol, peaks at 2.05, 7.57, 7.63, and 7.82 ppm are corresponding to the catalyst (**Table 1**, entry 5).

Figure SC 16. ^{1}H NMR spectrum of ECH conversion in DMSO-d_6 using **1**, **S**: solvent, **x**: H_2O, **a**: 1,2-diol, peaks at 2.15, 7.65,7.73,7.80, and 9.14 ppm are corresponding to the catalyst (**Table 1**, entry 6).

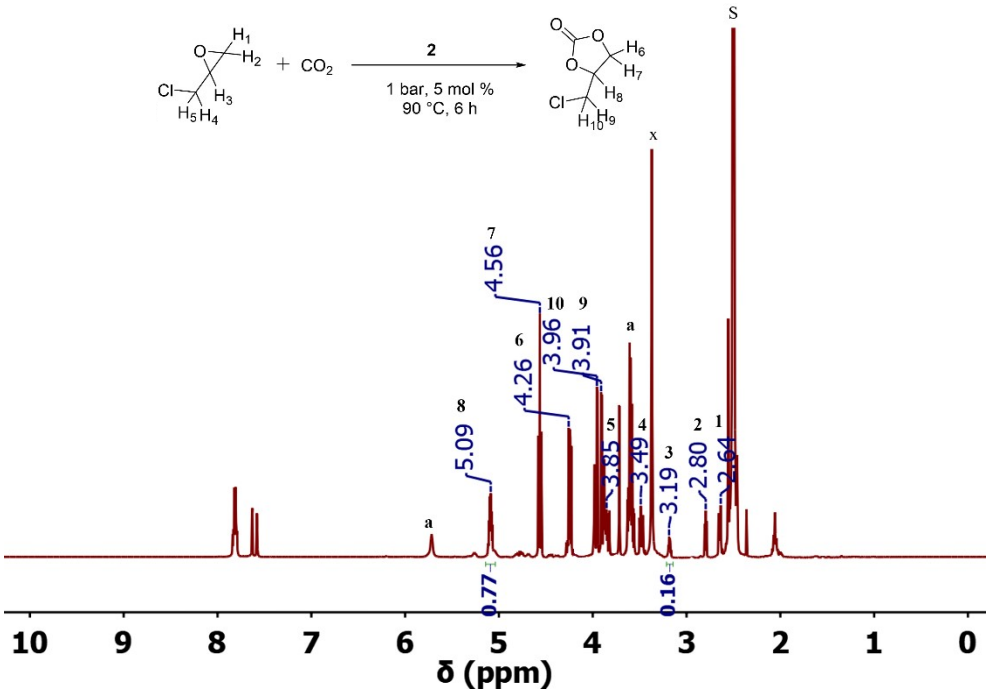

Figure SC 17. ^{1}H NMR spectrum of ECH conversion in DMSO-d_6 using **2**, **S**: solvent, **x**: H_2O, **a**: 1,2-diol, peaks at 2.05, 7.57, 7.63, and 7.82 ppm are corresponding to the catalyst (**Table 1**, entry 7).

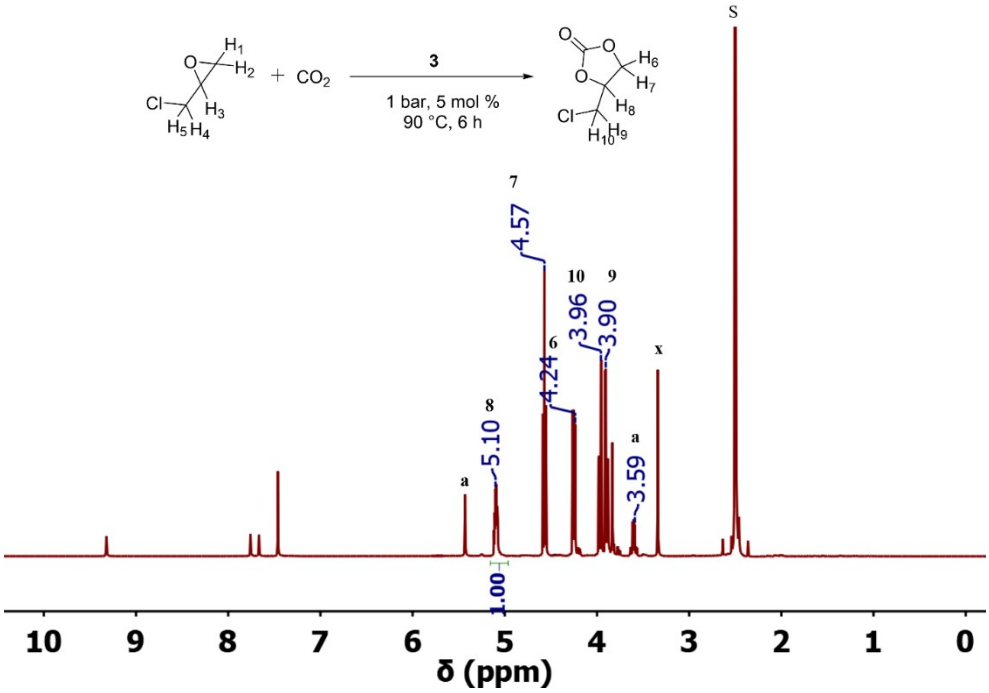

Figure SC 18. ^{1}H NMR spectrum of ECH conversion in DMSO-d_6 using **3**, **S**: solvent, **x**: H_2O, **a**: 1,2-diol, peaks at 7.46, 7.66, 7.75, and 9.32 ppm are corresponding to the catalyst (**Table 1**, entry 8).

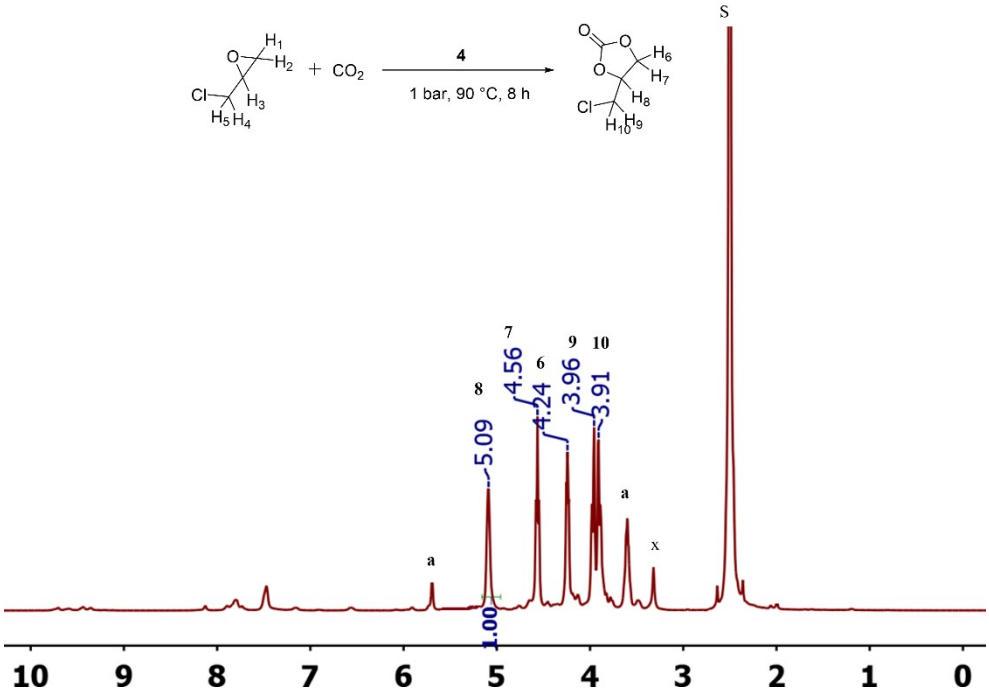

Figure SC 19. ^{1}H NMR spectrum of ECH conversion in DMSO-d_6 using **4**, **S**: solvent, **x**: H_2O, **a**: 1,2-diol, peaks around 7.46 ppm are corresponding to the catalyst (**Table 1**, entry 9).

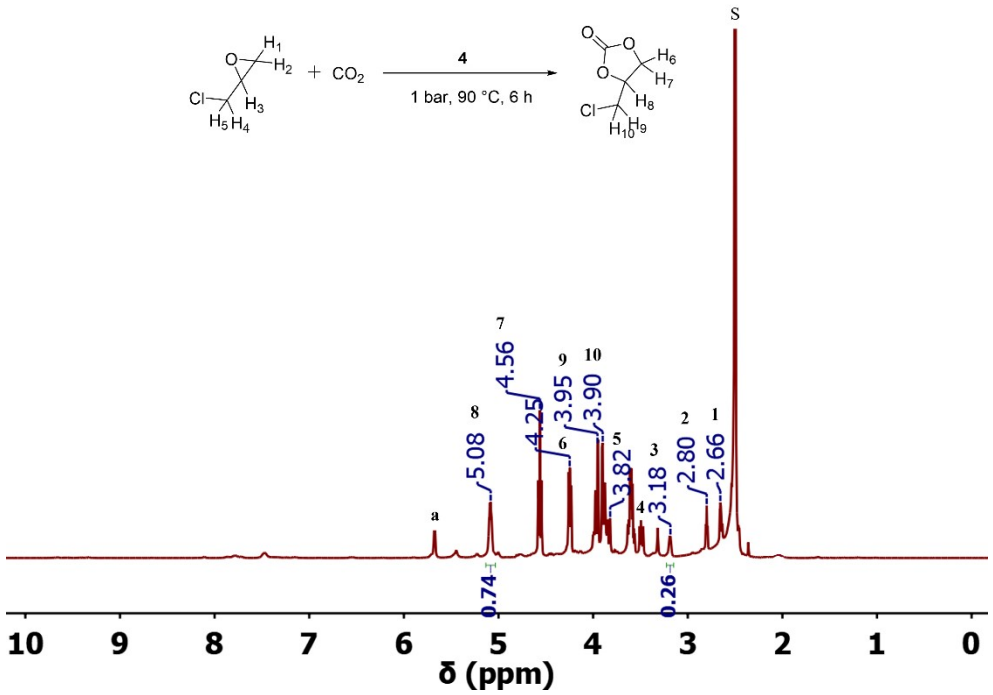

Figure SC 20. ^{1}H NMR spectrum of ECH conversion in DMSO-d_6 using **4**, **S**: solvent, **x**: H_2O, **a**: 1,2-diol, peaks around 7.46 ppm are corresponding to the catalyst (**Table 1**, entry 10).

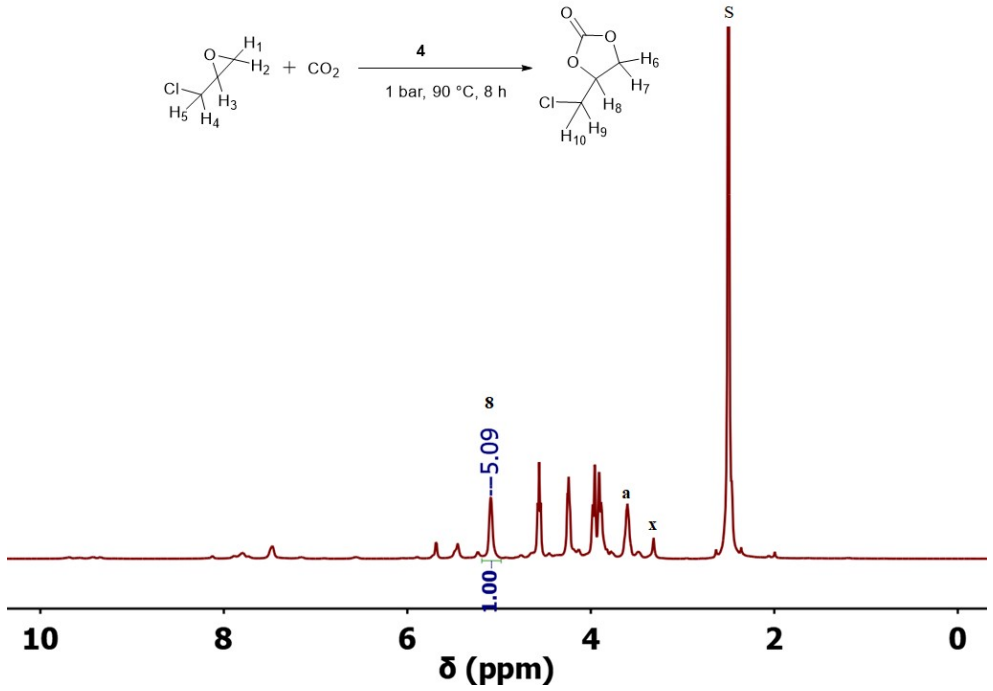

Figure SC 21. ^{1}H NMR spectrum of ECH conversion in DMSO-d_6 using **4**, **S**: solvent, **x**: H_2O, **a**: 1,2-diol, peaks around 7.46 ppm are corresponding to the catalyst (**catalytic cycle 1**).

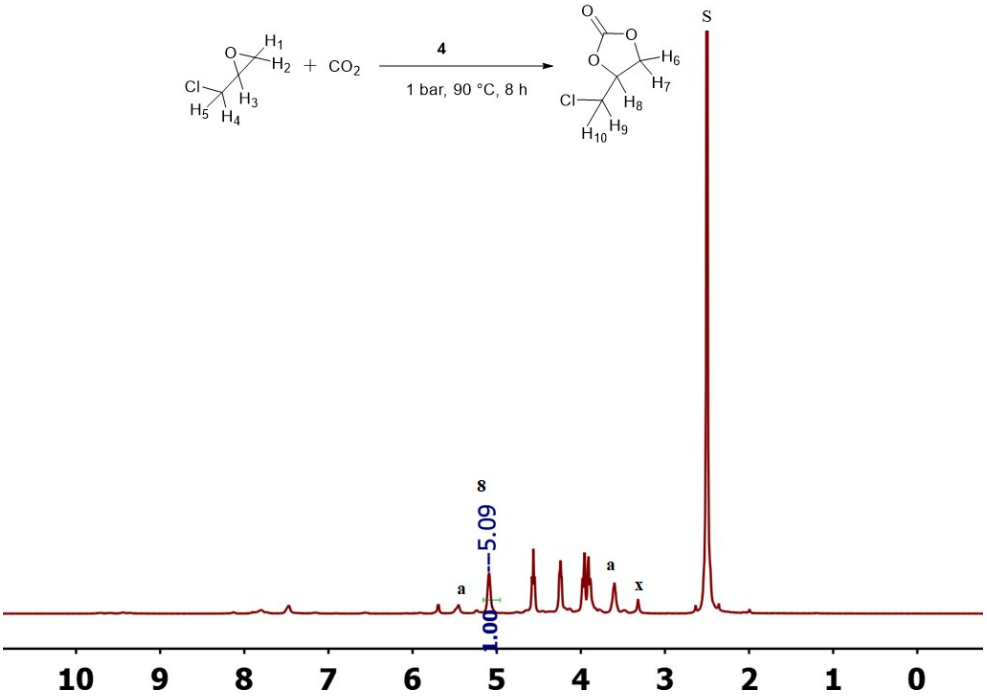

Figure SC 22. ^{1}H NMR spectrum of ECH conversion in DMSO-d_6 using **4**, **S**: solvent, **x**: H_2O, **a**: 1,2-diol, peaks around 7.46 ppm are corresponding to the catalyst (**catalytic cycle 2**).

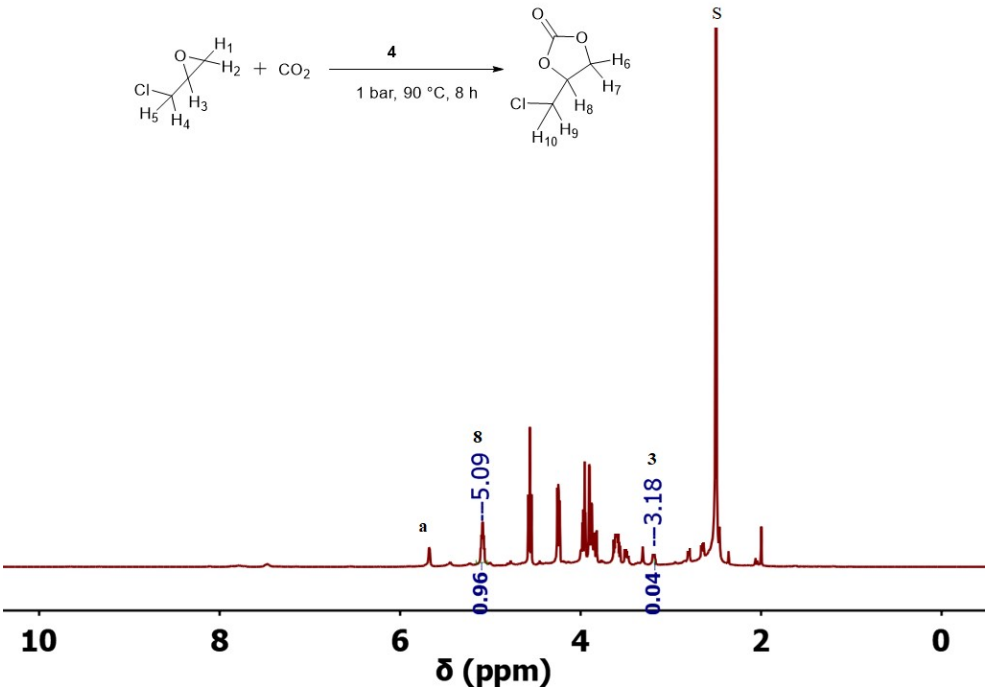

Figure SC 23. ^{1}H NMR spectrum of ECH conversion in DMSO-d_6 using **4**, **S**: solvent, **x**: H_2O, **a**: 1,2-diol, peaks around 7.46 ppm are corresponding to the catalyst (**catalytic cycle 3**).

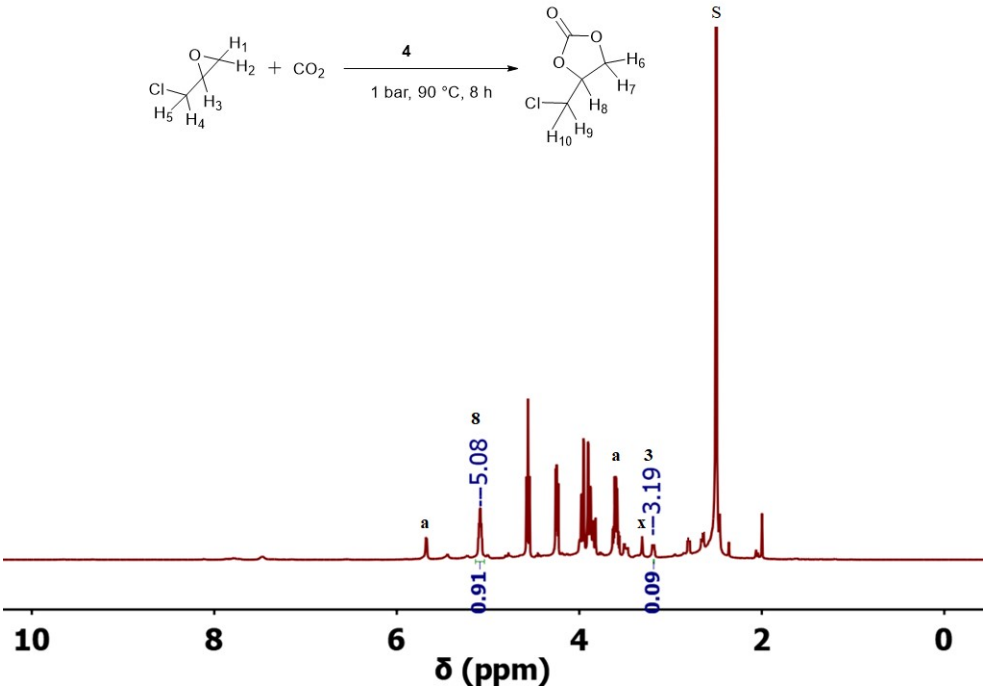

Figure SC 24. ^{1}H NMR spectrum of ECH conversion in DMSO-d_6 using **4**, **S**: solvent, **x**: H_2O, **a**: 1,2-diol, peaks around 7.46 ppm are corresponding to the catalyst (**catalytic cycle 4**).

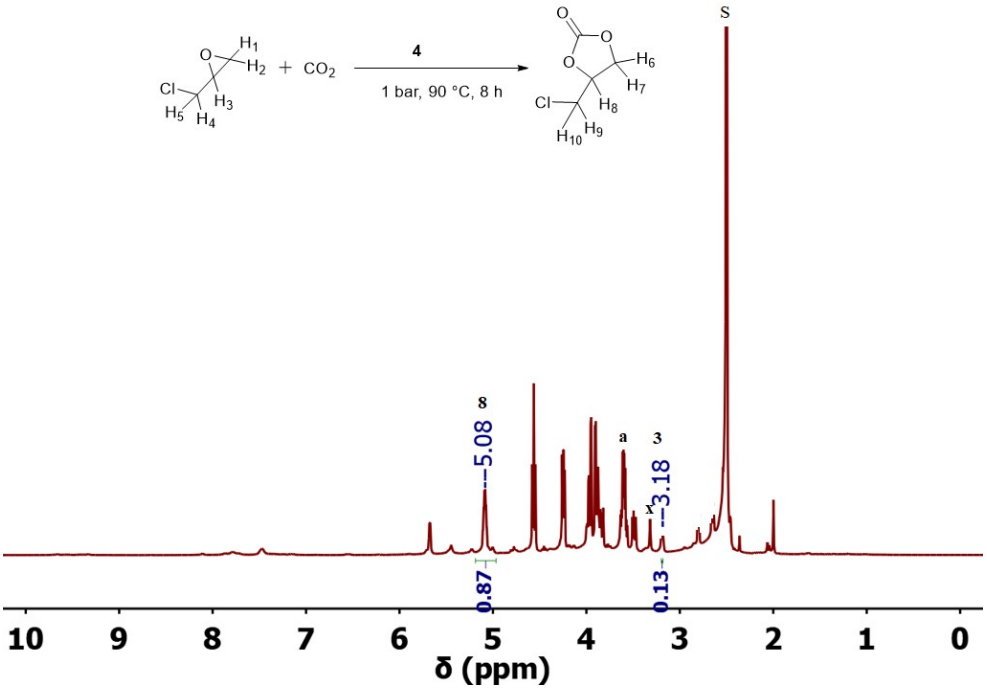

Figure SC 25. ^{1}H NMR spectrum of ECH conversion in DMSO-d_6 using **4**, **S**: solvent, **x**: H_2O, **a**: 1,2-diol, peaks around 7.46 ppm are corresponding to the catalyst (**catalytic cycle 5**).

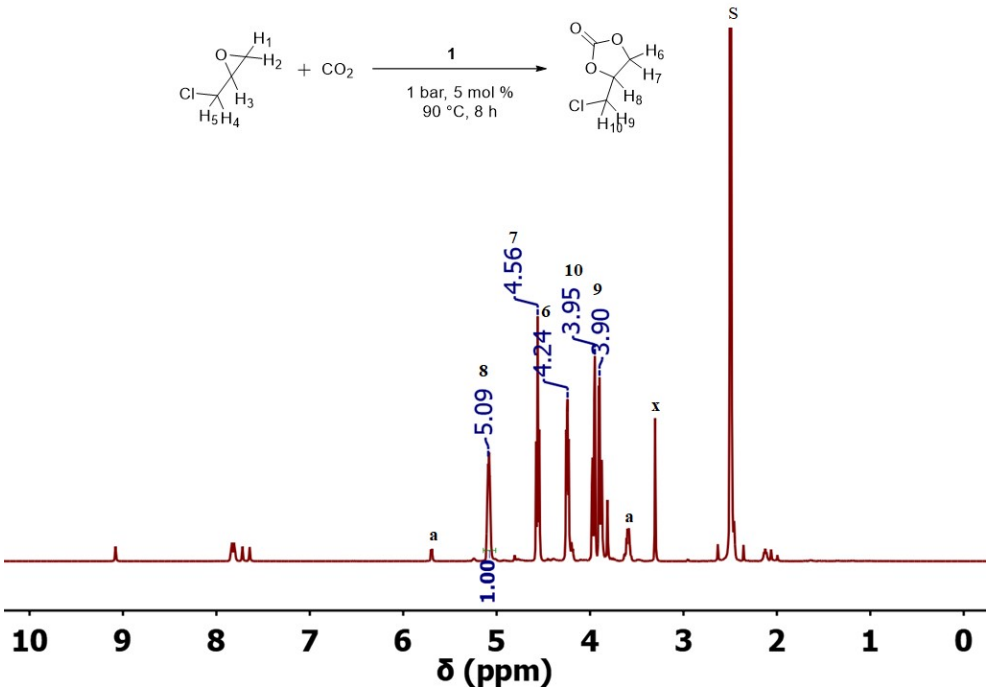

Figure SC 26. ^{1}H NMR spectrum of ECH conversion in DMSO-d_6 using **1**, **S**: solvent, **x**: H_2O, **a**: 1,2-diol, peaks at 2.15, 7.65,7.73,7.80, and 9.14 ppm are corresponding to the catalyst (**Table 2**, entry 1).

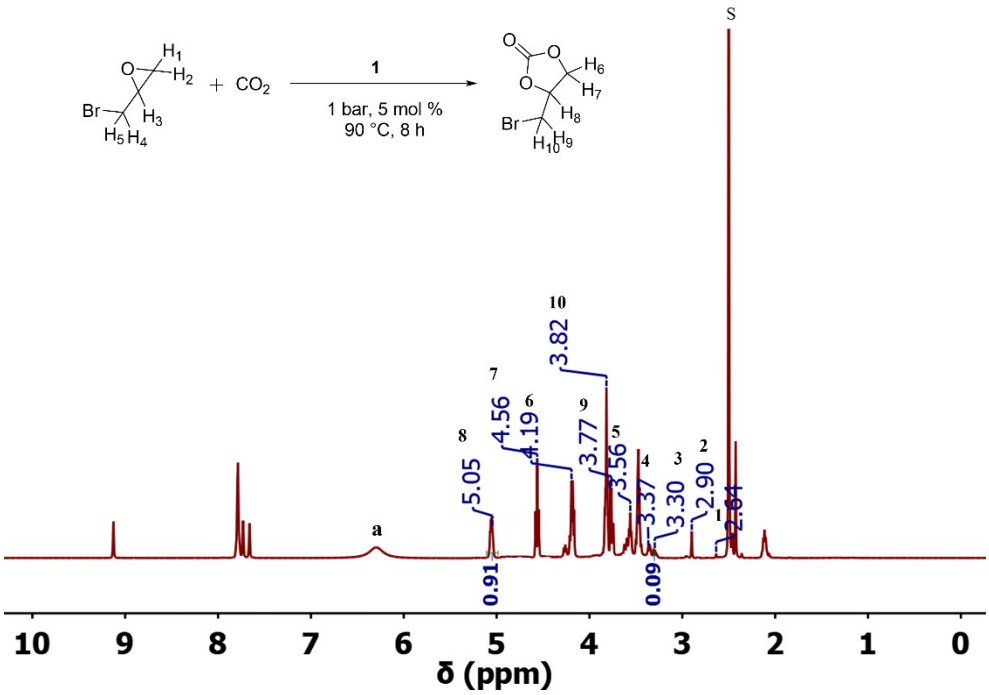

Figure SC 27. ^{1}H NMR spectrum of EBH conversion in DMSO-d_6 using **1**, **S**: solvent, **x**: H_2O, **a**: 1,2-diol, peaks at 2.15, 7.65,7.73,7.80, and 9.14 ppm are corresponding to the catalyst (**Table 2**, entry 2).

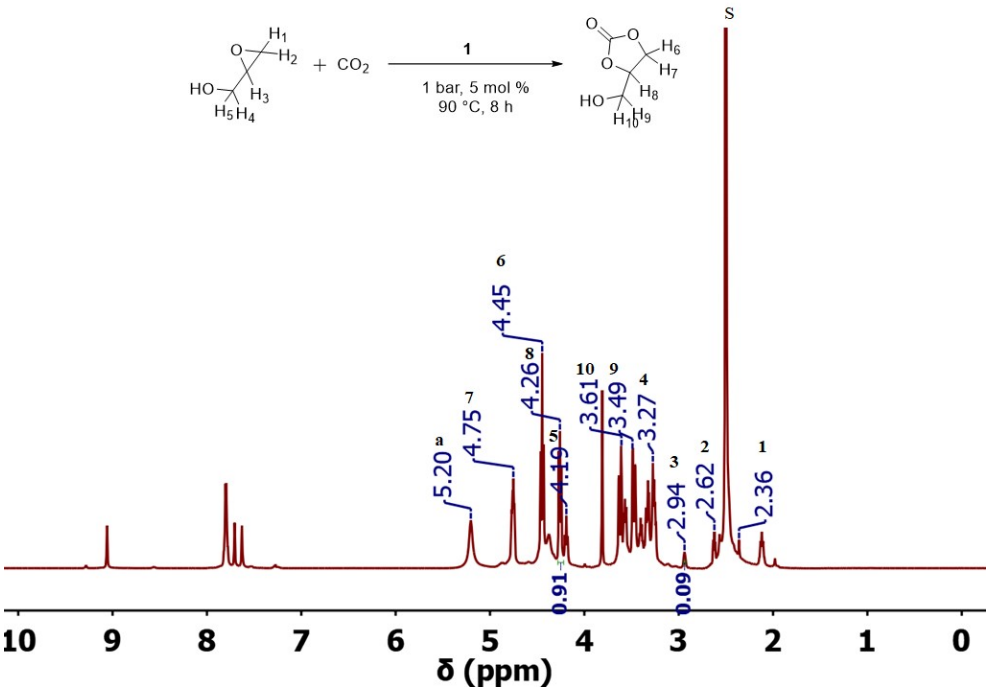

Figure SC 28. ^{1}H NMR spectrum of glycidol conversion in DMSO-d_6 using **1**, **S**: solvent, **x**: H_2O, **a**: 1,2-diol, peaks at 2.15, 7.65,7.73,7.80, and 9.14 ppm are corresponding to the catalyst (**Table 2**, entry 3).

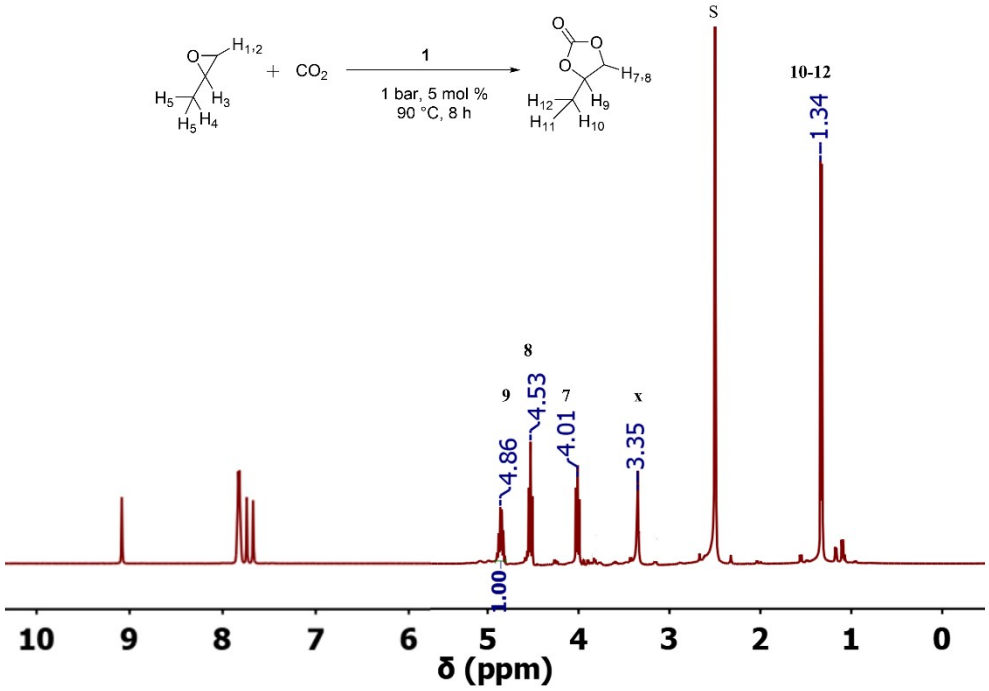

Figure SC 29. ^{1}H NMR spectrum of PO conversion in DMSO-d_6 using **1**, **S**: solvent, **x**: H_2O, peaks at 7.65,7.73,7.80, and 9.14 ppm are corresponding to the catalyst (**Table 2**, entry 4).

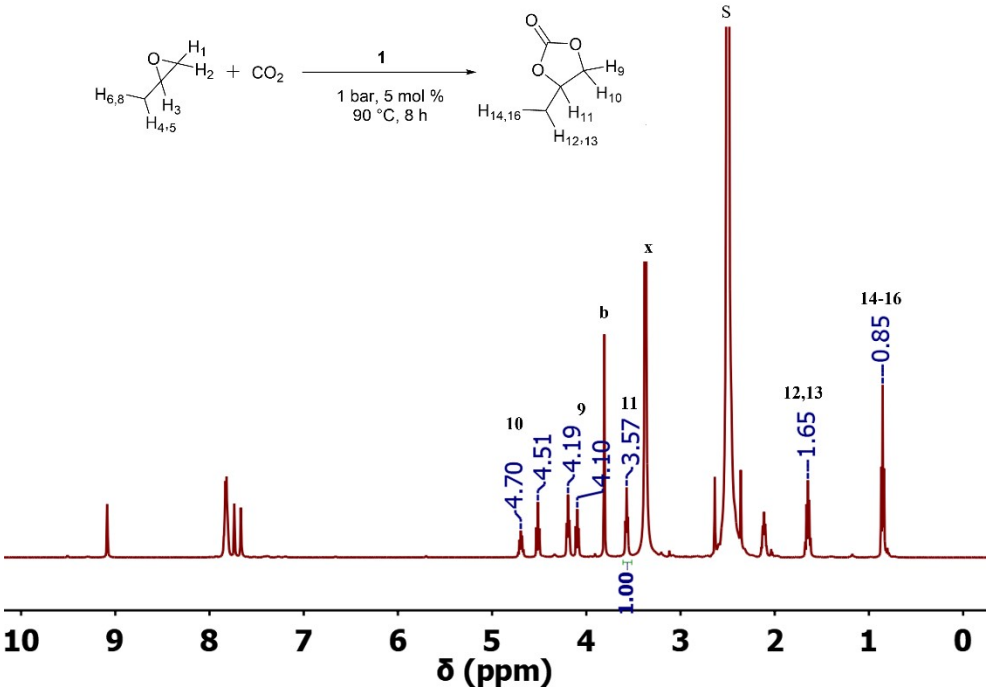

Figure SC 30. ^{1}H NMR spectrum of 1,2-epoxybutane conversion in DMSO-d_6 using **1**, **S**: solvent, **x**: H_2O, **b:** impurity from the starting material (1,2-epoxybutane), peaks at 7.65,7.73,7.80, and 9.14 ppm are corresponding to the catalyst (**Table 2**, entry 5).

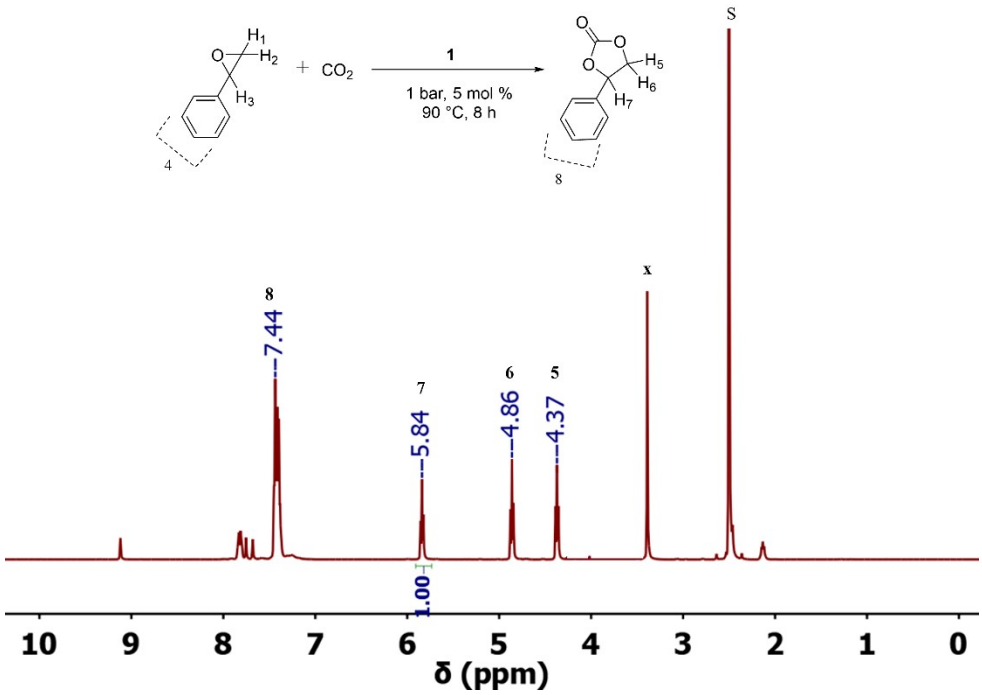

Figure SC 31. ^{1}H NMR spectrum of SO conversion in DMSO-d_6 using **1**, **S**: solvent, **x**: H_2O, peaks at 2.15, 7.65,7.73,7.80, and 9.14 ppm are corresponding to the catalyst (**Table 2**, entry 6).

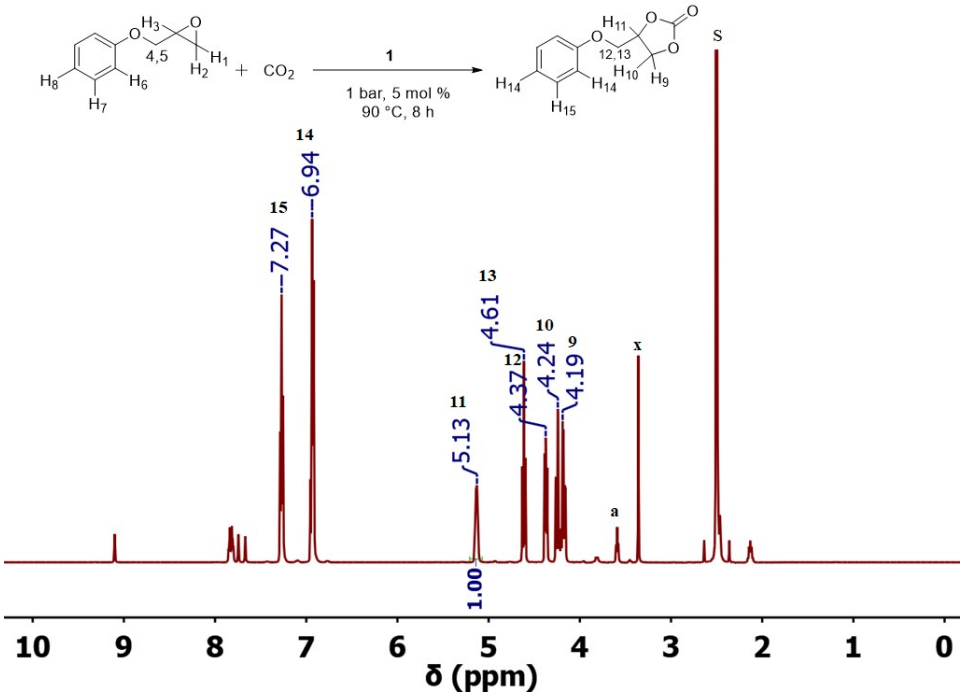

Figure SC32. ^{1}H NMR spectrum of 1,2-epoxy-3-phenoxypropane conversion in DMSO-d_6 using **1**, **S**: solvent, **x**: H_2O, peaks at 2.15, 7.65,7.73,7.80, and 9.14 ppm are corresponding to the catalyst (**Table 2**, entry 7).

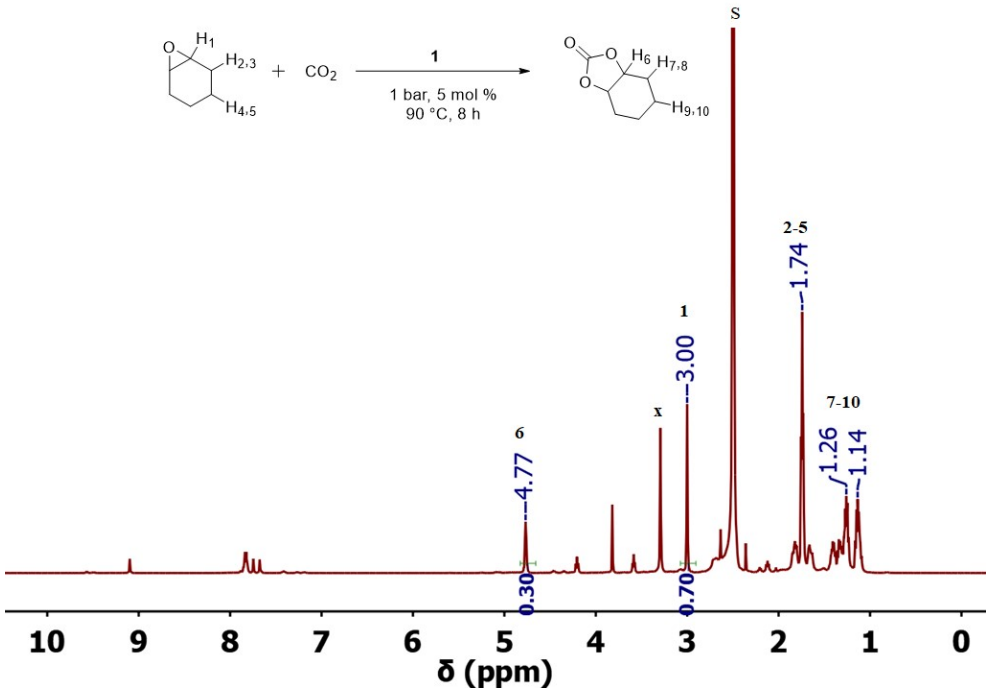

Figure SC33. ^{1}H NMR spectrum of cyclohexene oxide conversion in DMSO-d_6 using **1**, **S**: solvent, **x**: H_2O, peaks at 7.65,7.73,7.80, and 9.14 ppm are corresponding to the catalyst (**Table 2**, entry 8).

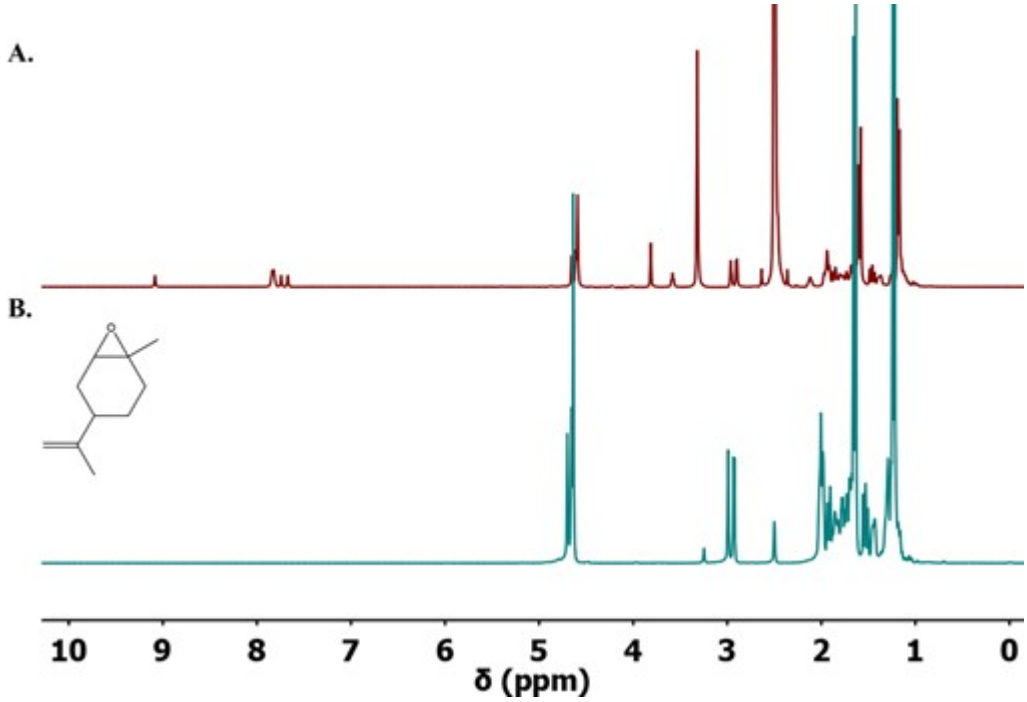

Figure SC 34. ^{1}H NMR spectra in DMSO-d_6 of: **A.** LO coupled with CO_2 in the presence of **3**, peaks at,7.73,7.80, and 9.14 ppm are corresponding to the catalyst (maroon traces); **B.** LO (blue trace). The CC peaks are not observed (**Table 2**, Entry 9).

Figure SC35. ^{1}H NMR spectrum of ECH conversion in DMSO-d_6 using **1**, **S**: solvent, **x**: H_2O, **a**: 1,2-diol, peaks at 2.15, 7.65,7.73,7.80, and 9.14 ppm are corresponding to the catalyst (**Table 3**, entry 1).

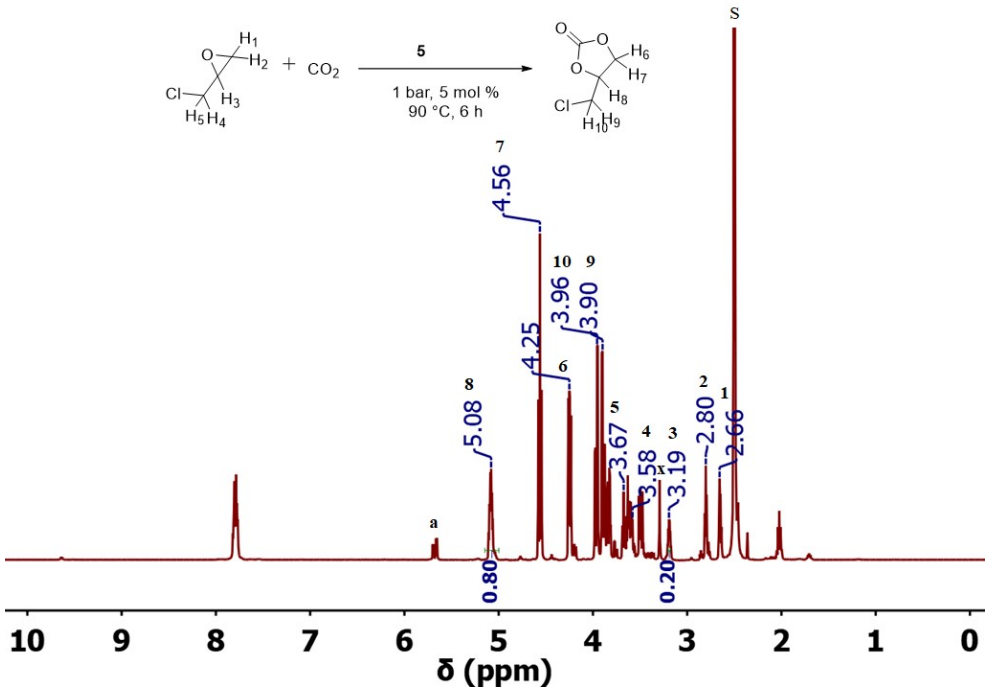

Figure SC36. ^{1}H NMR spectrum of ECH conversion in DMSO-d_6 using **5**, **S**: solvent, **x**: H_2O, **a**: 1,2-diol, peaks at 2.15 and 7.80 ppm are corresponding to the catalyst (**Table 3**, entry 2).

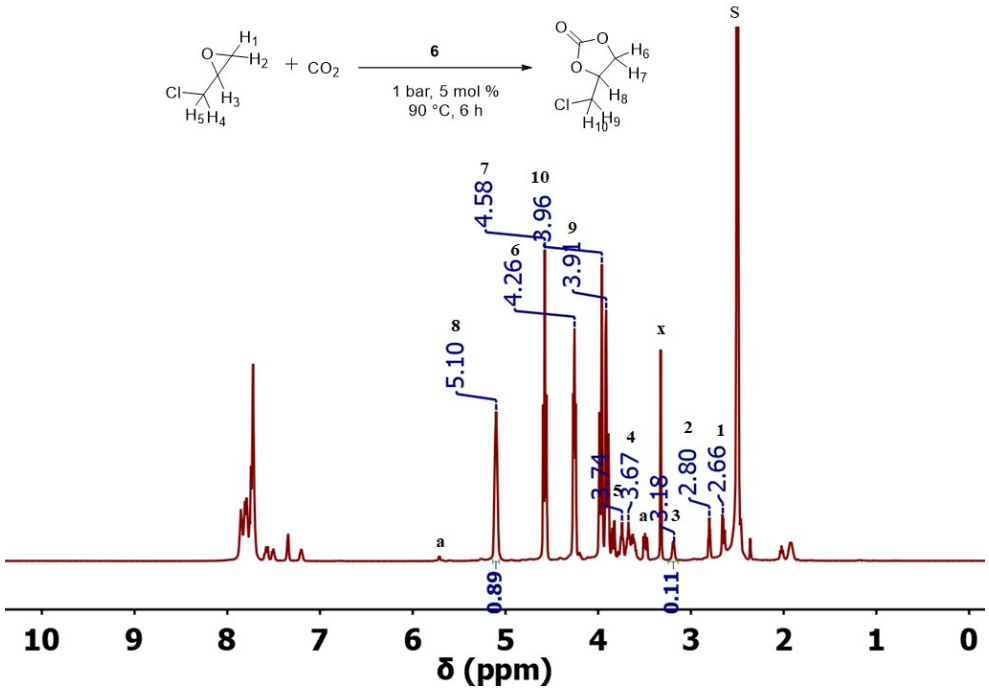

Figure SC37. ^{1}H NMR spectrum of ECH conversion in DMSO-d_6 using **6**, **S**: solvent, **x**: H_2O, **a**: 1,2-diol, peaks at 2.15 and 7.20-7.80 ppm are corresponding to the catalyst (**Table 3**, entry 3).

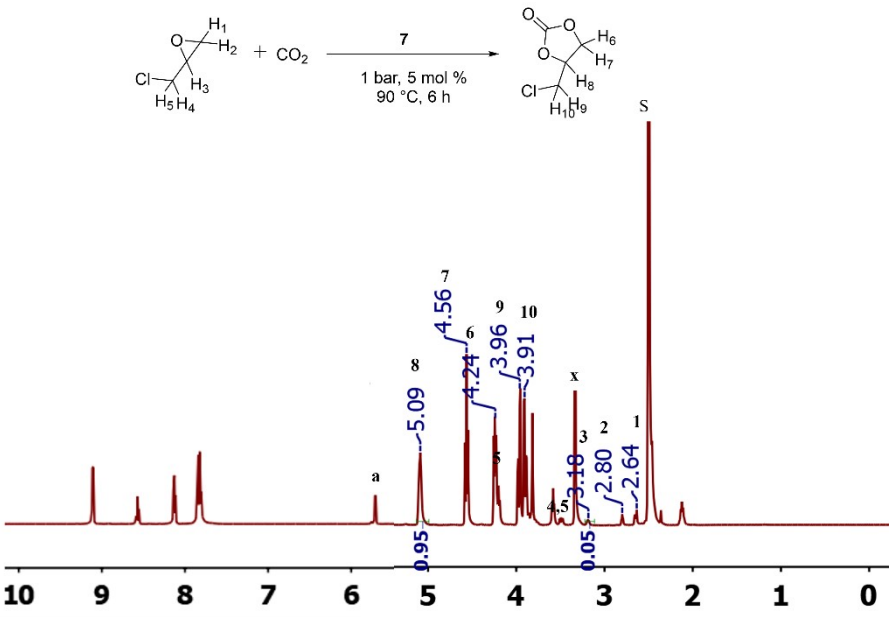

Figure SC38. ^{1}H NMR spectrum of ECH conversion in DMSO-d_6 using **7**, **S**: solvent, **x**: H_2O, **a**: 1,2-diol, peaks at 2.15, 7.84, 8.13, 8.57, and 9.11 ppm are corresponding to the catalyst (**Table 3**, entry 4).

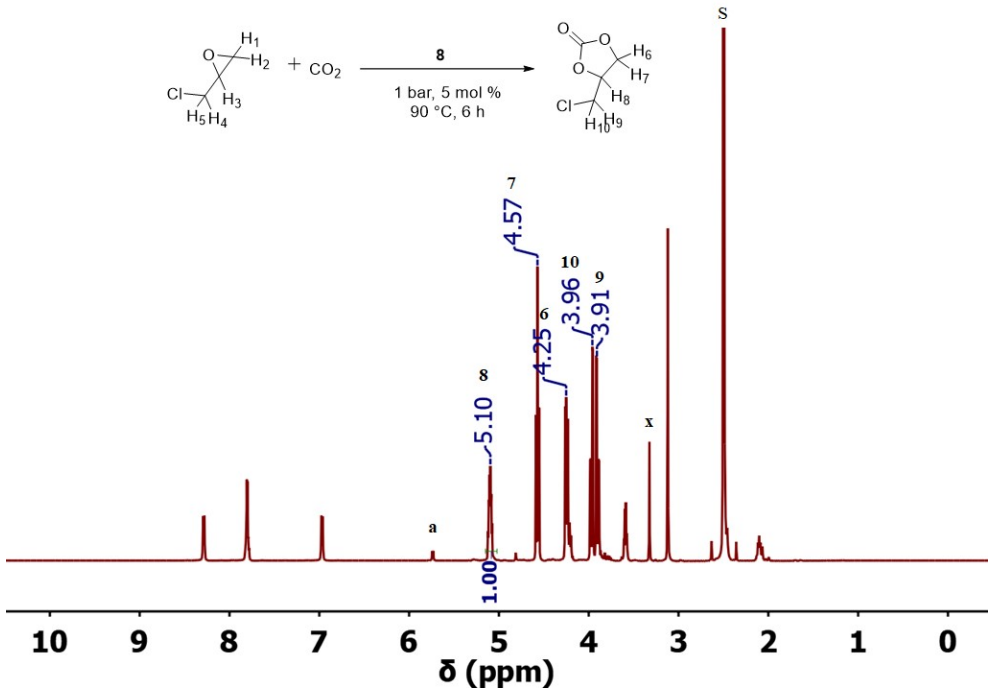

Figure SC39. ^{1}H NMR spectrum of ECH conversion in DMSO-d_6 using **8**, **S**: solvent, **x**: H_2O, **a**: 1,2-diol, peaks at 2.15, 3.11, 7.80, and 8.29 ppm are corresponding to the catalyst (**Table 3**, entry 5).

4. CCs Isolation

In order to get realistic quantities of CCs that can be handled and examined, the cycloaddition experiment for the isolation purpose was scaled up using 2 ml of ECH rather than 0.5 ml. The traditional isolation approaches were reported for CC isolation mainly depending on the column chromatography techniques.[10,11] Herein, using DMSO as a solvent caused real complications during separation due to its high polarity and viscosity, then it was necessary to get rid of it in the first step. To remove DMSO, ice cubes were added to the crude reaction until melting, followed by the addition of EtOAc: Et_2O to extract CC. Fortunately, the catalyst remained dissolved in the aqueous layer, then it was eliminated in this step. The organic layer was rinsed three times with cold water with good shaking to remove any DMSO and catalyst traces, dried with anhydrous sodium sulfate, and concentrated using rotary evaporation. The crude product was further purified using either recrystallization for solid CCs or silica plug for liquid CCs.

4-(chloromethyl)-1,3-dioxolane-2-one (**9**): obtained as a pale-yellow liquid upon filtration through a silica plug, eluting with hexane: EtOAc (3:1). **^{1}H NMR** (**500 MHz, DMSO-*d*$_6$**): δ 5.12 (m, J = 8.8, 4.2 Hz, 1H), 4.60 (t, J = 8.6 Hz, 1H), 4.28 (dd, J = 8.7, 5.6 Hz, 1H), 4.01 (dd, J = 12.5, 3.3 Hz, 1H), 3.93 (dd, J = 12.4, 4.2 Hz, 1H). **^{13}C NMR** (**126 MHz, DMSO-*d*$_6$**): δ 154.49, 74.96, 66.89, 45.30. **ATR-FTIR** (**400-4000 cm^{-1}**): 2964, 1778, 1159, 1066.

4-(bromomethyl)-1,3-dioxolane-2-one (**10**): obtained as a yellow liquid upon filtration through a silica plug, eluting with hexane: EtOAc (3:1). **^{1}H NMR** (**500 MHz, DMSO-*d*$_6$**): δ 5.08 (m, J = 9.0, 4.5 Hz, 1H), 4.60 (t, J = 8.6 Hz, 1H), 4.24 (dd, J = 8.7, 5.8 Hz, 1H), 3.77 (dd, J = 11.4, 4.3 Hz, 1H), 3.70 (dd, J = 19.6, 11.2, 3.9 Hz, 1H), 3.57 – 3.47 (m, 4H). **^{13}C NMR** (**126 MHz, DMSO-*d*$_6$**): δ 154.38, 74.49, 67.99, 36.68, 34.21. **ATR-FTIR** (**400-4000 cm^{-1}**): 2966, 1791, 1157, 1060.

4-methyl-1,3-dioxolan-2-one (**11**): obtained as a colorless liquid. **^{1}H NMR** (**500 MHz, DMSO-*d*$_6$**: δ 4.90 (h, *J* = 6.7 Hz, 1H), 4.57 (t, *J* = 8.0 Hz, 1H), 4.06 (t, *J* = 7.7 Hz, 1H), 1.37 (d, *J* = 6.3 Hz, 3H).**^{13}C NMR** (**126 MHz, DMSO-*d*$_6$**): δ 154.94, 73.79, 70.50, 18.78.

4-phenyl-1,3-dioxoalne-2-one (12): obtained as a white solid upon recrystallization using hot hexane. Melting point: 52-54 °C (Corrected: 49-51 °C)[11]. **^{1}H NMR** (**500 MHz, DMSO-*d*$_6$**): δ 7.47 (q, J = 7.5 Hz, 5H), 5.86 (t, J = 8.0 Hz, 1H), 4.89 (t, J = 8.3 Hz, 1H), 4.42 (t, J = 8.2 Hz, 1H). **^{13}C NMR** (**126 MHz, DMSO-*d*$_6$**): δ 154.72, 136.28, 129.36, 128.90, 126.68, 77.77, 70.81. **ATR-FTIR** (**400-4000 cm^{-1}**): 3068. 3037, 2925, 1770, 1552, 1166, 1057. **TGA**: No weight loss up to 150°C, the decomposition temperature at 50% weight loss (**T**$_{d50}$) took place at 256 °C.

4-(phenoxymethyl)-1,3-dioxoalne-2-one (**13**): obtained as a white solid upon recrystallization using a mixture of hexane: EtOAc (1:1). Melting point: 98-101 °C (Corrected: 94-97 °C)[14]. **^{1}H NMR** (**500 MHz, DMSO-*d*$_6$**): δ 7.39 – 7.22 (m, 2H), 7.05 – 6.88 (m, 3H), 5.23 – 5.08 (m, 1H),

4.64 (t, J = 8.5 Hz, 1H), 4.40 (dd, J = 8.4, 6.0 Hz, 1H), 4.28 (dd, J = 11.4, 2.6 Hz, 1H), 4.20 (dd, J = 11.3, 4.7 Hz, 1H). **^{13}C NMR (126 MHz, DMSO-*d*$_6$)**: δ 157.93, 129.60, 121.25, 114.61, 74.84, 67.39, 66.03. **ATR-FTIR (400-4000 cm^{-1})**: 3062, 2927, 1782, 1600, 1162, 1081. **TGA**: No weight loss up to 200 °C, the decomposition temperature at 50% weight loss (T_{d50}) took place at 296 °C.

hexahydrobenzo[d][1,3]dioxol-2-one (14): obtained as a white solid upon recrystallization using a mixture of hexane: EtOAc (1:1). **^{1}H NMR (500 MHz, DMSO-*d*$_6$)**: δ 4.79 – 4.71 (m, 2H), 1.83 (tt, J = 8.7, 4.3 Hz, 2H), 1.68 (ddt, J = 14.9, 10.2, 4.3 Hz, 2H), 1.43 (dtd, J = 14.8, 8.2, 4.0 Hz, 2H), 1.34 (dp, J = 11.9, 4.8, 4.1 Hz, 2H).). **^{13}C NMR (126 MHz, DMSO-*d*$_6$)**: δ 157.88, 75.44, 26.13,18.76.

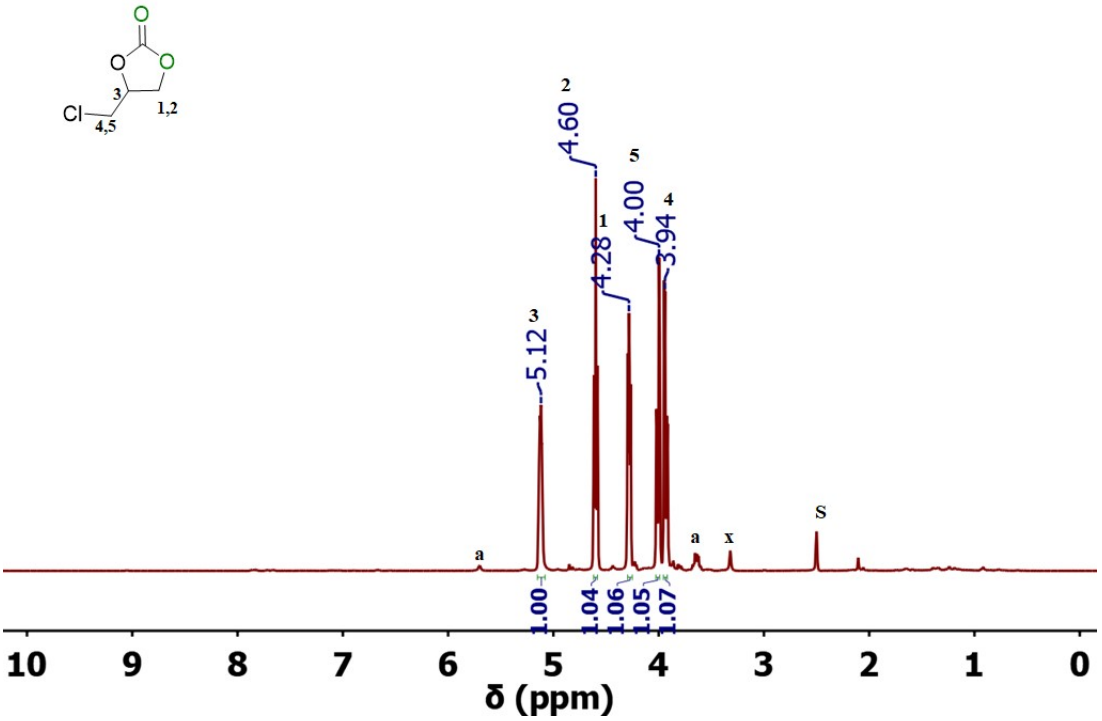

Figure SD 1. ^{1}H NMR spectrum of **9** in DMSO-*d*$_6$, **s**: solvent, **x**: H_2O, **a**: 1,2-diol.

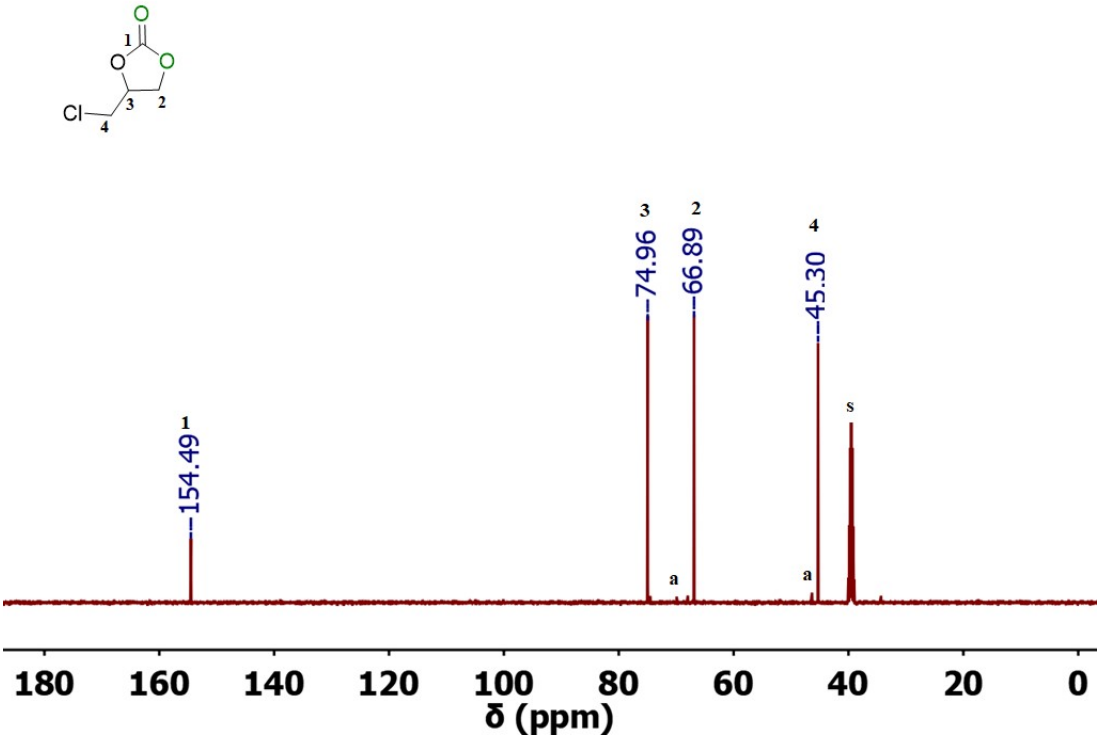

Figure SD 2. ^{13}C NMR spectrum of isolated **9** in DMSO-d_6, **s**: solvent, **a**: 1,2-diol.

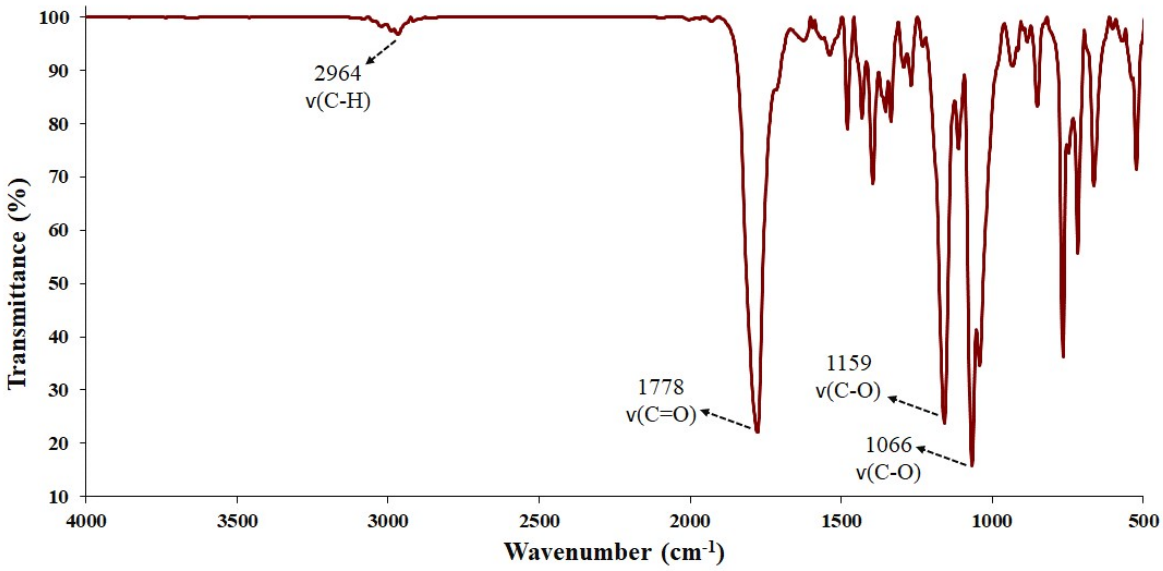

Figure SD 3. ATR-FTIR spectrum of **9**.

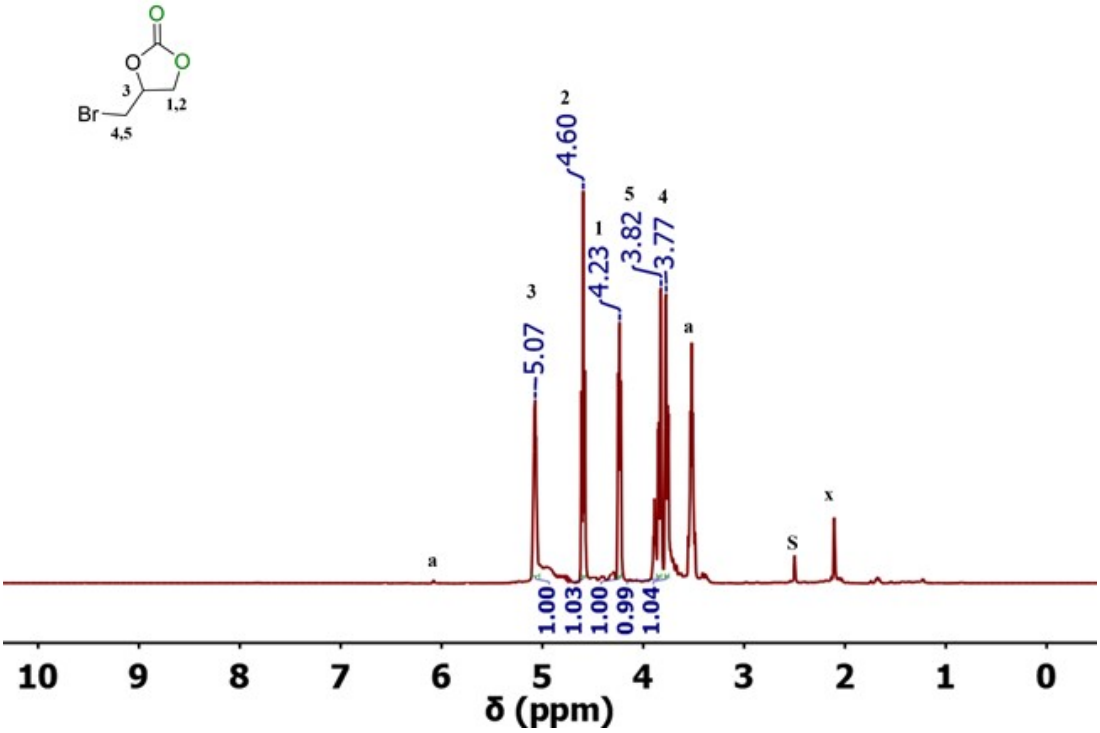

Figure SD 4.[1]H NMR spectrum of **10** in DMSO-d_6, **s**:solvent, **a**: 1,2-diol. **x**: impurities.

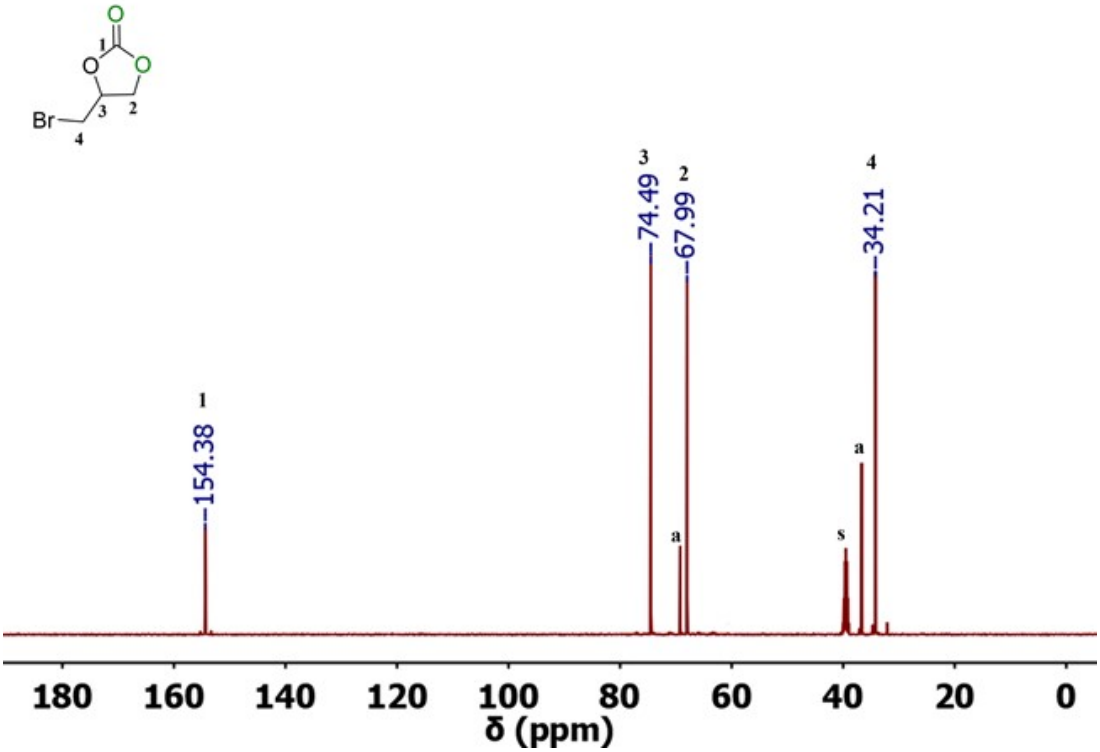

Figure SD 5.[13]C NMR spectrum of **10** in DMSO-d_6, **s**: solvent, **a**: 1,2-diol.

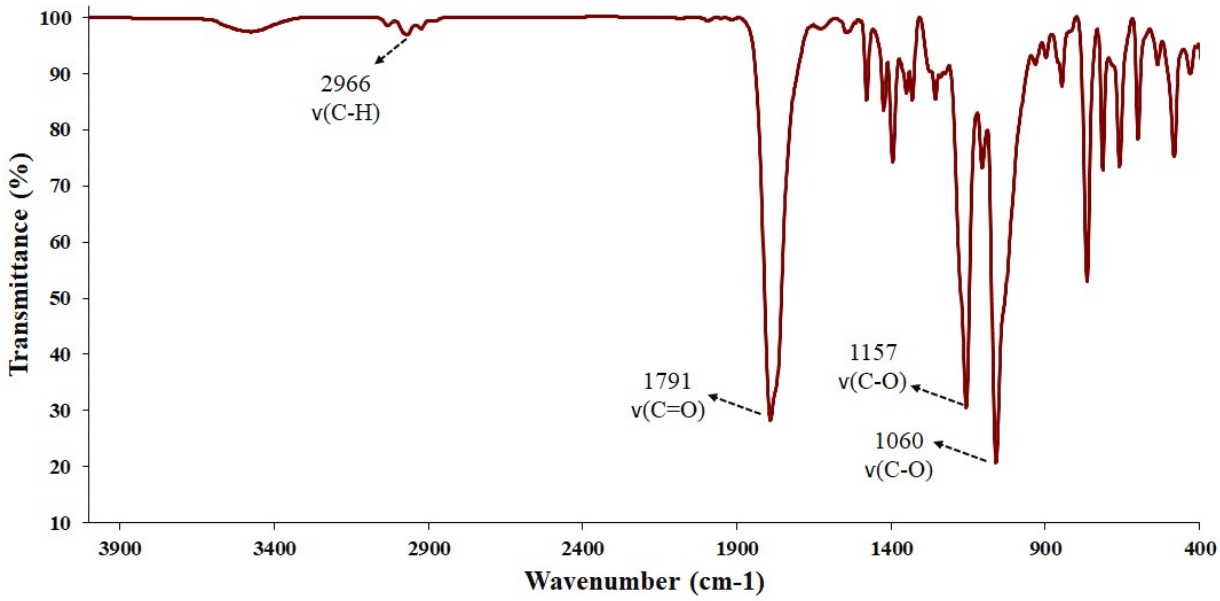

Figure SD 6. ATR-FTIR spectrum of **10**.

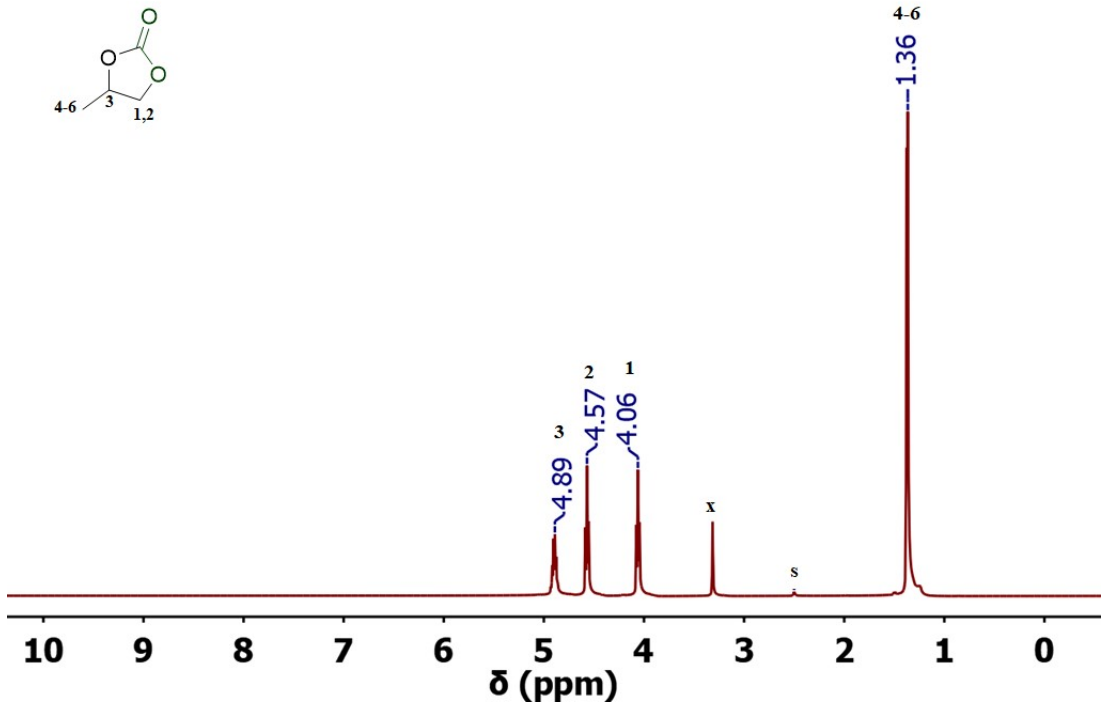

Figure SD 7. ^{1}H NMR spectrum of **11** in DMSO-d_6, **s**:solvent, **x**: H_2O.

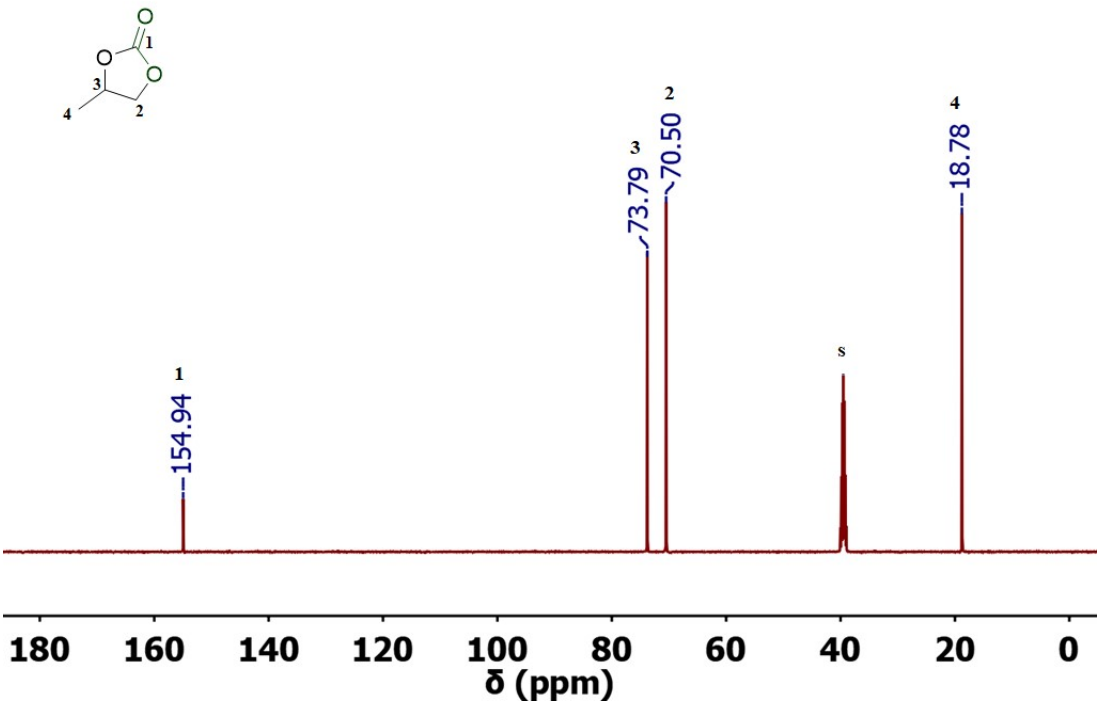

Figure SD 8. ^{13}C NMR spectrum of **11** in DMSO-d_6, **s**:solvent.

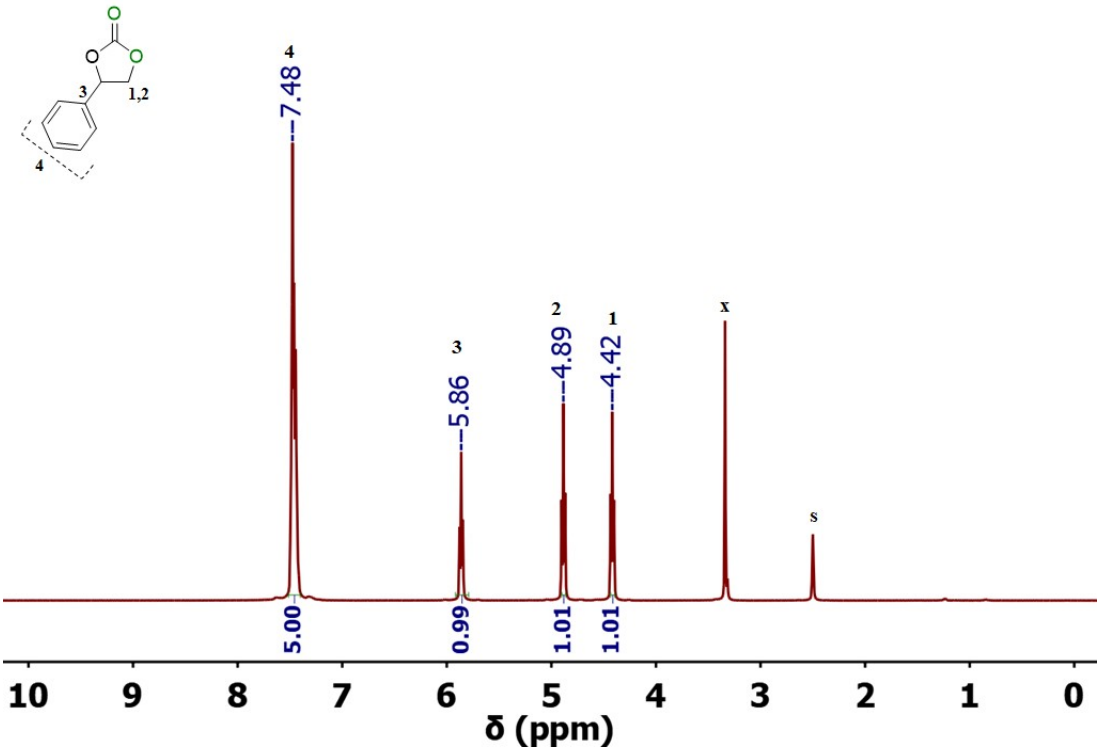

Figure SD 9. ^{1}H NMR spectrum of **12** in DMSO-d_6, **s**: solvent, **x**: H_2O.

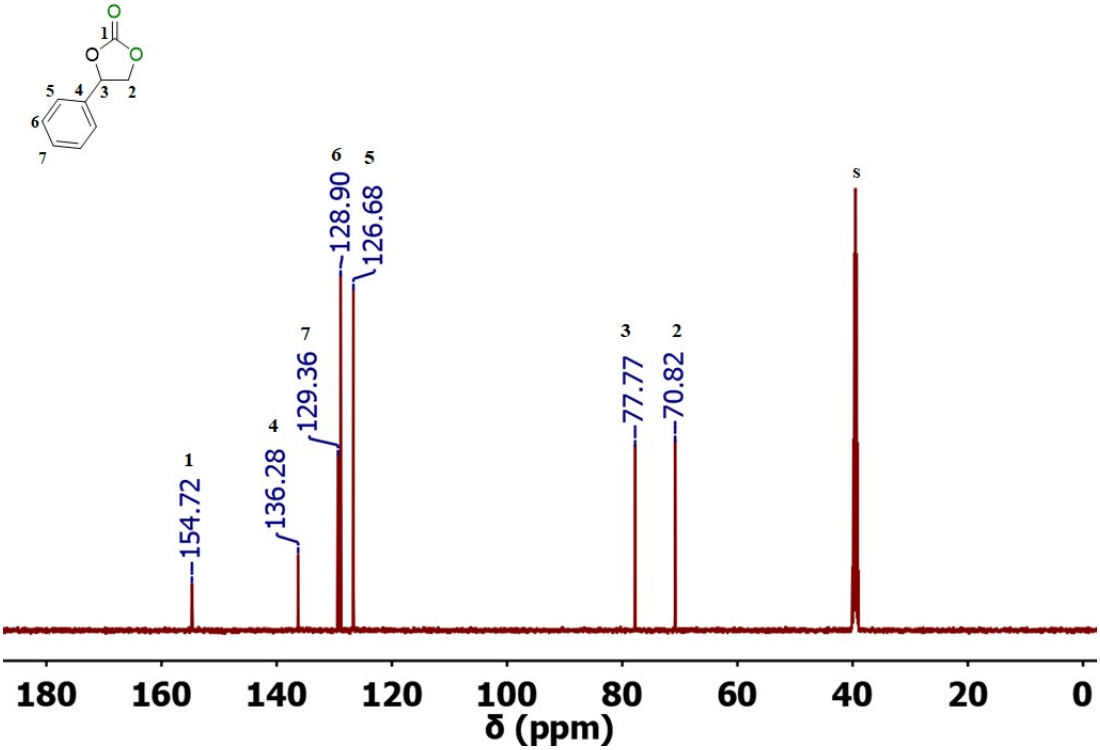

Figure SD 10. ^{13}C NMR spectrum of **12** in DMSO-d_6, **s**: solvent.

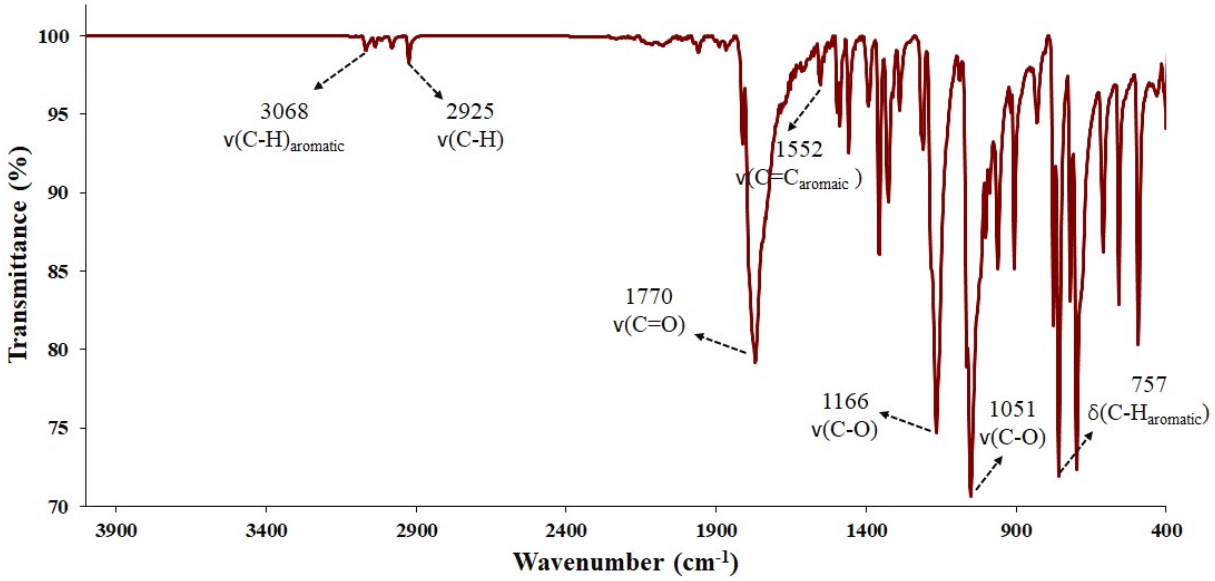

Figure SD 11. ATR-FTIR spectrum of **12**.

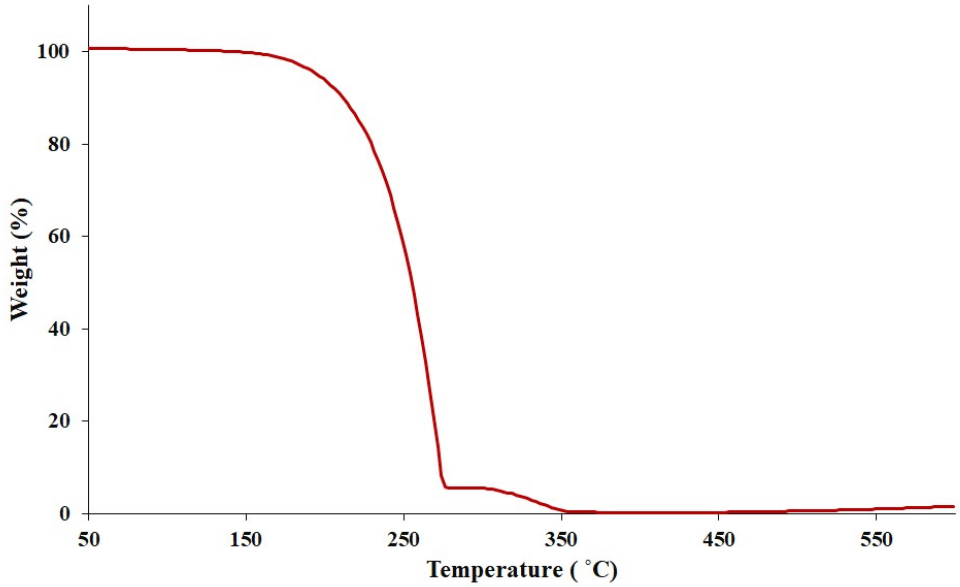

Figure SD 12. TGA traces of **12**.

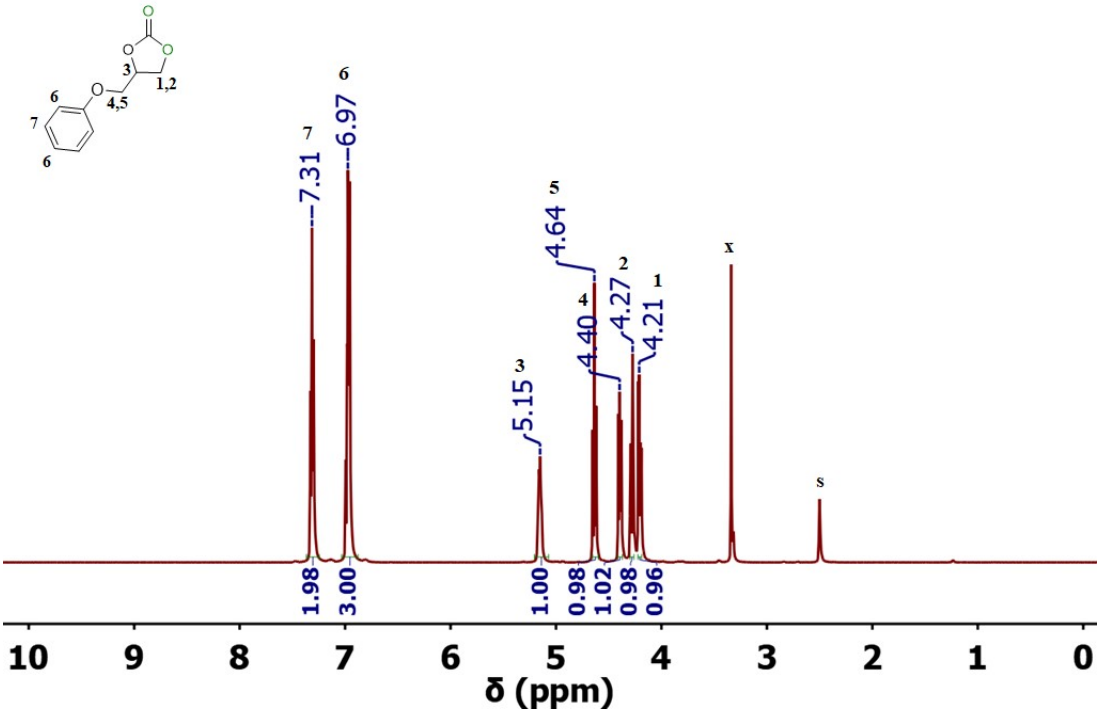

Figure SD13. ^{13}C NMR spectrum of 1**3** in DMSO-d_6, **s**: solvent **x**: H_2O.

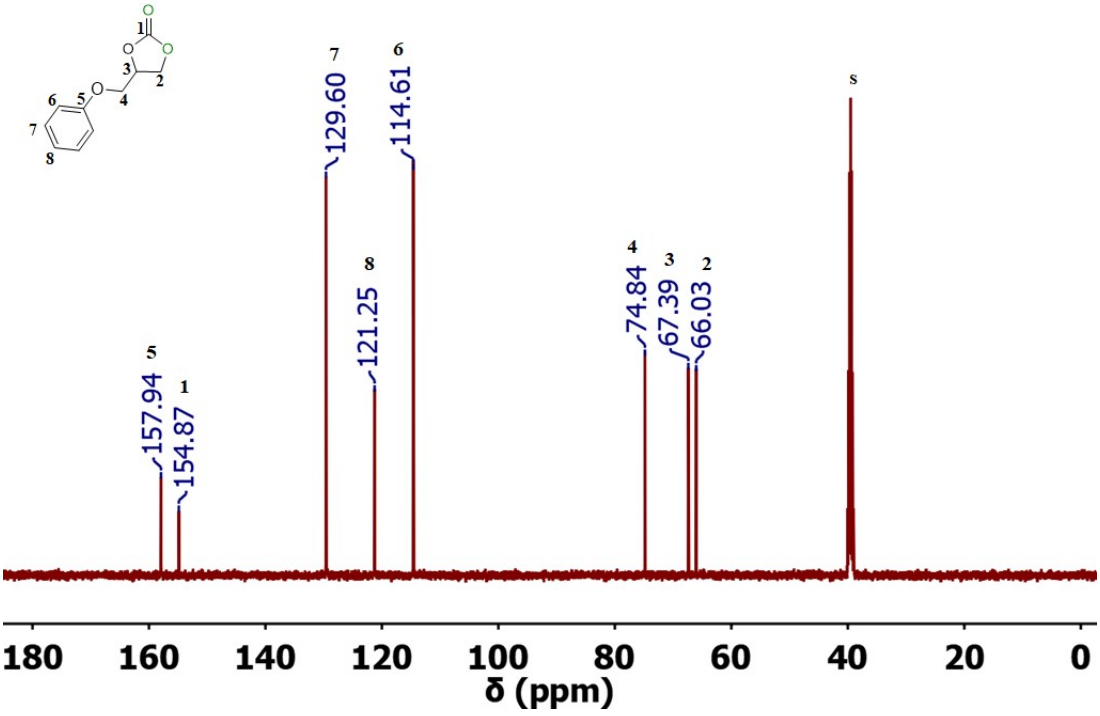

Figure SD14. ^{13}C NMR spectrum of 1**3** in DMSO-d_6, **s**: solvent.

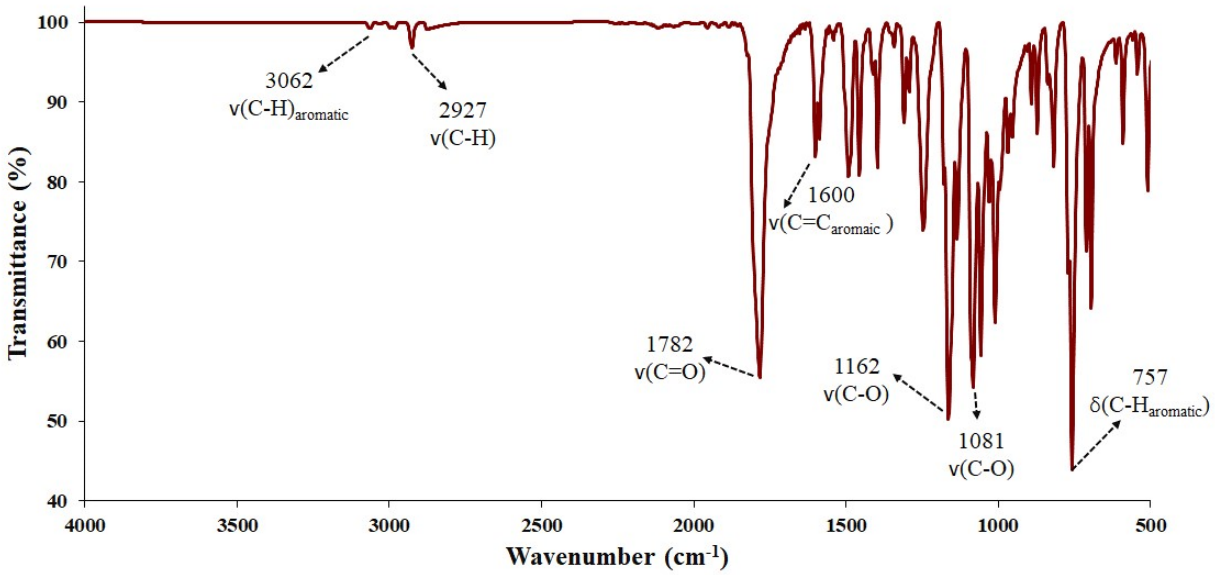

Figure SD 15. ATR-FTIR spectrum of **13.**

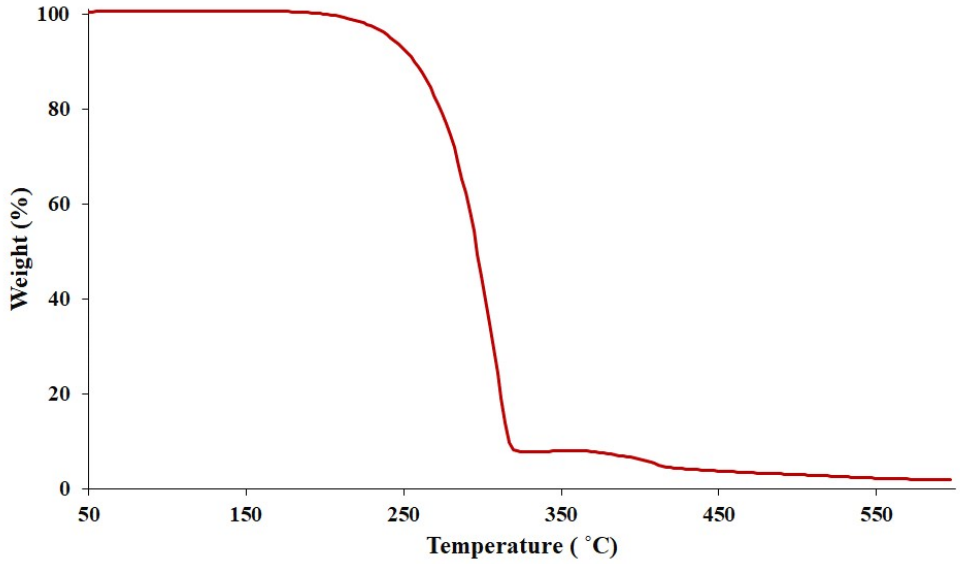

Figure SD 16. TGA traces of **13**.

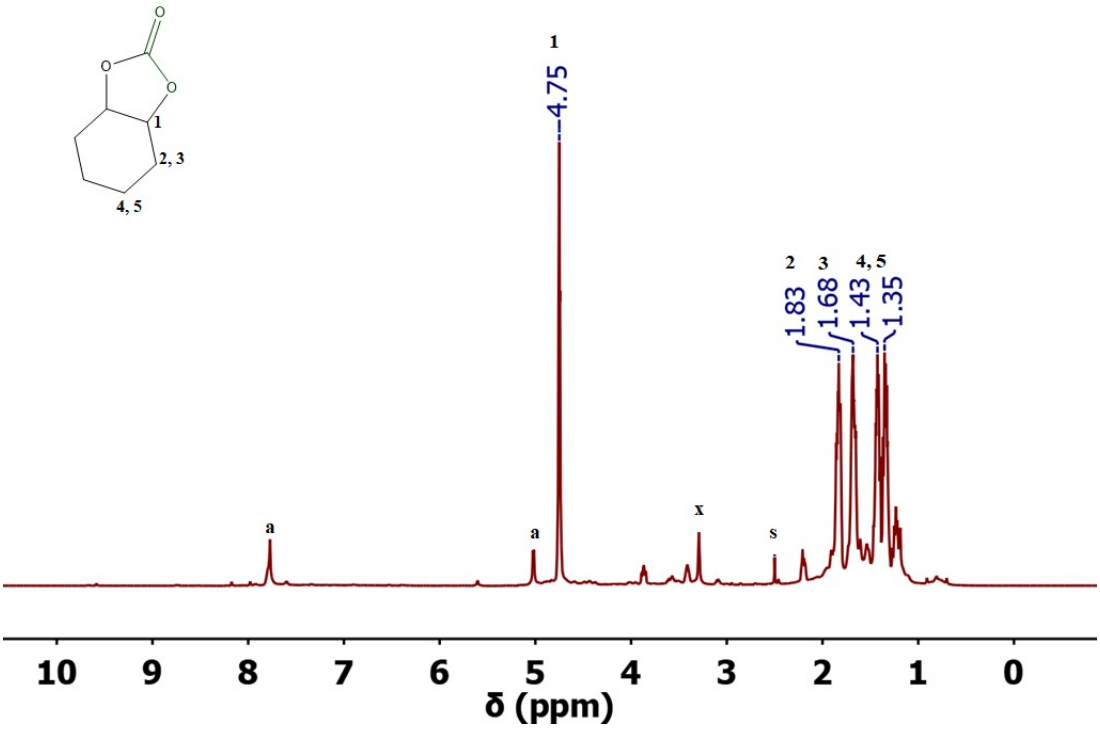

Figure SD 17. [1]H NMR spectrum of **14** in DMSO-d_6, **s**:solvent, **x**:impurities, **a**: 1,2-diol.

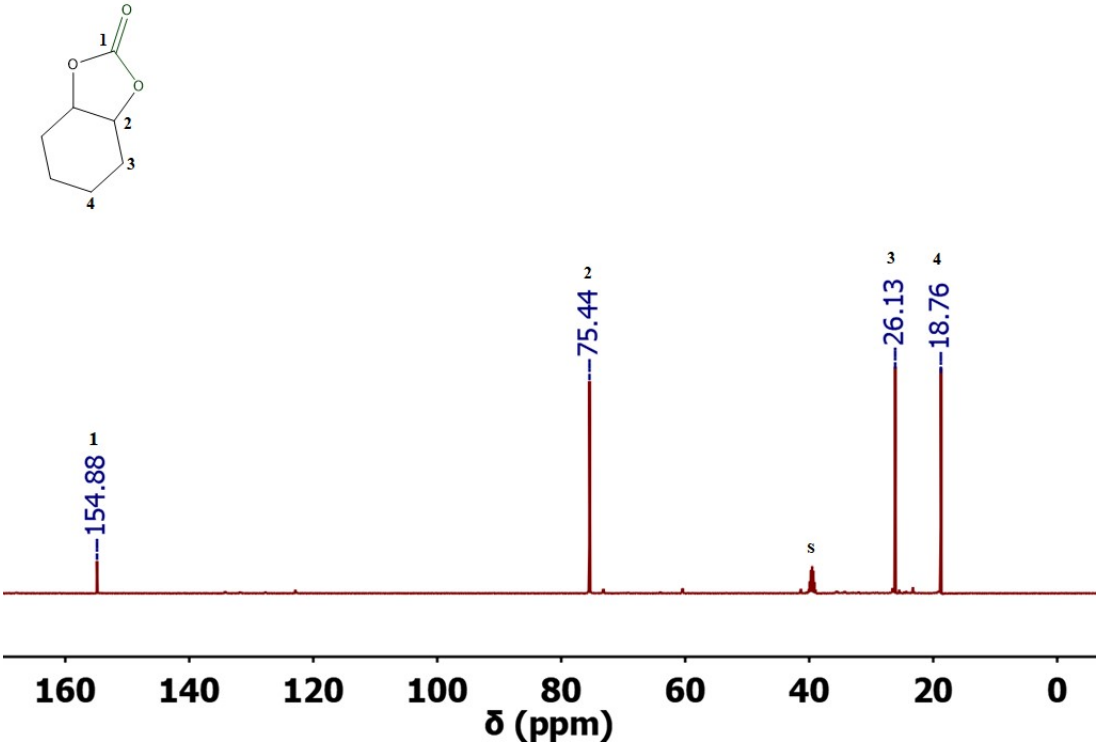

Figure SD 18. [13]C NMR spectrum of 1**4** in DMSO-d_6, **s**: solvent.

Table S2. Relative energies (kcal/mol) for the intermediates and transition states of the catalytic cycles for the different organocatalysts (**1', 5'-7'**)

	1	**$TS_{1\text{-ring opening}}$**	**2**	**3**	**$TS_{2\text{-ring close}}$**	**X'-CC**
Imidazolium (Route 1)	-1.45	34.58	-30.07	-22.10	19.93	-32.50
Imidazolium (Route 2)	-1.30	34.30	-31.39	-15.63	15.09	-26.09
Ammonium	-2.19	36.81	-28.53	-24.15	19.92	-33.00
Phosphonium	-2.58	35.88	-30.41	-23.15	17.14	-30.17
Pyridinium	-1.80	36.43	-31.54	-19.91	18.38	-27.67

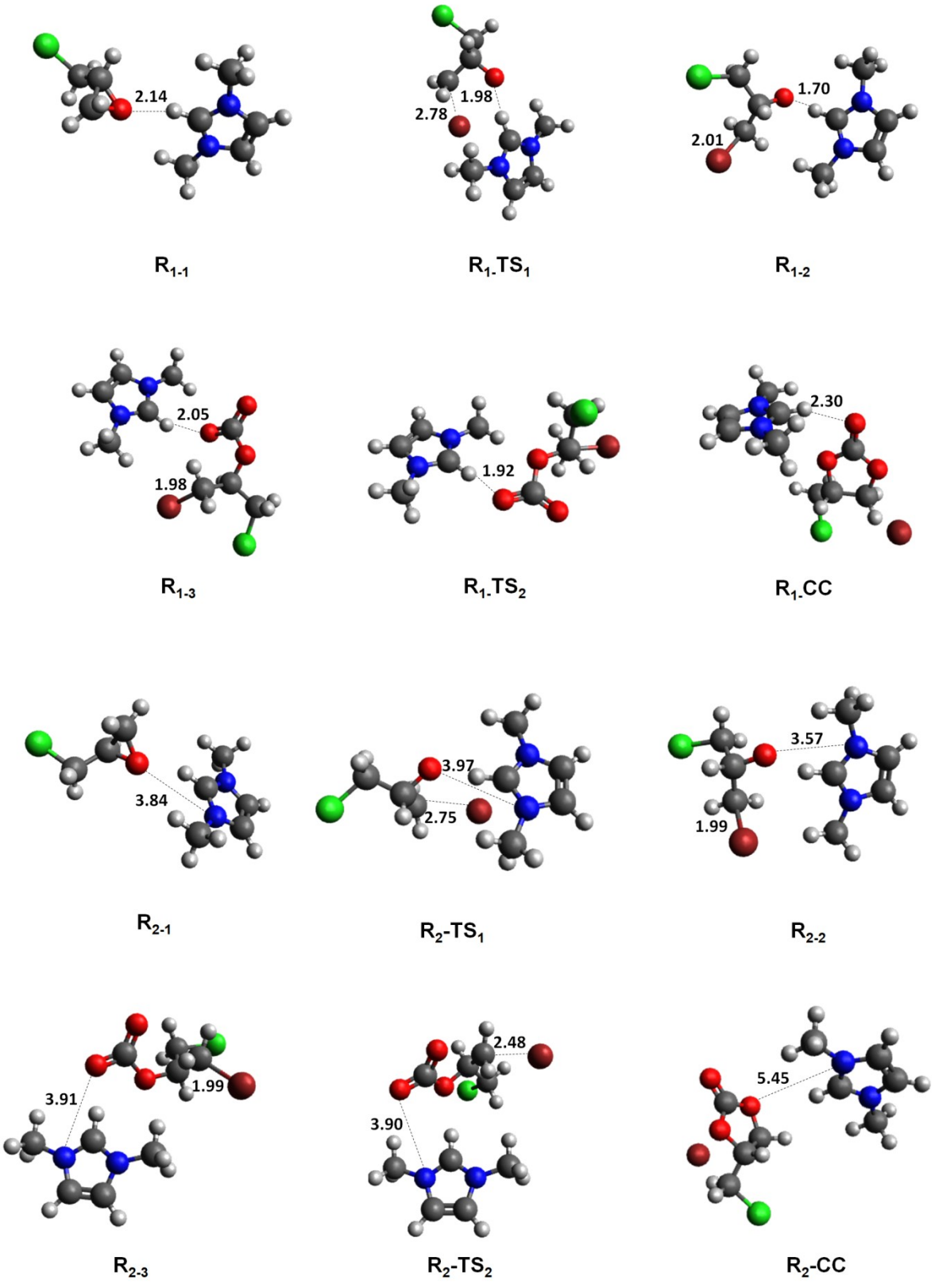

Figure SE 1. The DFT-optimized molecular geometries of the species present in the reaction profile of ECH and CO_2 to form CC catalyzed by (**1'**). The reported bond lengths are in angstrom (Å).

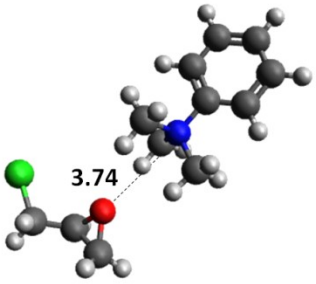

5'-1

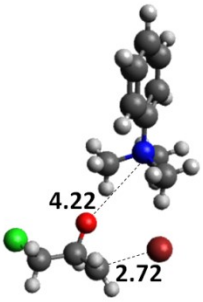

5'-TS$_1$

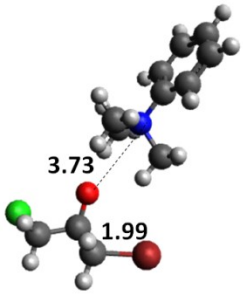

5'-2

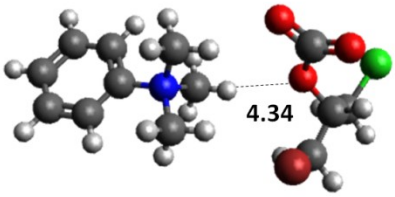

5'-3

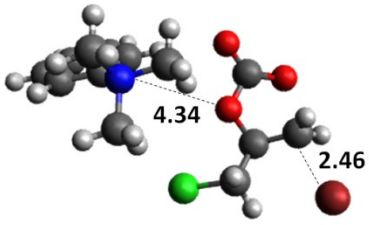

5'-TS$_2$

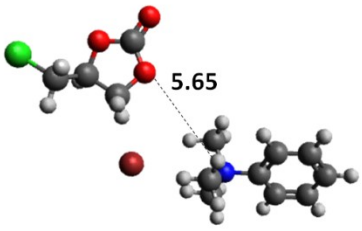

5'-CC

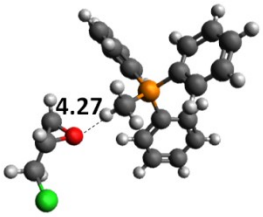

6'-1

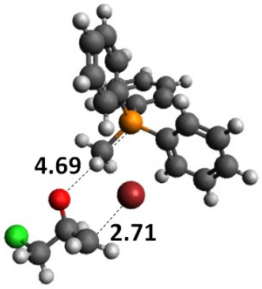

6'-TS$_1$

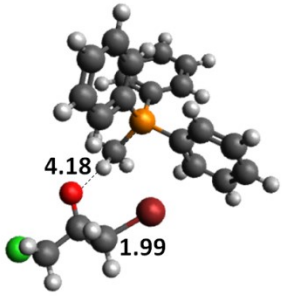

6'-2

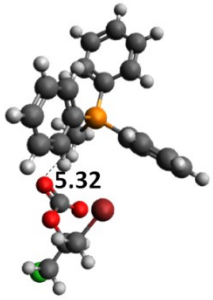

6'-3

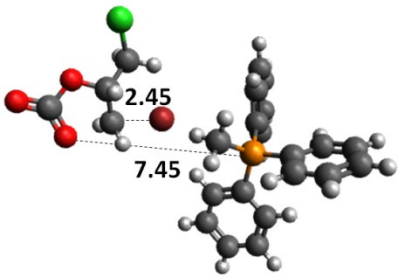

6'-TS$_2$

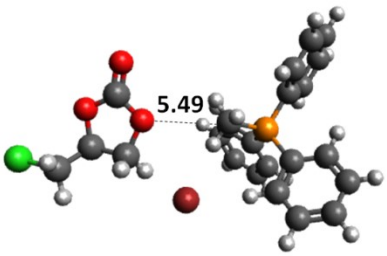

6'-CC

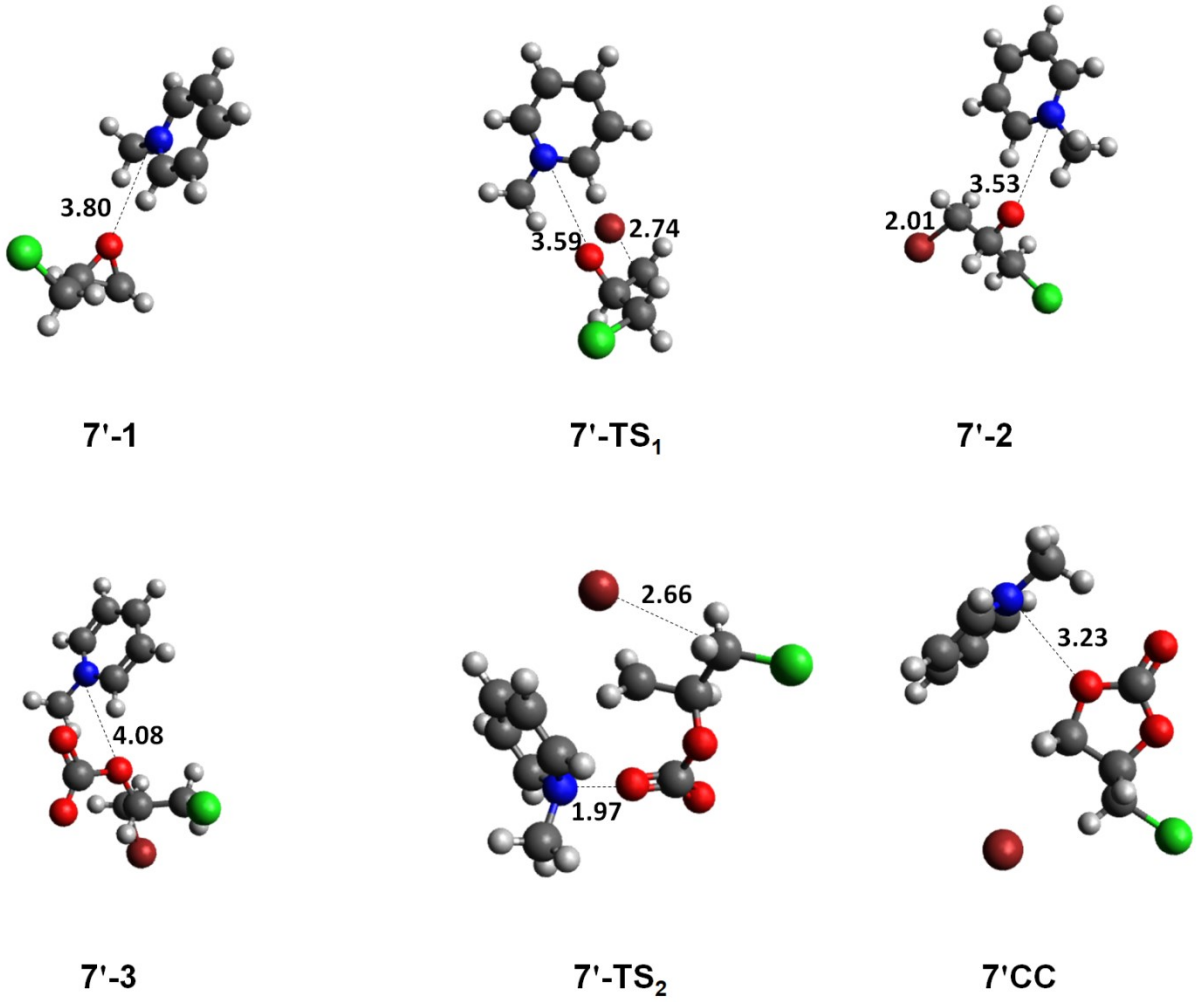

Figure SE 2. The DFT-optimized molecular geometries of the species present in the reaction profile of ECH and CO_2 to form CC catalyzed by (**5'**, **6'**, and **7'**). The reported bond lengths are in angstrom (Å).

References

1. Bobbink, F. D. *et al.* Intricacies of cation–anion combinations in imidazolium salt-catalyzed cycloaddition of CO2 into epoxides. *ACS Catal.* **8**, 2589–2594 (2018).
2. Steinbauer, J., Kubis, C., Ludwig, R. & Werner, T. Mechanistic study on the addition of CO2 to epoxides catalyzed by ammonium and phosphonium salts: a combined spectroscopic and kinetic approach. *ACS Sustain. Chem. Eng.* **6**, 10778–10788 (2018).
3. Xiao, L., Su, D., Yue, C. & Wu, W. Protic ionic liquids: A highly efficient catalyst for synthesis of cyclic carbonate from carbon dioxide and epoxides. *J. CO2 Util.* **6**, 1–6 (2014).
4. Wang, Y. *et al.* Imidazolium-based polymeric ionic liquids for heterogeneous catalytic conversion of CO2 into cyclic carbonates. *Microporous Mesoporous Mater.* **292**, 109751 (2020).
5. Liu, J., Ma, D. & Li, Z. FTIR studies on the compatibility of hard–soft segments for polyurethane–imide copolymers with different soft segments. *Eur. Polym. J.* **38**, 661–665 (2002).
6. Arjunan, V., Subramanian, S. & Mohan, S. FTIR and FTR spectral studies of 2-amino-6-bromo-3-formylchromone. *Spectrochim. Acta. A. Mol. Biomol. Spectrosc.* **60**, 995–1000 (2004).
7. Silverstein, R. M. & Bassler, G. C. Spectrometric identification of organic compounds. *J. Chem. Educ.* **39**, 546 (1962).
8. Sorte, E. G., Rimsza, J. M. & Alam, T. M. Computational and Experimental 1H-NMR Study of Hydrated Mg-Based Minerals. *Molecules* **25**, 933 (2020).
9. Washington, J. B. *et al.* Trialkylammonium salt degradation: implications for methylation and cross-coupling. *Chem. Sci.* (2021).
10. Fiorani, G. *et al.* Catalytic Coupling of Carbon Dioxide with Terpene Scaffolds: Access to Challenging Bio-Based Organic Carbonates. *ChemSusChem* **9**, 1304–1311 (2016).
11. Castro-Osma, J. A. *et al.* Development of hydroxy-containing imidazole organocatalysts for CO 2 fixation into cyclic carbonates. *Catal. Sci. Technol.* **8**, 1981–1987 (2018).